

Evaluation of *Brassica* root architectural traits

by

Chunxiao Yang

A thesis submitted in partial fulfillment of the requirements for the degree of

Master of Science

in

Plant Science

Department of Agricultural, Food and Nutritional Science
University of Alberta

© Chunxiao Yang, 2023

Abstract

Given the roles of roots in water and nutrient uptake, anchorage, and storage of resources, root system architecture (RSA) can have a major impact on plant growth and development. The root systems of *Brassica* species, an important group that includes many field and horticultural crops, is complex. Comparative studies of RSA that combine morphological and genetic analyses are limited, particularly because the evaluation of root traits can be tedious and time-consuming. In this thesis, a semi-hydroponic system was optimized for phenotyping RSA traits in *Brassica napus*, and then utilized for the study of eight RSA traits in a collection of 379 *Brassica* accessions representing six species (*B. napus*, *B. juncea*, *B. carinata*, *B. oleracea*, *B. nigra* and *B. rapa*). The phenotypic data, assessed with an image analysis system, indicated that *B. napus* and *B. oleracea* have the most complex and largest root systems among the species evaluated, with relatively larger values for six of the eight traits measured. In contrast, *B. nigra* had the smallest root systems. The two species *B. juncea* and *B. carinata* shared comparable root system complexity and had thicker root systems compared with the other species. In addition, 313 of the *Brassica* accessions were genotyped using a 19K *Brassica* single nucleotide polymorphism (SNP) array. After removing monomorphic and low-coverage site markers, markers with a minor allele frequency (MAF) ≤ 0.05 , and those missing data for $> 5\%$ of the accessions, a total of 6,213 SNP markers, comprising 5,103 markers on the A genome and 1,110 markers on the C genome, were selected for genome wide association studies (GWAS). These markers effectively covered genomic regions of 302.5 Mb for the A-genome and 452.8 Mb for the C-genome. Four mixed linear models (MLM), and two general linear models (GLM) were tested to identify the genomic regions and SNPs associated with the RSA traits. The GWAS identified 79 significant SNP markers associated with the eight root-related traits under investigation. These markers were distributed across the 18 chromosomes of *B. napus*, excluding chromosome C06. Sixty-five markers were located on the A-genome, while

14 were found on the C-genome. Furthermore, three specific genomic regions located on chromosomes A02, A03, and A06 were identified as hotspots containing genes associated with root traits. This work paves the way for additional research and exploration of these regions, offering new opportunities to deepen understanding of RSA traits and their genetic basis in the *Brassic*as.

Preface

I, Chunxiao Yang, affirm that this thesis is an original piece of work conducted by me. I carried out all experiments and wrote the first drafts of each thesis chapter. Dr. Stephen Strelkov, my supervisor, reviewed and revised all chapters and provided me with suggestions for improvement. Dr. Rudolph Fredua-Agyeman, a Senior Research Associate in our group, assisted with the data analysis and reviewed Chapter 3 prior to sharing it with Dr. Strelkov. I incorporated all of the suggested revisions. Once the draft thesis was completed, Dr. Strelkov and my Co-Supervisor, Dr. Sheau-Fang Hwang, approved it to proceed to defense.

The *Brassica* seeds utilized in this thesis were acquired originally from the Leibniz Institute of Plant Genetics and Crop Plant Research (IPK, Germany), and were multiplied by Dr. Fredua-Agyeman. Additionally, Dr. Linda Gorim (University of Alberta) provided me with guidance and mentorship with respect to the experimental design for Chapter 2. The phenotyping work described in Chapter 3 benefited from the support and contributions of two undergraduate students, Ms. Na Chen and Ms. Chenyu Wu, from the University of Alberta.

Funding for this research was provided by Results Driven Agriculture Research (RDAR), the Western Grains Research Foundation (WGRF) and Alberta Canola via Project No. 2021F063R, and by RDAR and the Canadian Agriculture Partnership (CAP) via Project No. 2022N029R. Dr. Strelkov as the Principal Investigator received these grants, with Drs. Fredua-Agyeman and Hwang as Co-Investigators. The University of Alberta provided in-kind support, including access to growth chambers and laboratory infrastructure.

Acknowledgements

I would like to express my deepest gratitude to my supervisors, Dr. Stephen Strelkov, and Dr. Sheau-Fang Hwang, for their unwavering support and encouragement throughout my MSc journey. I am grateful for their patience and dedication in helping me to refine my ideas, develop my research skills, and enhance my understanding of science.

I am also immensely grateful to Dr. Rudolph Fredua-Agyeman, who provided constant mentorship and support for my project. His expertise in plant molecular biology and genomics has been instrumental in shaping the direction of my thesis.

I would like to extend my sincere thanks to Dr. Linda Gorim, Assistant Professor and WGRF Chair in Cropping Systems, Department of Agricultural, Food and Nutritional Science (AFNS), for providing kind guidance for my research. I also would like to thank Dr. Malinda Thilakarathna, also of AFNS, for serving as my “arm’s length” examiner.

Special thanks go to two students, Ms. Na Chen and Ms. Chenyu Wu at the U of Alberta, who helped me conduct my experiments and complete my thesis successfully.

A special mention goes to my cat, Oliver, whose companionship has been a source of comfort and happiness during my late-night writing sessions and stressful moments.

Finally, I am eternally grateful to my parents Mr. Litao Yang and Ms. Yuye Han and my partner Mr. Shichen Hu for their unwavering love, understanding, patience, encouragement, and endless support as I pursued my dreams in life, and for always being there for me.

I would also like to acknowledge the financial support provided by Results Driven Agriculture Research (RDAR), the Canadian Agriculture Partnership (CAP), the Western Grains Research Foundation (WGRF), and Alberta Canola. The in-kind support from the U of Alberta is also gratefully acknowledged.

This thesis is dedicated to all those who have contributed to my growth as a young female researcher to the continued pursuit of knowledge in the fascinating field of science.

Table of Contents

Chapter 1: Introduction and Literature Review.....	1
1.1 The <i>Brassicas</i>	1
1.1.1 Introduction to the Genus <i>Brassica</i>	1
1.1.2 Origin, Taxonomy and Growing Regions.....	1
1.2 Roots.....	5
1.2.1 Introduction to the Root System and Root System Architecture (RSA).....	5
1.2.1 Importance of the Root System and Root System Architecture.....	6
1.2.2.1 General Functions of the Root System.....	7
1.2.2.2 Relationship between Root System Architecture and Abiotic Stress Tolerance....	8
1.2.2.3 Relationship between Root System Architecture and Biotic Stress Tolerance....	10
1.2.2.4 Root Architecture in the Brassicas.....	11
1.2.3 Phenotyping Root System Architectural Traits: Models, Technologies, and Challenges	12
1.2.3.1 Overview of Models for Root System Architecture Phenotyping.....	13
1.2.3.2 Overview of Technologies for RSA Phenotyping.....	14
1.3 Marker-based Approaches for Identifying Genes Controlling Root Architectural Traits..	16
1.3.1 Marker-Assisted Techniques for Identifying Genes of Interests.....	16
1.3.2 Linkage Disequilibrium-based Association Mapping and Genome-Wide Association Studies.....	18
1.3.3 Genetic Studies Associated with Root Architectural Traits in <i>Brassica</i> Crops.....	19
1.4 Thesis Objectives.....	21

Chapter 2: Optimizing the Evaluation of *Brassica* Root System Architectural Traits:

Determining the Ideal Timeframe.....	24
2.1 Introduction.....	24
2.2 Materials and Methods.....	25
2.2.1 Plant Materials	25
2.2.2 Scanning and Root Trait Measurement.....	26
2.3 Statistical Analyses	26
2.4 Results and Discussion	27
2.5 Conclusion	30

Chapter 3: Genome-wide Association Studies (GWAS) of Root Architectural Traits in A

Large Collection of <i>Brassica</i> Genotypes	36
3.1 Introduction.....	36
3.2 Materials and Methods.....	38
3.2.1. Plant Materials	38
3.2.2. Growth Conditions and RSA Trait Phenotyping	38
3.2.3. Statistical Analyses	39
3.2.4. SNP Genotyping	40
3.2.5. Linkage Disequilibrium Estimation.....	40
3.2.6. Bayesian Population Structure Analysis.....	41
3.2.7. Genome-wide Association Studies	41
3.2.8. Identification of Candidate Genes	41
3.3 Results.....	42

3.3.1 Phenotypic Variation for RSA Traits.....	42
3.3.2 Correlation Analysis Between Selected RSA Traits.....	42
3.3.3 Comparisons of RSA Traits Within and Among Species	43
3.3.3.1 Comparisons Among the Six Brassica Species	43
3.3.3.2 Comparisons Within the Six Brassica Species	44
3.3.4. SNP Genome Coverage and Marker Density	44
3.3.5. Estimation of Linkage Disequilibrium.....	45
3.3.6 Population Structure.....	45
3.3.7. Marker-RSA Trait Associations (MTA).....	45
3.3.8. Functions of Proteins Encoded by Significant Sequences	46
3.4 Discussion.....	46
3.5 Conclusion	51
Chapter 4: Conclusions	70
4.1 Introduction.....	70
4.2 Optimizing the Evaluation of <i>Brassica</i> Root System Architectural Traits.....	70
4.3 Evaluation of Root Architectural Traits in A Collection of <i>Brassica</i> Genotypes.....	71
4.4 Future studies	72
References	74

List of Tables

Table 2.1 Values for a suite of root system architecture traits in the <i>Brassica napus</i> cultivars ‘L255PC’, ‘Westar’, ‘L150’ and ‘Mendel’ as assessed with WinRHIZO software (Regent Instruments Inc., Quebec, Canada)	32
Table 2.2 Classification of the percentage of the total root length (% TRL), percentage total root surface area (% TRSA) and the percentage of the root volume (% Vol) falling into seven root diameter classes (0 – 0.5 mm, > 0.5 – 1.0 mm, > 1.0 – 1.5 mm, > 1.5 – 2.0 mm, > 2.0 – 2.5 mm, > 2.5 – 3.0 mm, > 3.0 – 3.5 mm) as assessed with WinRHIZO software (Regent Instruments Inc., Quebec, Canada)	33
Table 3.1 Summary and phenotypic variations of eight root system architectural traits in a collection of 379 <i>Brassica</i> genotypes representing <i>B. napus</i> , <i>B. oleracea</i> , <i>B. rapa</i> , <i>B. nigra</i> , <i>B. carinata</i> and <i>B. juncea</i>	53
Table 3.2 Least square means of eight root system architectural traits among six the <i>Brassica</i> species <i>B. napus</i> , <i>B. oleracea</i> , <i>B. rapa</i> , <i>B. nigra</i> , <i>B. carinata</i> and <i>B. juncea</i> based on Duncan’s test. Traits examined included total root length (TRL/cm), total surface area of roots (TRSA/cm ²), average root diameter (RAD/cm), number of tips (NTP), total primary root length (TPRL/cm), total lateral root length (TLRL/cm), total tertiary root length (TTRL/cm) and basal link length (BLL/cm)	54
Table 3.3 SNP marker density and extent of intra-chromosomal linkage disequilibrium in <i>Brassica napus</i> , <i>B. rapa</i> and <i>B. juncea</i> accessions used in genome-wide association studies for the determination of root architectural traits	55
Table 3.4 SNP markers in the <i>Brassica</i> species <i>B. napus</i> , <i>B. rapa</i> and <i>B. juncea</i> , including their chromosomal location and linkage association with root architectural traits	56

Table A1 List of 379 genotypes of <i>Brassica</i> used in the root system architecture studies under semi-hydroponic system	94
Table A1a Commercial lines	95
Table A1b <i>Brassica napus</i>	96
Table A1c <i>Brassica rapa</i>	98
Table A1d <i>Brassica juncea</i>	100
Table A1e <i>Brassica oleracea</i>	102
Table A1f <i>Brassica carinata</i>	104
Table A1g <i>Brassica nigra</i>	105

List of Figures

Figure 1.1 The Triangle of U showing the evolution and genetic relationships among the six most important <i>Brassica</i> species	23
Fig 2.1 A semi-hydroponic system for evaluation of root system architecture in <i>Brassica napus</i>	34
Fig 2.2 Representative roots of the <i>Brassica napus</i> cultivars ‘L255PC’, ‘Westar’, ‘L150’ and ‘Mendel’ after 7, 14 and 21 days in Hoagland’s solution	35
Figure 3.1 Correlation analysis between eight root system architecture (RSA) traits as determined by a Spearman rank-based variable correlation test	60
Figure 3.2 Scree plot explaining cumulative variance of the principal components	61
Figure 3.3. Scree plot for all variables of principal components 1 and 2	62
Figure 3.4 Principal components analysis (PCA) biplot among six <i>Brassica</i> species including <i>B. napus</i> , <i>B. oleracea</i> , <i>B. rapa</i> , <i>B. nigra</i> , <i>B. carinata</i> and <i>B. juncea</i>	63
Figure 3.5 Percentage of genotypes with small, medium, or large sized root systems in six <i>Brassica</i> species – <i>B. napus</i> (a), <i>B. juncea</i> (b), <i>B. rapa</i> (c), <i>B. nigra</i> (d), <i>B. oleracea</i> (e) and <i>B. carinata</i> (f)	64
Figure 3.6 Bar plot of eight root system architecture (RSA) traits among six <i>Brassica</i> species	65
Figure 3.7 Quantile-Quantile comparison of six GWAS models for identifying loci associated with root architecture (RSA) traits in 313 <i>Brassica</i> accessions representing five species, including <i>B. napus</i> , <i>B. oleracea</i> , <i>B. rapa</i> , <i>B. carinata</i> and <i>B. juncea</i>	66
Figure 3.8 Manhattan plots of the PCA + K MLM models for identifying root system architecture (RSA) trait loci in 313 <i>Brassica</i> accessions representing five species, including <i>B. napus</i> , <i>B. oleracea</i> , <i>B. rapa</i> , <i>B. carinata</i> and <i>B. juncea</i>	67

Figure 3.9 Bayesian cluster analysis of 313 *Brassica* accessions representing five species, including *B. napus*, *B. oleracea*, *B. rapa*, *B. carinata* and *B. juncea*, estimated with STRUCTURE based on 6,213 SNP markers using 50,000 burn-in iterations and Markov Chain Monte Carlo (MCMC) lengths 69

Figure A1a Quantile-Quantile comparison of GWAS model PCA + K for identifying loci associated with eight root architectural traits in 313 *Brassica* accessions representing five species *B. napus*, *B. oleracea*, *B. rapa*, *B. carinata* and *B. juncea* except *B. nigra*108

Figure A1b Quantile-Quantile comparison of GWAS model PCA + D for identifying loci associated with eight root architectural traits in 313 *Brassica* accessions representing five species *B. napus*, *B. oleracea*, *B. rapa*, *B. carinata* and *B. juncea* except *B. nigra* 110

Figure A1c Quantile-Quantile comparison of GWAS model Q + D for identifying loci associated with eight root architectural traits in 313 *Brassica* accessions representing five species *B. napus*, *B. oleracea*, *B. rapa*, *B. carinata* and *B. juncea* except *B. nigra* 112

Figure A1d Quantile-Quantile comparison of GWAS model Q + K for identifying loci associated with eight root architectural traits in 313 *Brassica* accessions representing five species *B. napus*, *B. oleracea*, *B. rapa*, *B. carinata* and *B. juncea* except *B. nigra* 114

Figure A1e Quantile-Quantile comparison of GWAS model PCA-only for identifying loci associated with eight root architectural traits in 313 *Brassica* accessions representing five species *B. napus*, *B. oleracea*, *B. rapa*, *B. carinata* and *B. juncea* except *B. nigra* 116

Figure A1f Quantile-Quantile comparison of GWAS model Q-only for identifying loci associated with eight root architectural traits in 313 *Brassica* accessions representing five species *B. napus*, *B. oleracea*, *B. rapa*, *B. carinata* and *B. juncea* except *B. nigra* 118

Figure A2a Manhattan plots of the PCA + D MLM models for identifying root architecture traits loci in 313 <i>Brassica</i> accessions representing five species <i>B. napus</i> , <i>B. oleracea</i> , <i>B. rapa</i> , <i>B. carinata</i> and <i>B. juncea</i>	120
Figure A2b Manhattan plots of the Q + D MLM models for identifying root architecture traits loci in 313 <i>Brassica</i> accessions representing five species <i>B. napus</i> , <i>B. oleracea</i> , <i>B. rapa</i> , <i>B. carinata</i> and <i>B. juncea</i>	122
Figure A2c Manhattan plots of the Q + K MLM models for identifying root architecture traits loci in 313 <i>Brassica</i> accessions representing five species <i>B. napus</i> , <i>B. oleracea</i> , <i>B. rapa</i> , <i>B. carinata</i> and <i>B. juncea</i>	124
Figure A2d Manhattan plots of the PCA-only GLM models for identifying root architecture traits loci in 313 <i>Brassica</i> accessions representing five species <i>B. napus</i> , <i>B. oleracea</i> , <i>B. rapa</i> , <i>B. carinata</i> and <i>B. juncea</i>	126
Figure A2e Manhattan plots of the Q-only GLM models for identifying root architecture traits loci in 313 <i>Brassica</i> accessions representing five species <i>B. napus</i> , <i>B. oleracea</i> , <i>B. rapa</i> , <i>B. carinata</i> and <i>B. juncea</i>	128
Figure A3 Plots of correlation coefficient (r^2) and physical distance (in Mb) for SNP markers on chromosomes A01 – A10 (a-j) and chromosomes C01 – C09 (k-s)	130

List of Abbreviations

Abbreviation	Definition
AFLP	Amplified fragment length polymorphism
AM	Association mapping
ARM	Armadillo
BLL	Basal link length
CAPS	Cleaved amplified polymorphic sequences
CCD	Canadian Clubroot Differential
ECD	European Clubroot Differential
GIP1	G-box-binding factor Interacting Protein 1
GLM	General linear models
GSLs	Glucosinolates
GWAS	Genome-wide association studies
LD	Linkage disequilibrium
LPR1	Low Phosphate Root 1
LRR	Leucine-rich repeat
MLM	Mixed linear models
MTA	Marker-traits association
N	Nitrogen
NAC	N-acetylcysteine
NB-ARC	Central nucleotide-binding
NTP	Number of tips
P	Phosphorus

PCA	Principal component analysis
QTLs	Quantitative trait loci
RAD	Average root diameter
RAPD	Random amplified polymorphic DNA
RFLP	Restriction fragment length polymorphism
RSA	Root system architecture
SAUR	Small auxin up-regulated RNA
SCAR	Sequence characterized amplified region
SNP	Single nucleotide polymorphism
SSR	Simple sequence repeat
STS	Sequence-tagged sites
TLRT	Total lateral root length
TPRL	Total tertiary root length
TRL	Total root length
TRSA	Total root surface area
TTRL	Total tertiary root length

Chapter 1: Introduction and Literature Review

1.1 The *Brassicaceae*

1.1.1 Introduction to the Genus *Brassica*

Brassica is the most economically important genus of the *Brassicaceae* family and includes many major cash crops grown worldwide. This genus shows significant genetic diversity and species are grown for use in condiments (brown mustard, white mustard), as oilseeds (canola, rapeseed), vegetables (cabbage, kale, broccoli), and soil conditioners (composting crops, green manure). *Brassica* species are also regarded as functional foods, with a long history of use in the prevention and treatment of cardiovascular and cancer disorders (Dixon, 2006). Genetic resources associated with the *Brassicaceae* include novel genes for stress tolerance, traits of agronomic importance, high seed and oil quality, and male sterility, all of which are important for long-term crop improvement (Sharma et al., 2022). Many *Brassica* species and other members of the *Brassicaceae*, such as *Arabidopsis thaliana* (L.) Heynh., can serve as models for research into plant systems because of their rapid life cycles and straightforward cultivation under lab and greenhouse conditions (Williams and Hill, 1986). The genus *Brassica* includes 37 species, six of which are widely grown: *B. napus* L., *B. rapa* L., *B. nigra* (L.) Koch, *B. oleracea* L., *B. juncea* (L.) Czern & Coss, and *B. carinata* A. Braun (Branca and Cartea, 2011). These species originated from the Mediterranean region of Europe and Asia, with the ancient Greeks, Romans, Indians, and Chinese all placing a high value on *Brassica* crops (Dixon, 2006).

1.1.2 Origin, Taxonomy and Growing Regions

The *Brassicaceae* includes 3709 species and 338 genera with a broad variety of morphologies and uses (Sharma et al., 2022). Taxonomic studies of the genus *Brassica* were initiated around 1700 by Tournefort and have continued since then (Branca and Cartea, 2011).

Numerous cytogenetic studies have been conducted over the past century to identify the genomes and evolutionary relationships among *B. napus*, *B. rapa*, *B. nigra*, *B. oleracea*, *B. juncea*, and *B. carinata* (Sharma et al., 2022). These relationships are illustrated in the well-known “Triangle of U” (Figure 1.1), first published by the Korean-Japanese botanist U in 1935. This triangle shows how the amphidiploid species *B. napus* (AACC, $n = 19$), *B. juncea* (AABB, $n = 18$), and *B. carinata* (BBCC, $n = 17$) resulted from interspecific hybridizations between the diploid species *B. rapa* (AA, $n = 10$) and *B. oleracea* (CC, $n = 9$), *B. rapa* and *B. nigra* (BB, $n = 8$), and *B. nigra* and *B. oleracea*, respectively.

Brassica rapa (A genome) originated in the Fertile Crescent in the high plateaus of the Middle East, where environmental conditions were hot and dry, resulting in fast growth and reproduction (Dixon, 2006). This species include numerous popular crops like turnips (mostly in Europe), Chinese cabbage (mostly in Asia), and some turnip rapes (oilseed crops in North America) (Branca and Cartea, 2011). In addition, *B. rapa* contains many weedy types, and hence is considered as a key candidate for studies to improve understanding of the basic genomics of weeds (Cardoza and Stewart, 2004).

Brassica nigra (B genome), also known as black mustard, is commonly cultivated for condiment and rapeseed oil production. This species originated in Eurasia but is now grown globally (Obayuwana and Obayuwana, 2022). With the highest output-to-input ratio among the *Brassicaceae*, *B. nigra* has been shown to be an energy-efficient plant, increasing its importance as a crop in addition to its medicinal benefits (Davydenko et al., 2018). Due to its short life cycle and copious pollen production, *B. nigra* is also regarded as an excellent model plant for research on pollination (Davydenko et al., 2018).

Brassica oleracea (C genome) includes a significant important group of extremely varied cash crops grown worldwide (Cardoza and Stewart, 2004). Wild *B. oleracea* was found in southern

and western Europe in the Middle Ages (Liu et al., 2014). Cultivated *B. oleracea* has diversified into 6 groups including *B. oleracea* var. *capitata* L. (cabbage), *B. oleracea* var. *acephala* L. (kale), *B. oleracea* var. *botrytis* L. (cauliflower), *B. oleracea* var. *italica* (broccoli), *B. oleracea* var. *alboglabra* L. (Chinese kale), *B. oleracea* var. *gongylodes* L. (kohlabi), and *B. oleracea* var. *gemmifera* (DC.) Zenker (Brussels sprouts) (Branca and Cartea, 2011). Its morphological diversity and ability to adapt to different environments contribute to the important role of *B. oleracea* in the human diet (Liu et al., 2014). The majority of *B. oleracea* crops also have significant protein and carotenoid content and produce a variety of glucosinolates (GSLs), which are phytochemicals involved in plant defence against bacterial and fungal diseases (Liu et al., 2014). This wide variation and high plasticity makes *B. oleracea* a good model for comparative genomics and evolutionary biology studies (Ayele et al., 2005; Wang et al., 2011; Yu et al., 2013).

Brassica napus (AACC), commonly known as oilseed rape or canola is the third most important oilseed crop worldwide, after soybean (28%) and oil palm (35%), and accounts for 13% of global oil production. Hu et al. (2021) estimated global yields of *B. napus* at approximately 75 million tons, grown across 37.58 million ha worldwide. This species arose through the spontaneous hybridization of *B. rapa* and *B. oleracea* (Nesi et al., 2008). The term “canola” is a trademark registered by the Canadian Canola Association in 1979, and refers to rapeseed cultivars producing seed oil with a low content of erucic acid (< 2%) and seed meal with a low concentration of aliphatic glucosinolates (< 30 $\mu\text{mol/g}$) (Raymer, 2002). It was bred to be an edible oil and is a good source of heart-healthy unsaturated fats, making it a nutritious choice for cooking and baking. The canola meal left over after extraction of the oil from the seeds is widely used as animal feed because it is high in amino acids and fibre, with a low glucosinolate content (So and Duncan, 2021). Several centers of origin have been reported for *B. napus*, including northern Europe, the Iran-Turanian region and the Mediterranean (Dixon, 2006).

The cultivation of *B. napus* started in Europe in the Middle Ages and spread globally (Chalhoub et al., 2014). Today, *B. napus* is an important cash crop cultivated across temperate and subtropical areas including Europe, China, South Asia, Australia and Canada (Neik et al., 2017). Depending on the need for vernalization, *B. napus* canola has three distinct growth types: spring, winter, and semi-winter (Ferreira et al., 1995; Rahman and McClean, 2013a; Arifuzzaman et al., 2019). Spring and winter types of canola varieties are genetically distinct (Diers and Osborn, 1994; Becker et al., 1995; Kebede et al., 2010). Other physical traits that set spring and winter types apart from one another include their different flowering times (Arifuzzaman et al., 2019). In comparison to spring canola, winter-type canola has bigger leaves, wider stem diameters, greater plant heights, more robust root systems, and better yields (Rahman and McClean, 2013a; Arifuzzaman et al., 2016, 2019; Arifuzzaman and Rahman, 2017).

Brassica juncea (AABB), also known as Indian or Chinese mustard, is mostly cultivated in temperate regions, and in some tropical or subtropical climates (Shekhawat et al., 2012). It originated in northwest India, with supplementary centers of diversity in western and central China, Burma, eastern India, the Near East and southern Iran (Kumar et al., 2011). This species is grown as an oilseed in India and as a leafy vegetable in China (Rakow, 2004). The seeds and vegetative tissue of Indian oilseed varieties contain 3-butenyl glucosinolate, whereas only trace levels of this compound and 2-propenyl (allyl) glucosinolate are present in the Chinese varieties (Rakow, 2004). In western nations, *B. juncea* is also cultivated for the production of condiment mustard (brown and oriental mustard), especially in western Canada (Rakow, 2004). It is also considered a weed in the United States, Fiji, Mexico, Australia and Argentina; in Canada, it is regarded as a potential weed (Kumar et al., 2011).

Brassica carinata (BBCC) is a crop that originated and is primarily cultivated in the Ethiopian highlands. It is believed to have developed through hybridization between wild or

cultivated *B. nigra* and kale (*B. oleracea* Acephala Group), as described by Rakow (2004). This versatile crop is grown both for its leafy vegetables and oil, and has recently gained attention as a promising source for biodiesel (Cardone et al., 2003). Despite its slow growth, *B. carinata* has demonstrated strong agronomic performance under unfavorable conditions, which can be attributed to the beneficial traits inherited from its parental species *B. nigra* and *B. oleracea* (Cardone et al., 2003).

1.2 Roots

1.2.1 Introduction to the Root System and Root System Architecture (RSA)

Roots are vital organs of vascular plants that grow underground and serve several critical functions, including water and nutrient uptake and anchorage. The root is composed of several distinct zones that each play a unique role in root growth and function. The root cap, located at the bottom of the root, serves two essential purposes: protecting the stem cell zone/meristems responsible for cell division and differentiation, and sensing environmental changes for soil penetration (Arnaud et al., 2010). The root apical meristem, where cell division takes place, is the source of undifferentiated cells that give rise to the adult root architecture, supporting continuous primary root growth and expansion (Perilli et al., 2012). In the elongation zone, cells that do not divide elongate rapidly, roughly ten-times faster than meristem cells (Baskin et al., 2020). The maturation zone is where cells undergo terminal differentiation and reach their full length (Cajero Sánchez et al., 2018).

The root system is divided into different parts based on morphological traits and functions. In dicots, the primary root system consists of taproots and lateral roots, while in monocots, the root system includes seminal roots, nodal roots, and their lateral roots (de Dorlodot et al., 2007). As such, two types of root systems have been defined for angiosperms: the taproot system, mostly found in dicots, and the fibrous system/adventitious root system, mostly found in monocots (Ito,

1996). Root system architecture (RSA) refers to the spatial arrangement of a plant's root system and is regulated by both endogenous genetic programs and environmental factors (Hodge, 2004; Malamy, 2005). The development of crops with improved RSA traits to efficiently acquire and conserve resources is a critical strategy for reducing costs in the agricultural supply chain. The RSA is significant because essential nutrients are unevenly distributed in the soil, and the spatial arrangement of a plant's roots largely determines its ability to store and transfer nutrients (Lynch, 1995; Robinson et al., 2018). Additionally, RSA plays a crucial role in supporting the shoot mechanically (Lynch, 1995). Individual plants generate different types of roots and RSA; the term heterorhizy is used to describe a plant producing roots that are morphologically distinct with different RSA traits (de Dorlodot et al., 2007). These morphological variations often correspond to physiological or functional variations, highlighting the importance of understanding RSA in improving crop yield and resource efficiency (de Dorlodot et al., 2007).

1.2.1 Importance of the Root System and Root System Architecture

The issue of global food security for a growing population is a mounting concern in the face of climate variability and global warming. Various unfavorable climatic factors such as excessive heat, salinity, acidity, drought, flooding, and frost, along with increased greenhouse gas levels and other mechanical impedances, negatively impact a plant's physiology and its quantitative and qualitative traits (Panjabi et al., 2019). Additionally, diseases and nutrient deficiencies can further impede a plant species' performance. RSA is influenced by various factors, including species, environmental cues such as nutrients, water, temperature, microbial activity, soil pH and chemicals, and pests, all of which can significantly affect the final RSA traits (Ingram and Malamy, 2010). A lack of resources in the soil area occupied by the root system is a significant barrier to plant productivity (Wang et al., 2017). Moreover, resources may exist in other parts of the soil that cannot be reached easily by some root systems, such as when nutrients leach beyond

the depth that roots can penetrate (Wang et al., 2017). Roots play a crucial role in water and nutrient uptake for plant growth, energy storage, and anchorage, making them an excellent model for studying developmental plasticity in plant responses to various environmental conditions (Ingram and Malamy, 2010; Paez-Garcia et al., 2015).

1.2.2.1 General Functions of the Root System

The primary functions of the root system are anchorage and resource uptake (Hodge et al., 2009a). Plants require sufficient nutrients and water from the soil to grow and produce a crop, necessitating an extensive root system in close proximity to a substantial amount of soil (Bengough et al., 2016). The uptake of nutrients and water is regulated by the demand of the shoot system in coordination with the root system (Engels and Marschner, 1992). Root hair cells facilitate the uptake of water from the soil through osmosis, and the water then diffuses and flows into the root cortex. The uptake of nutrients occurs through three pathways: root interception, mass flow, and diffusion (Barber, 1995; Waisel et al., 2002; Wang et al., 2006). Root interception occurs when roots grow towards nutrient-rich areas in the soil, and the amount of nutrients absorbed by the growing root is proportional to the quantity of nutrients in a soil volume equivalent to the root volume (Wang et al., 2006). The transfer of nutrients from the bulk soil to the root surface involves both mass flow and diffusion (Wang et al., 2006). The water potential gradient generated by roots absorbing water from the soil drives mass flow, which is the convective transfer of dissolved nutrients from the soil towards the root (Barber, 1995; Waisel et al., 2002; Wang et al., 2006).

Roots are vital for plant anchorage and growth, with the root hairs playing a particularly important role (Choi and Cho, 2019). Root hairs, which are outgrowths of the epidermal cells that increase the root surface area, absorb nutrients and water, penetrate soil particles, and interact with microbiomes (Grierson et al., 2014). Additionally, root hairs anchor individual root tips as they develop in soil pores, facilitating root penetration (Bengough et al., 2016). They also allow roots

to adhere to soil pore walls, reducing frictional resistance and axial cell wall tension, and enabling cavity expansion pressure (Bengough et al., 2016). Root hairs can increase the absorptive surface area of the root system by 2-3 fold, providing a high degree of developmental plasticity in response to drought and nutrient deficiency (Choi and Cho, 2019).

In mature plants with fully developed secondary root systems, lateral roots are primarily responsible for mechanical support (Bailey et al., 2002). For trees and woody plants, anchorage is primarily for root support and development, rather than resource absorption and acquisition below ground, while anchorage is a secondary function for smaller plant species (Choi and Cho, 2019).

1.2.2.2 Relationship between Root System Architecture and Abiotic Stress Tolerance

The response of crop plants to abiotic stresses is strongly influenced by their RSA. Nutrient and water uptake from the soil is a complex process that involves several abiotic interactions, and RSA is modulated when the intrinsic root developmental program perceives changes in the plant's nutritional status and external nutrient and water supply over time (Khan et al., 2016). Modulation of the root growth program occurs through changes in carbon allocation from the root to the shoot and/or initiation of signaling cascades involving hormones, RNAs, and proteins, among others (Fritsche-Neto and Borém, 2015). Certain RSA traits, such as longer primary roots (Wasson et al., 2012), a larger root diameter (Uga et al., 2013), abundant and steeper lateral roots (Lynch, 2013), and larger root cortical aerenchyma (Comas et al., 2013), can contribute to a deeper and stronger root system, increasing the radial hydraulic conductivity at depth and decreasing metabolic costs for drought adaptation (Khan et al., 2016). Similarly, root systems with abundant lateral roots (Richardson et al., 2009), longer root hairs (Lynch and Brown, 2001), many adventitious roots (Gruber et al., 2013; Forde, 2014), more aerenchyma (Chalhoub et al., 2014), and a high efficiency in the exudation of organic anions (Lynch, 2015) will exhibit higher tolerance to nutrient deficiency (Khan et al., 2016).

Reducing elongation of the main root (Munns and Tester, 2008) to decrease the transport of sodium from roots to shoots (Rus et al., 2006; Katori et al., 2010) and compartmentalizing sodium ions into the root vacuoles and steles (Gupta and Huang, 2014) can enhance the efficiency of water extraction and ion exclusion for salinity tolerance (Khan et al., 2016). Plants respond to abiotic stresses in diverse ways, depending on the type of stress they encounter. A plant's ability to take up water and nutrients from the soil is largely dependent on the depth of its roots (Lynch and Wojciechowski, 2015; Khan et al., 2016). The distribution of water and nutrients in the soil affects the development of lateral roots, which are a key determinant of RSA (Deak and Malamy, 2005; Postma and Lynch, 2011; Khan et al., 2016). For example, drought conditions can inhibit lateral root production in *Arabidopsis* by interacting with genes that regulate hormone signaling pathways (Deak and Malamy, 2005; Khan et al., 2016). In some root crops, such as sweet potato, the ability to produce lateral roots determines the yield of storage roots (Khan et al., 2016).

Root hairs, which project from the root epidermis, also play an important role in nutrient uptake (Tanaka et al., 2014). Higher nutrient absorption is associated with higher densities of both root hairs and lateral roots, especially in the topsoil (Postma et al., 2014; Khan et al., 2016). However, an increase in root hairs and lateral roots comes with a higher metabolic cost (Zhan et al., 2015; Khan et al., 2016).

Low levels of soil phosphate inhibit primary root growth but promote lateral root growth, resulting in a shallower root system (Khan et al., 2016). This can be detrimental under drought stress conditions, where deep roots are necessary to access water (Wasson et al., 2012; Khan et al., 2016). Similarly, genotypes with fewer but longer lateral roots have deeper roots, longer axial roots, and better nitrogen uptake than those with more lateral roots (Zhan and Lynch, 2015; Khan et al., 2016).

It is important to note that there is no one-size-fits-all solution to adapt to abiotic stresses, as plants often experience multiple stresses simultaneously in the field (Khan et al., 2016).

Therefore, it is essential to consider the specific circumstances of each stress when determining the best adaptation strategies for plants.

1.2.2.3 Relationship between Root System Architecture and Biotic Stress Tolerance

Most studies have focused primarily on exploring the relationship between RSA and abiotic stress tolerance, with relatively less emphasis on biotic stress tolerance. This is likely due to the fact that roots exhibit a high degree of flexibility in their responses to various environmental factors, making it particularly challenging to assess their unique characteristics and disease tolerance mechanisms in specific contexts (Snapp et al., 1995). Only a limited amount of research has been published on the relationship between RSA and disease resistance in crops, as noted by Desgroux et al. (2018). It is worth noting that there are variations in root branching and elongation rates between different plant genera, species, and cultivars within a species, as shown in several studies (Gabelman et al., 1986; Lynch and van Beem, 1993; Jackson, 1995; Leskovar and Stoffella, 1995; Zobel, 1995; Gallardo et al., 1996; Bingham and Bengough, 2003; Vercambre et al., 2003; Desgroux et al., 2018). However, some studies have demonstrated the impact of RSA traits on disease severity caused by soil-borne pathogens (Desgroux et al., 2018). For instance, it has been shown that leguminous plants such as common bean and pea exhibit resistance to *Fusarium* root rot when they have a larger average root diameter, a higher number and volume of lateral roots, or a higher root dry weight (Kraft and Boge, 2001; Snapp et al., 2003; Román-Avilés et al., 2004; Cichy et al., 2007; Hagerty et al., 2015; Desgroux et al., 2018). Pathogen infections can lead to a reduction in root density, potentially affecting the functional effectiveness of the remaining infected roots (Román-Avilés et al., 2004). In cases where the primary root dies because of infection, young roots emerging from the root-shoot transition zone may take on its role (Jackson,

1995). Promoting the growth of adventitious and lateral roots may also aid plant survival in roots infected by pathogens (Snapp et al., 2003).

Plants subjected to elevated levels of stress, in conjunction with indigenous soil-borne pathogens and other soil microorganisms, frequently exhibit greater development of adventitious roots when contrasted with plants grown under less stressful conditions. (Román-Avilés et al., 2004). Furthermore, many *Brassica* species are capable of producing chemical substances in their roots that can be toxic to soil-borne pathogens such as nematodes and fungi, as well as certain weeds (Admin, 2015). Therefore, having quantitative information on RSA linked to specific disease resistance could significantly enhance selection criteria in resistance-breeding programs.

1.2.2.4 Root Architecture in the *Brassic*s

Mustards such as *B. juncea* and *B. nigra* typically have fibrous roots (Admin, 2015), whereas crops such as *B. napus* (Arif et al., 2019), *B. rapa* (Admin, 2015), *B. oleracea* (Admin, 2015), and *B. carinata* (Barro and Martín, 1999) have a large taproot system with a single main root axis and lateral roots. Winter-type *Brassic*s are well-suited for collecting soil nitrogen (N) after the previous crop's harvest, given their rapid fall growth (Admin, 2015). In *Brassic*a species, there is a negative correlation between phosphorus (P) concentration and total root length (Hunter et al., 2014). P starvation has been shown to result in shorter primary roots and increased number and length of lateral roots in *B. napus* (Shi et al., 2013) and *B. oleracea* (Hammond et al., 2009; Wang et al., 2017). In many *Brassic*a species, increasing root architectural complexity is positively correlated with yield per unit P concentration in plant tissue (Hammond et al., 2004; Akhatar and Banga, 2015). However, within-species variation in *B. napus* suggests that the period of exposure to P deficiency is a factor influencing the yield, as this relationship was only observed in plants that had been exposed to P deficiency up until flowering (Marschner et al., 2007).

The primary root axes of oilseed rape often grow more centrally down biopores (voids formed by the activity of soil life) in the soil, relying on lateral roots to contact the biopore walls (Bengough et al., 2016). *B. juncea* is known for its ability to accumulate and withstand high concentrations of heavy metals in polluted soil due to up-regulation of proteins related to redox homeostasis, sulfur assimilation, and xenobiotic detoxification in the roots (Alvarez et al., 2009). *Brassica* species exhibit significant interspecific variation in salt tolerance, which can impair growth, seed yield, and oil production under salinity stress (Ashraf and McNeilly, 2004). Studies have shown that some *Brassica* crops exhibit reduced shoot/root ratios as an adaptation to salinity stress (Maggio et al., 2005; Arif et al., 2019). Many root architecture characteristics in *Brassica* are heritable, suggesting underlying genetic regulatory mechanisms that could be exploited in breeding programs (Shi et al., 2013). These features, however, are often under complex genetic regulation with significant environmental influences, despite their obvious phenotypic variation (Lynch, 2007).

1.2.3 Phenotyping Root System Architectural Traits: Models, Technologies, and Challenges

The breeding of plants with improved root traits has the potential to enhance stress tolerance and yields by facilitating their capacity to explore the soil and take up water and nutrients (Paez-Garcia et al., 2015). However, the subterranean nature of roots poses a challenge for breeders, as it is difficult to phenotype and select for specific root trait characteristics (Paez-Garcia et al., 2015). The study of RSA also has been hampered by a lack of consistent terminology, which has made communication difficult between researchers and among workers focused on different species (Zobel and Waisel, 2010). Moreover, the diverse range of terminologies used to describe RSA in different plant species and communities has led to the use of a wide variety of models and technologies, making it challenging to conduct cross-species comparisons (Pagès et al., 2014). Furthermore, the specific requirements for RSA studies vary widely across plant species, growth

stages, soil systems, environmental conditions, and parameters considered in specific studies, complicating the development of models that can be applied to investigate RSA in a broad range of crops (Pagès et al., 2014).

1.2.3.1 Overview of Models for Root System Architecture Phenotyping

Three-dimensional (3D) root system models that include both RSA traits and root-environment interactions are interesting because they provide information on the structural properties of the root system, location of roots underground, and various aspects of rhizosphere behavior and plant resource allocation. Unlike pure RSA models that focus only on RSA traits, such models provide a more comprehensive understanding of root system development.

The first 3D model, called "ROOTMAP," was developed by Diggle (1988) to project the fibrous root system of wheat. This model created a representation of the root system by updating it at discrete time-points and storing the locations of all root tips and branches in 3D coordinates until the specific growing time was attained. Although this model displayed the root tip number profiles and root length in pictorial and graphic formats by root branching order classes, it had some drawbacks, such as its significant memory and processing time (about 40 min) requirements.

Other models, such as "SimRoot" and "ArtRoot," were developed based on ROOTMAP. "SimRoot" differentiated itself from prior models by including a kinematic treatment of root axes and an explicit consideration of the spatial variability of physiological processes in the root system. In contrast, "ArtRoot" estimated and calculated the size of the entire root system by using data from the diameters of the roots connecting to shoots, the branching ratios, and the minimum branch diameters based on the "branching-rule" or "pipe-model."

To address dynamic interactions with soil variables and architectural qualities on resource uptake and root growth dynamics, Pagès et al. (2004) proposed a generic model called "Root Typ" that quantifies and analyzes RSA in a more representative way. However, the modeling of root

flexibility in response to environmental growth conditions remains challenging. Recently, more advanced models have been developed using programming languages such as Turbo Pascal, C, C++, Fortran, Java, Matlab, and Python (Jakobsen and Dexter, 1987; Diggle, 1988; Pagès et al., 2004; Le Bot et al., 2010; Schnepf et al., 2018). For instance, "PlanNet Maize" was created for whole-plant architecture studies including root and water flow in the vascular tissues of plants, while "OpenSimRoot," based on "SimRoot," is a functional-structural model that combined the soil system with root phenotypes to develop a mechanistic understanding at the whole-system scale.

To make models more widely applicable, "ArchiSimple" was proposed by Pagès et al. (2014) as a relatively straightforward and simple approach that models the diversity in RSA resulting from different plant species interacting with diverse environmental factors. This dynamic functional and architectural model divided the root system into collections of tiny segments and meristems, and calibrated and validated the diversity of RSA and the potential influence of those root traits on plant behavior more comprehensively and easily.

Although some models may be overly complex or specific to particular species or growing stages, root system models continue to evolve, providing greater insights into root system development, RSA traits, and interactions with the environment.

1.2.3.2 Overview of Technologies for RSA Phenotyping

In 1966, Newman introduced the 'line intersect' method for estimating total root length by counting the number of root intercepts in a regular space with total length lines that are randomly placed and orientated (Tennant, 1975). This method enabled an accurate and comprehensive assessment of root length in a root sample (Bouma et al., 2000). After several generations of improvement, this method, known as Tennant's statistical method, is still used by agronomists for measuring rooting depth and root length density (Smith et al., 2020). However, this method can be time-consuming, tedious, labour-intensive, and sometimes inaccurate, especially with a large

amount of fine roots, and it cannot directly measure root length or reveal certain details about RSA traits such as lateral branching, diameter, tip count, or growth rate (Smith et al., 2020). In recent years, the automated phenotyping of RSA via computer hardware or software has been extensively advanced (Wang and Zhang, 2009). Several software programmes, such as RootScan (Burton et al., 2012), RootReader3D (Clark et al., 2011), RootReader (Clark et al., 2013), RootSystemAnalyzer (Leitner et al., 2014), RootNav (Pound et al., 2013), RooTrak (Mairhofer et al., 2012), DART (Le Bot et al., 2010), GiA Roots (Galkovskyi et al., 2012), and IJ_Rhizo (Pierret et al., 2013), have been created for photographing roots and extracting quantitative information from the photos. More information regarding these software tools and models can be found online (www.plant-image-analysis.org) (Paez-Garcia et al., 2015).

When phenotyping a large amount of root material, choosing the most effective and economical approach is crucial (Pang et al., 2011). WinRHIZO (Régent Instruments Inc., Quebec, Canada) is a relatively efficient and cost-effective image tool for phenotyping and quantifying the root system of plants, which is widely used for root stress studies (Luc et al., 2006; Schwartz et al., 2010; Pang et al., 2011). Paired with root scanning, it can provide rapid and relatively accurate assessment of RSA, including root length, volume, average diameter, surface area, number of tips, crossings, and color analyses (Régent Instruments Inc.). Unlike other image analysis tools, WinRHIZO provides diameter distributions of the whole root system by identifying areas of root overlap and correcting them through its overlap algorithm, which assigns root lengths to specified diameter classes, offering a more complete RSA assessment (Arsenault et al., 1995). The software determines average diameter by dividing the projected area of the photographed root sample by its total length, and it derives total root length from a one-pixel thinned image by multiplying the number of pixels by pixel size, while the surface area is calculated through root length and diameter

(Wang and Zhang, 2009). Additionally, WinRHIZO's automated threshold can be adjusted to account for image contrast, making it a beneficial tool for routine scanning.

Selection of the best approach for culturing and phenotyping plants for quantification requires considering various parameters, including the specific root characteristics of interest (e.g., main roots vs. crown roots), preferred timescale for sampling (hours vs. days/months), infrastructure capability, and cost (Paez-Garcia et al., 2015). Nonetheless, the use of imaging software tools like WinRHIZO has revolutionized the study of root systems and enabled more comprehensive and accurate assessments of RSA traits.

1.3 Marker-based Approaches for Identifying Genes Controlling Root Architectural Traits

Knowledge of the molecular processes that drive root developmental flexibility is important for crop improvement (Hodge et al., 2009). Significant advances have been made in our understanding of the developmental mechanisms underlying root system architecture (RSA), along with the identification of several quantitative trait loci (QTLs) for root architectural features (Robinson et al., 2018). Plants have the ability to adjust the number of lateral root primordia they initiate and the rate at which their primary or lateral roots develop in response to environmental cues (Desgroux et al., 2018). RSA is therefore the result of several quantitative features that are regulated primarily by numerous loci (Desgroux et al., 2018; Hodge et al., 2009). To improve understanding of the interaction between genes and the environment, the RSA properties of a genotype can be examined in various controlled situations (Paez-Garcia et al., 2015) employing a variety of methods.

1.3.1 Marker-Assisted Techniques for Identifying Genes of Interests

Enhancement of *Brassica* germplasm requires the introduction of superior alleles related to disease resistance, oil content, and crop phenology, which would lead to improved agronomic performance and end-products (Akhtari and Banga, 2015). Research on natural plant populations

has made it possible to understand genetic exchange or gene flow within and across populations (Schaal et al., 1998; Yu et al., 2021). Marker-assisted studies of genetic diversity, including important quantitative features, offer a feasible way to establish the linkage between traits of interest and molecular markers (Akhtatar and Banga, 2015).

Marker-assisted selection (MAS) using DNA markers has the potential to increase the effectiveness and precision of conventional plant breeding. Many QTL mapping studies have been conducted for several crop species, resulting in an abundance of DNA marker-trait connections (Collard and Mackill, 2008). Various molecular markers, such as sequence characterized amplified region (SCAR), sequence-tagged sites (STS), random amplified polymorphic DNA (RAPD), amplified fragment length polymorphism (AFLP), cleaved amplified polymorphic sequences (CAPS), and restriction fragment length polymorphism (RFLP) markers, have been developed and widely used in crop improvement studies, usually in combination with gel electrophoresis for detection of the markers (Landry et al., 1992; Voorrips and Visser, 1993; Shan et al., 1999; Sanchez et al., 2000; Sharp et al., 2001; Piao et al., 2004; Saito et al., 2006; Suwabe et al., 2006; Collard and Mackill, 2008; Ueno et al., 2012; Zhang et al., 2014; Hasan and Rahman, 2016; Yu et al., 2021). These types of markers, however, have been largely supplanted in recent years by simple sequence repeat (SSR) and single nucleotide polymorphism (SNP) markers; these markers are now widely used due to their prevalence and co-dominant nature (Yu et al., 2021).

While SSRs are highly reliable, polymorphic, co-dominant, relatively cost-effective, and simple to use, they can produce sequence artifacts during PCR amplification due to errors associated with the formation of heteroduplexes and chimeric molecules and the activity of Taq DNA polymerase (Brakenhoff et al., 1991; Cline et al., 1996; Acinas et al., 2005; Yu et al., 2021). This can lead to difficulties in allele size calling and affect the quality of genotyping data (Kulibaba

and Liashenko, 2016; Yu et al., 2021). Moreover, SSRs can only provide information about a single locus per test and require polyacrylamide gel electrophoresis (Collard and Mackill, 2008).

Compared with SSRs, SNPs have several advantages, including higher heritability and a biallelic nature, which increases genotyping accuracy; SNP arrays can also be used to screen a large number of markers quickly and have high reproducibility and stability (Clarke et al., 2016; Yu et al., 2021). Bio-chipped SNPs offer fine resolution and ultra-high throughput discovery and detection (Syvänen, 2001; Mason et al., 2017). However, SNP calling for polyploid species such as *B. napus* can be difficult (Clarke et al., 2016; Yu et al., 2021). To avoid selection bias, it is important to use neutral or non-coding SNPs for genetic diversity studies. SNP arrays may also have limitations, such as being constrained to the variations originally utilized for array construction, which can introduce bias and miss rare alleles (Ganal et al., 2012; Mason et al., 2017). Therefore, it is crucial to validate SNP arrays thoroughly to ensure their suitability for widespread application (Yu et al., 2021).

1.3.2 Linkage Disequilibrium-based Association Mapping and Genome-Wide Association Studies

Association mapping (AM) is a reliable method for identifying marker-trait relationships based on linkage disequilibrium (LD). This approach takes advantage of the extensive historical recombination events in the evolutionary history of an association phylogenetic panel, which provides a way for association studies of historically measured traits (Akhtar and Banga, 2015). AM is the only method that allows for broad sampling from a population of interest, involving a diverse group of unrelated individuals (Jannink et al., 2001). This makes it a powerful tool for assessing the associations between multi-allelic markers and quantitative traits (Akhtar and Banga, 2015).

LD-based association mapping, such as genome-wide association studies (GWAS), offers significant advantages over conventional linkage-based association mapping (Gupta et al., 2014; Fredua-Agyeman et al., 2020). GWAS can be used to analyze genotypes from any crop species, without the need for ancestry or pedigree information for QTL mapping. Additionally, it captures higher allelic diversity, offers higher resolution, and can be used to analyze a variety of traits of interest. This approach is less costly and time-consuming than other methods, since it does not require the creation of a mapping population (Fredua-Agyeman et al., 2020).

It should be noted that AM has higher type I and type II error rates than biparental QTL mapping (Zondervan and Cardon, 2004). However, these errors can be minimized by incorporating the population structure of the association panel in the analysis (Pritchard et al., 2000; Flint-Garcia et al., 2003; Akhatar and Banga, 2015). On the other hand, GWAS filters out SNPs with minor alleles (5-10%), which limits its ability to detect small alleles (Brachi et al., 2011; Fredua-Agyeman et al., 2020). Overall, both AM and GWAS are useful methods for identifying marker-trait relationships, and the choice of which one to use depends on the specific research objectives and available resources.

1.3.3 Genetic Studies Associated with Root Architectural Traits in *Brassica* Crops

Breeding and research efforts have long been focused on identifying agronomic traits that contribute to higher yield and stress tolerance in the *Brassicac*s (Rahman and McClean, 2013). Among these traits, root system architecture (RSA) is particularly challenging to assess and breed for (Courtois et al., 2013). To overcome this challenge, indirect selection methods based on molecular markers linked to root traits have been suggested as a potential solution (Courtois et al., 2013). Recent studies on specific QTL associated with RSA have deepened understanding of the physiology and evolution of root traits and functions, which are important for developing RSA adapted to specific conditions (Ibrahim et al., 2021). As QTL for root traits often overlap with

those for productivity (water use, yield, or nutrient acquisition), the former may significantly affect the latter (Steele et al., 2006).

Despite the potential significance of RSA traits in crop productivity, only a limited number of genetic studies have been conducted on RSA traits in *Brassica* crops. These have been related mainly to the critical role of root traits in the uptake of nutrients such as boron, nitrogen, and phosphorus (Yang et al., 2010; Shi et al., 2013; Zhang et al., 2016; Ibrahim et al., 2021). The *Brassicac*s exhibit a high degree of genetic diversity, which, along with the phenotypic variation in their root systems, provides many opportunities for identifying genetic markers and loci associated with root system traits. The development of the *Brassica* 60-K Illumina SNP array has facilitated the genetic dissection of complex agronomic traits and greatly enabled the development of beneficial alleles in *Brassica* crops (Wang et al., 2019). In one of the first studies on canola, it was found that the root architecture of *B. napus* varies significantly depending on its developmental habits, with winter-type parents exhibiting a more vigorous root system controlled by three dominant genes. A strong positive correlation was also observed between root length and seed yield (Rahman and McClean, 2013).

Arifuzzaman et al. (2016) found a QTL mapping for root vigor on chromosome A01 (24.7 Mb) in rapeseed. The QTL region contained two candidate genes, G-box-binding factor Interacting Protein 1 (GIP1) and small auxin up-regulated RNA (SAUR)-like family proteins, associated with root growth and development in *B. napus*. Moreover, dynamic unconditional and conditional QTL mapping studies in rapeseed identified 28 stage-specific and 23 persistent QTL associated with root development, explaining from 5.1% to 36.2% of the genetic variation (Wang et al., 2019; Ibrahim et al., 2021). Despite the significant impact of root traits on productivity, only a limited number of genetic studies have focused on RSA traits in *Brassica* crops, especially the critical role

of root traits in nutrient uptake (Yang et al., 2010; Shi et al., 2013; Zhang et al., 2016; Ibrahim et al., 2021).

Researchers have identified several genes involved in root development that are located close to genetic regions linked to root-related characteristics or nutrient consumption efficiency in rapeseed (Ibrahim et al., 2021). For instance, Alock et al. (2018) found that genes regulating root and root hair development are located near genetic regions on QTL A10 associated with leaf P concentration (Fletcher et al., 2016; Ibrahim et al., 2021). Additionally, BnNRT2.1, a protein predominantly expressed in roots, can be up-regulated under low-N stress (Tong et al., 2020; Ibrahim et al., 2021). QTL mapping of *B. napus* under low-P conditions has revealed three distinctive QTL, uq.A1, uq.C3a, and uq.C3b, which were low-P specific. uq.C3a and uq.C3b were discovered specifically for root characteristics and P absorption under low-P stress and may help *B. napus* adapt to P deprivation (Yang et al., 2010). The confidence intervals of uq.C3a and uq.C3b contained two functional markers, BnIPS2-C3 and BnGPT1-C3, respectively, generated from the *Arabidopsis* genes AtIPS2 and AtGPT1 (Yang et al., 2010). In a recombinant inbred line (RIL) population of *A. thaliana* grown under low-P conditions, the QTL LPR1 (Low Phosphate Root 1) has been located to a 36-kb area on chromosome 1 (Svistoonoff et al., 2007).

Despite these findings, there is still a need for more in-depth genetic studies of RSA traits in the *Brassicaceae*. The identification of genes and QTL associated with root development and nutrient uptake efficiency in canola or rapeseed provides an opportunity to improve the RSA of this crop, potentially leading to increased yields and stress tolerance.

1.4 Thesis Objectives

The root system of *Brassica* crops is complex, and comparative studies that combine both morphological and genetic analyses of root architecture are limited. While previous work has highlighted the important role of root traits in nutrient uptake and the plasticity of RSA under stress,

only a few studies have focused on RSA in the *Brassic*s. Given the significance of the root system for plant growth and development, it is crucial to assess RSA traits thoroughly. The current study aims to increase knowledge of *Brassica* root systems by: (1) evaluating RSA traits of 379 *Brassica* accessions representing six species (*B. napus*, *B. juncea*, *B. carinata*, *B. oleracea*, *B. nigra* and *B. rapa*); and (2) identifying the genetic regions controlling RSA via a genome-wide association study (GWAS). The work presented in this thesis may contribute to the development of new and improved *Brassica* cultivars with improved root system architecture.

1.5 Figures

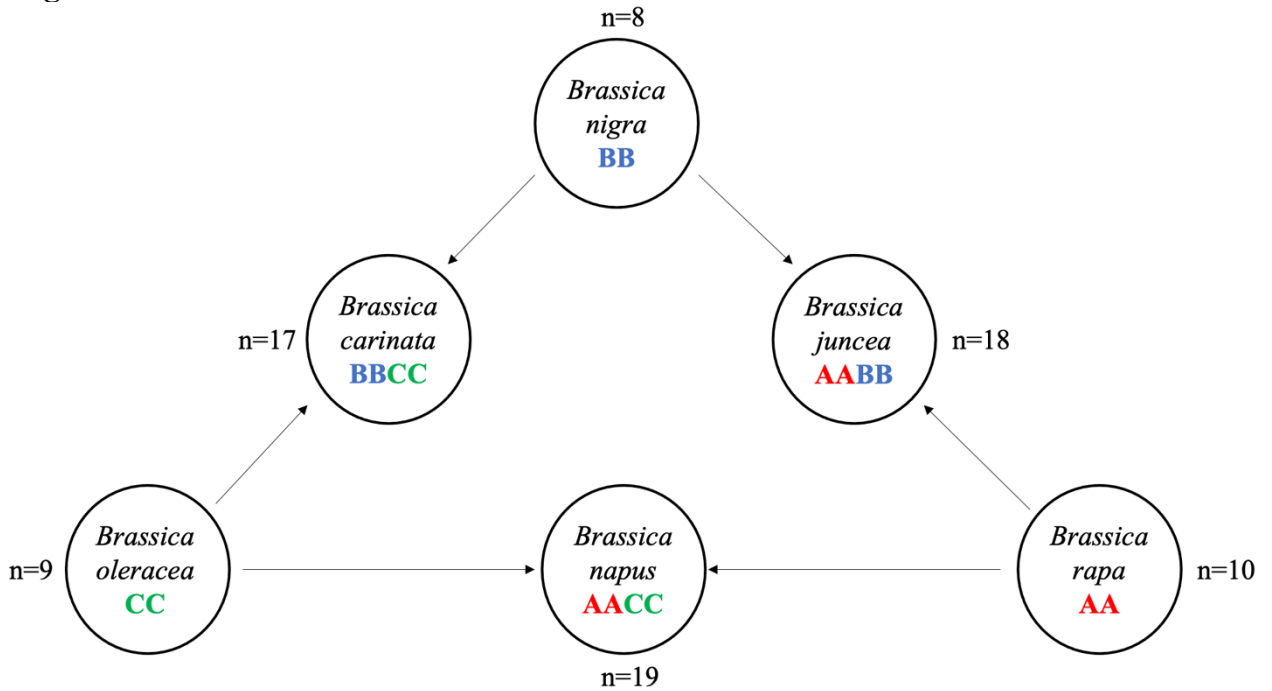


Figure 1.1 The Triangle of U showing the evolution and genetic relationships among the six most important *Brassica* species. The A (red), B (blue), and C (green) genomes are indicated in different colours; n represents the chromosome number.

Chapter 2: Optimizing the Evaluation of *Brassica* Root System Architectural Traits:

Determining the Ideal Timeframe

2.1 Introduction

Root system architecture (RSA) refers to the spatial structure of a root system, including its topology, distribution, and morphology in the growth medium (Lynch, 1995; Wang et al., 2019). Studies have shown that RSA traits such as surface area, root length, volume, and quantity of tips and forks play a crucial role in nutrient and water absorption (Zhao et al., 2004; Comas et al., 2013; Li et al., 2015; Gu et al., 2016; Wang et al., 2019). However, given the complexities involved in collecting undamaged roots and accurately phenotyping many samples, research on RSA traits is limited compared with other, aboveground agronomic traits (Meister et al., 2014). While several tools that combine photography and automated algorithms have been developed for RSA trait phenotyping in controlled environments (Armengaud et al., 2009; French et al., 2009; Clark et al., 2011; Basu and Pal, 2012), many researchers continue to use manual techniques like hand measuring or tracing roots (Clark et al., 2013). To address these issues, novel approaches are being developed to collect and extract phenotypes from a broader range of root systems with higher throughput (French et al., 2009).

Hydroponic systems are ideal for studying plant roots because they enable precise control over the growing conditions and allow for non-destructive sampling. These soilless systems are widely used in plant biology studies and for the commercial production of many high-value greenhouse crops (Nguyen et al., 2016). Different kinds of hydroponic or semi-hydroponic systems have been used to characterize RSA traits in several crop species, including maize (*Zea mays* L.) (Qiao et al., 2019), chickpea (*Cicer arietinum* L.) (Chen et al., 2017), narrow-leafed lupin (*Lupinus angustifolius* L.) (Chen et al., 2011, 2012, 2016), wheat (*Triticum aestivum* L.) (Chen et al., 2020;

Halder et al., 2021), barley (*Hordeum vulgare* L.) (Wang et al., 2021) and soybean (*Glycine max* L. Merr.) (Liu et al., 2021). The use of such systems, however, has been limited in studies with the *Brassicaceae*. The main objective of this study was to determine the optimal number of days required to measure RSA traits accurately in *Brassica napus* L. under semi-hydroponic conditions. To facilitate this objective, we also developed a modified semi-hydroponic system that is cost-effective, high-throughput, and suitable for the phenotyping of RSA in this species.

2.2 Materials and Methods

2.2.1 Plant Materials

A semi-hydroponic system was developed based on the ‘cigar roll’ system of Zhu et al. (2005). Briefly, seeds of four *B. napus* cultivars ‘L255PC’, ‘Westar’, ‘L150’ and ‘Mendel’ were pre-germinated on moistened filter paper in Petri dishes for 7 days (Fig 2.1a) and transferred to moist germination paper (approximately 25.4 cm × 30.5 cm in size) (Anchor Paper Company, St. Paul, USA) (Fig 2.1b). Four pre-germinated seedlings of relatively similar vigour were placed 2 cm from the edge of each piece of paper (Fig 2.1c) and the paper with the seeds was rolled up and secured with rubber bands (Fig 2.1d). Each experiment consisted of six germination paper rolls (i.e., 24 seedlings per cultivar) immersed in a 2 L beaker filled with 1 L of half-strength Hoagland’s No. 2 Basal Salt Mixture (Sigma-Aldrich Co., Ontario, Canada) solution (Fig 2.1e). The beakers were placed in a growth chamber under a 16 h photoperiod at 20°C (day)/18°C (night) (Fig 2.1f). Every 5 days, the paper rolls were removed so that the beakers could be sterilized with a diluted (1% v/v) bleach solution to minimize bacterial and fungal contamination. The beakers were then rinsed with sterile distilled water, refilled with fresh Hoagland’s solution, and the paper rolls placed back inside. The root systems were examined after 7, 14 and 21 days in the growth cabinet.

2.2.2 Scanning and Root Trait Measurement

Prior to root scanning, the germination paper was unrolled, and 16 plants of each cultivar were selected randomly for analysis (Fig 2.1g). The plant roots were excised and placed on a scanning tray, then gently spread apart using forceps. Roots were scanned in a Perfection V800 scanner (Epson, Markham, ON) using WinRHIZO (Regent Instruments Inc., Quebec, Canada) (Fig 2.1h). Software settings included “multi-thread”, “normal crossing detection and standard precision for root morphology measurements”, the “grey” channel and “Log” scale with “automatic” threshold for root and background detection. Eight basic parameters related to root architecture were quantified, including total root length (TRL/cm per plant), total root surface area (TRSA/cm² per plant), average root diameter (RAD/mm per plant), number of tips (NTP per plant), total primary root length (TPRL/cm per plant), total lateral root length (TLRT/cm per plant), total tertiary root length (TTRL/cm per plant), and basal link length (BLL/cm per plant). WinRHIZO software can also generate output categorizing the root parameters into different root diameter classes (Gorim and Vandenberg, 2017). Here, TRL, TRSA and volume (cm³) data were classified into seven root diameter classes (0 – 0.5 mm, > 0.5 – 1.0 mm, > 1.0 – 1.5 mm, > 1.5 – 2.0 mm, > 2.0 – 2.5 mm, > 2.5 – 3.0 mm, > 3.0 – 3.5 mm) and the percentage of the three root traits in each class was determined relative to the total TRL, TRSA and volume.

2.3 Statistical Analyses

Statistical analyses of the root trait data were conducted with R: A Language and Environment for Statistical Computing (R Foundation for Statistical Computing, Vienna, Austria). Duncan’s multiple test (Heinisch, 1962) was used to assess differences ($P \leq 0.05$) among mean root trait values and to quantify these differences among the *B. napus* cultivars.

2.4 Results and Discussion

Root systems play a critical role in determining the growth and productivity of *Brassicas* and other plants (Lynch, 1995). Digital scanning of the roots can provide valuable insights into their architecture, but it is important to determine the ideal timeframe for this analysis to ensure its accuracy and relevance. In this study, it was difficult to detect differences in the root morphology of the *B. napus* cultivars at 7 days of growth in the semi-hydroponic system, as the seedlings were still too small and undeveloped (Table 2.1; Fig. 2.2). By 14 days, however, the roots had undergone further growth, resulting in increased complexity and enabling clearer detection of differences among cultivars (Table 2.1; Fig. 2.2). Similarly, Li et al. (2020) found that while significant differences in root dry weight (g per plant) among different *B. napus* genotypes could be observed after 5 days of growth in a hydroponic system, more pronounced differences were detected after 15 days. Although the root systems in the current study had developed further by day 21 (Table 2.1; Fig. 2.1), extracting the roots without overlap proved difficult at this stage, due to the large amount of tissue. Moreover, despite regular replacement of the Hoagland's solution and disinfection of the beakers with bleach, mold contamination of the seedlings and germination paper became more common after 14 days.

As expected, TRL for all cultivars increased over time from 7 to 14 to 21 days (Table 2.1). While some differences could be detected among cultivars at all three time-points, most of the significant differences in TRL were observed at 21 days; at this time, 'L255PC' had the longest roots (355 cm), 'L150' and 'Mendel' had roots of intermediate length (333 and 246 cm, respectively), and 'Westar' had the shortest roots (221 cm). Similarly, in a comparison of the primary roots of 40 *B. napus* accessions, Dun et al. (2016) observed greater variation in primary root length at 10 and 18 days vs. 5 days under similar paper roll conditions. This suggests that differences in root length among genotypes become more pronounced over time. TPRL, TLRL

and TTRL also increased over the time-course, with the greatest differences among cultivars generally detected at 14 and/or 21 days (Table 2.1). Nonetheless, the relative ranking of each cultivar for some of these traits sometimes changed over time; for example, at 14 days, the longest TPRL was observed for 'L150', but by 21 days, TPRL for 'L255PC' and 'Mendel' was not significantly shorter (Table 2.1). This likely reflects differential development in specific *B. napus* genotypes, which may exhibit varying growth rates over time (Gabelman et al., 1986; Lynch and van Beem, 1993; Jackson, 1995; Leskovar and Stoffella, 1995; Zobel, 1995; Gallardo et al., 1996; Bingham and Bengough, 2003; Vercambre et al., 2003; Desgroux et al., 2018).

Most crop species have root systems characterized by low tissue densities (Lynch, 2007) and extensively branched architectures (Lynch, 2007; White et al., 2013), increasing the root surface area for highly efficient nutrient uptake (White et al., 2013; Hunter et al., 2014). In this study, TRSA was consistently lowest for 'Westar', which may reflect its older, open-pollinated nature resulting in reduced root generation. Indeed, 'Westar' showed the lowest values for many other traits as well (Table 2.1). The relative ranking of the cultivars with respect to the number of root tips changed over time, although by 21 days it was lowest in the other open-pollinated cultivar, 'Mendel'. In trees, root tip abundance was reported to change in response to environmental gradients (Wang et al. 2019), suggesting patterns of root tip adjustments with fine-root systems. Other studies have indicated that in winter oilseed rape (*B. napus*), root tip abundance, root length, root surface area, and volume per unit area decline after flowering (Li et al., 2017b). This decline may be attributed to the plant's allocation of resources primarily towards seed filling, a process that demands significant quantities of carbohydrates (Li et al., 2017b). Additionally, higher plant densities result in greater competition for resources, leading to a more rapid decline in root parameters (Li et al., 2017b). This suggests that root morphology is flexible and can adapt to changing environmental conditions and resource availability. In highly controlled semi-

hydroponic systems such as the one utilized in this study, however, variation in root tips per plant may be indicative of inherent genetic disparities, a phenomenon well-established in rice through comprehensive genome-wide expression analysis (Abdirad et al., 2022).

Basal roots originate from the base of the hypocotyl (Basu et al., 2007), establishing the foundational structure of the mature root system (Miguel et al., 2013; Rangarajan et al., 2018). The spatial distribution of basal roots plays a crucial role in determining their capacity to explore the soil and facilitate nutrient uptake (Basu et al., 2007; Miguel et al., 2013; Rangarajan et al., 2018). In this study, the length of the uppermost basal root was measured and recorded as the BLL. There were no significant differences in BLL among the cultivars at 7 days. At 14 days, no differences were detected between 'L150' (3.22 cm) and 'L255PC' (3.62 cm) or between 'Westar' (1.59 cm) and 'Mendel' (1.91 cm), but BLL was significantly shorter for the latter two cultivars. By 21 days, BLL in 'L255PC' (5.71 cm), 'L150' (5.31 cm) and 'Westar' (4.96 cm) was not significantly different, while it was shorter in 'Mendel' (3.54 cm). Similar results have been reported in common bean (*Phaseolus vulgaris* L.), wherein the basal roots emerged simultaneously in different genotypes but subsequent growth varied, resulting in variation in basal root lengths (Basu and Pal, 2011; Basu et al., 2011).

A noticeable decline in the overall magnitude of root length, surface area, and volume was observed as root diameter increased. The highest proportion of TRL, TRSA, and volume occurred in the 0-2.0 mm diameter class for all cultivars, and there were no roots thicker than 2.5 mm (Table 2.2). These findings indicate that most of the root system consisted of fine roots, increasing the efficiency of nutrient and water uptake (Liu et al., 2010). Gorim and Vandenberg (2017) documented similar findings when investigating the root morphology of five wild lentil species and *Lens culinaris* (Medik.) across three soil horizons. A larger proportion of root traits in lentil was observed within the smaller diameter classes, particularly those below 2.0 mm (Gorim and

Vandenberg, 2017). Additionally, in the current study, the variability in TRL, TRSA, and volume diminished as the root diameter increased (Table 2.2).

Classic hydroponic systems involve immersing the plant roots in a nutrient solution, which can either be continuously flowing or stationary and aerated with an air pump (Albery et al., 1985; Saraswathi et al., 2018). In semi-hydroponic systems, plants are grown in a soilless medium where the plant is self-watered via a reservoir (Saraswathi et al., 2018). In the semi-hydroponic system used in this study, based on the ‘cigar roll’ system of Zhu et al. (2005), plants were grown in paper rolls and absorbed the nutrient solution at the bottom of a beaker. The use of semi-hydroponic systems with paper rolls is highly advantageous when intact root systems need to be phenotyped; they provide more space for root development, while also safeguarding delicate root systems, particularly fine roots and root hairs, from damage. While the bottom of the germination paper rolls was soaked in Hoagland's solution, most of the rolls containing the roots were exposed to air, ensuring sufficient oxygen supply for the entire plant. In this study, the pre-germination of the seedlings in Petri dishes prior to transfer to the paper rolls ensured uniform germination and vigor, reducing artefacts associated with reduced viability or seedling growth. In addition, the semi-hydroponic system in this study did not require any specialized equipment or complex setup, as the paper rolls in beakers could be maintained in a regular growth room.

2.5 Conclusion

The genetic dissection and enhancement of RSA is hindered by the difficulties involved in precise and efficient root phenotyping. In this study, a semi-hydroponic system was utilized to optimize the evaluation of *B. napus* RSA traits, with a particular focus on determining the ideal timeframe for assessments. By conducting a comprehensive evaluation of various RSA traits and taking into account factors such as the ability to discern varietal differences and minimize

microbial contamination, it appears that assessing the roots after 14 days in Hoagland's solution yields accurate results within a reasonable timeframe.

2.5 Tables

Table 2.1 Values for a suite of root system architecture traits in the *Brassica napus* cultivars ‘L255PC’, ‘Westar’, ‘L150’ and ‘Mendel’ as assessed with WinRHIZO software (Regent Instruments Inc., Quebec, Canada).

Trait*	7 days				14 days				21 days				Optimum day(s) to scan**
	L255PC	Westar	L150	Mendel	L255PC	Westar	L150	Mendel	L255PC	Westar	L150	Mendel	
TRL	6.89 ^b	10.1 ^b	7.97 ^b	16.77 ^a	87.3 ^b	68.8 ^b	116.6 ^a	63.6 ^b	355 ^a	221 ^c	333 ^{ab}	246 ^{bc}	21
TRSA	0.73 ^b	0.9 ^b	0.85 ^b	1.85 ^a	9.32 ^{ab}	6.08 ^b	12.25 ^a	6.65 ^b	35.3 ^a	18.2 ^b	33.9 ^a	32.1 ^a	14
RAD	0.35 ^a	0.31 ^a	0.36 ^a	0.37 ^a	0.33 ^{ab}	0.28 ^b	0.33 ^{ab}	0.35 ^a	0.32 ^b	0.29 ^b	0.33 ^b	0.42 ^a	14
NTP	8.69 ^b	13.75 ^{ab}	17.62 ^{ab}	24.81 ^a	108.6 ^b	101.5 ^b	163.4 ^a	91.4 ^b	379 ^a	293 ^{ab}	340 ^{ab}	270 ^b	7/21
TPRL	4.45 ^b	6.94 ^a	5.03 ^b	6.74 ^a	12.8 ^b	12.7 ^b	19.3 ^a	12.8 ^b	39.5 ^a	29.6 ^b	35.9 ^{ab}	34.0 ^{ab}	21
TLRL	2 ^b	2 ^b	2.23 ^b	7.37 ^a	56.2 ^{ab}	45.9 ^b	74.2 ^a	38.9 ^b	142 ^a	117 ^a	143 ^a	116 ^a	14
TTRL	0 ^b	0.04 ^b	0.05 ^b	0.66 ^a	11.51 ^a	6.20 ^a	13.56 ^a	6.36 ^a	136.8 ^a	32.5 ^b	122.4 ^a	82.7 ^{ab}	21
BLL	0.42 ^a	0.59 ^a	0.57 ^a	0.53 ^a	3.22 ^a	1.59 ^b	3.62 ^a	1.91 ^b	5.71 ^a	4.96 ^a	5.31 ^a	3.54 ^b	14/21

*The estimated mean of each root architectural trait is indicated for each cultivar after 7, 14 and 21 days growth in a semi-hydroponic system. The traits include total root length (TRL/cm), total root surface area (TRSA/cm²), average root diameter (RAD/mm), number of tips (NTP), total primary root length (TPRL/cm), total lateral root length (TLRL/cm), total tertiary root length (TTRL/cm), and basal link length (BLL/cm). Values denoted by a different letter were significantly different ($P \leq 0.05$) between cultivars for a given time-point as determined by Duncan’s multiple range test.

**The optimum day to scan for a particular trait was determined based on the time-point at which most of the significant differences could be detected for that trait (i.e., sufficient time allowed for the roots to develop so that the differences could most easily be detected); ND, no differences detected on any of the sampled days.

Table 2.2 Classification of the percentage of the total root length (% TRL), percentage total root surface area (% TRSA) and the percentage of the root volume (% Vol) falling into seven root diameter classes (0 – 0.5 mm, > 0.5 – 1.0 mm, > 1.0 – 1.5 mm, > 1.5 – 2.0 mm, > 2.0 – 2.5 mm, > 2.5 – 3.0 mm, > 3.0 – 3.5 mm) as assessed with WinRHIZO software (Regent Instruments Inc., Quebec, Canada).

Trait	7 days				14 days				21 days			
	L255PC*	Westar	L150	Mendel	L255PC	Westar	L150	Mendel	L255PC	Westar	L150	Mendel
% TRL 0-0.5	88.4 ^a	91.1 ^a	88.5 ^a	84.2 ^a	91.6 ^{ab}	96.7 ^a	92.7 ^{ab}	89.1 ^b	88.8 ^a	95.3 ^a	87.7 ^a	75.1 ^b
% TRL >0.5-1.0	10.5 ^{ab}	7.87 ^b	10.16 ^{ab}	15.01 ^a	8.18 ^{ab}	2.95 ^b	6.92 ^{ab}	10.30 ^a	10.9 ^b	4.4 ^b	12.1 ^b	24.3 ^a
% TRL >1.0-1.5	1.08 ^a	1.03 ^a	1.26 ^a	0.78 ^a	0.18 ^b	0.36 ^{ab}	0.26 ^{ab}	0.52 ^a	0.25 ^{ab}	0.27 ^{ab}	0.18 ^b	0.5 ^a
% TRL >1.5-2.0	0 ^a	0 ^a	0.04 ^a	0.05 ^a	0.01 ^a	0.03 ^a	0.07 ^a	0.05 ^a	0.06 ^{ab}	0.02 ^b	0.04 ^{ab}	0.08 ^a
% TRL >2.0-2.5	0 ^a	0 ^a	0 ^a	0 ^a	0 ^a	0 ^a	0 ^a	0 ^a	0.0 ^a	0 ^a	0 ^a	0.02 ^a
% TRL >2.5-3.0	0 ^a	0 ^a	0 ^a	0 ^a	0 ^a	0 ^a	0 ^a	0 ^a	0 ^a	0 ^a	0 ^a	0 ^a
% TRL >3.0-3.5	0 ^a	0 ^a	0 ^a	0 ^a	0 ^a	0 ^a	0 ^a	0 ^a	0 ^a	0 ^a	0 ^a	0 ^a
% TRSA 0-0.5	75.8 ^a	79.1 ^a	77.0 ^a	71.3 ^a	85.9 ^{ab}	91.9 ^a	86.5 ^{ab}	80.3 ^b	78.3 ^a	89.7 ^a	77.8 ^a	62.0 ^b
% TRSA >0.5-1.0	20.7 ^a	17 ^a	18.6 ^a	25.8 ^a	13.42 ^{ab}	6.53 ^b	12.04 ^{ab}	17.55 ^a	20.28 ^b	8.89 ^b	21.21 ^b	36.17 ^a
% TRSA >1.0-1.5	3.53 ^a	3.98 ^a	4.22 ^a	2.68 ^a	0.65 ^b	1.42 ^{ab}	1.057 ^{ab}	1.88 ^a	1.03 ^a	1.25 ^a	0.7 ^a	1.39 ^a
% TRSA >1.5-2.0	0 ^a	0 ^a	0.186 ^a	0.23 ^a	0.04 ^a	0.12 ^a	0.36 ^a	0.24 ^a	0.32 ^a	0.15 ^a	0.25 ^a	0.32 ^a
% TRSA >2.0-2.5	0 ^a	0 ^a	0 ^a	0 ^a	0 ^a	0 ^a	0 ^a	0 ^a	0.02 ^a	0.02 ^a	0.06 ^a	0.10 ^a
% TRSA >2.5-3.0	0 ^a	0 ^a	0 ^a	0 ^a	0 ^a	0 ^a	0 ^a	0 ^a	0 ^a	0 ^a	0 ^a	0 ^a
% TRSA >3.0-3.5	0 ^a	0 ^a	0 ^a	0 ^a	0 ^a	0 ^a	0 ^a	0 ^a	0 ^a	0 ^a	0 ^a	0 ^a
% Vol 0-0.5	57.4 ^a	59.4 ^a	59.1 ^a	55.5 ^a	77.5 ^{ab}	80.5 ^a	76.5 ^{ab}	67.3 ^b	64.3 ^{ab}	79.2 ^a	64.2 ^{ab}	48.5 ^b
% Vol >0.5-1.0	34.1 ^a	29.1 ^a	29.2 ^a	36.5 ^a	20.1 ^a	14.3 ^a	18.2 ^a	25.8 ^a	30.7 ^b	15.2 ^c	31.8 ^{ab}	46.6 ^a
% Vol >1.0-1.5	8.55 ^a	11.36 ^a	10.85 ^a	7.26 ^a	2.16 ^b	4.74 ^{ab}	3.59 ^{ab}	5.77 ^a	3.45 ^a	4.65 ^a	2.24 ^a	3.32 ^a
% Vol >1.5-2.0	0 ^a	0 ^a	0.56 ^a	0.82 ^a	0.16 ^b	0.45 ^{ab}	1.66 ^a	1.09 ^{ab}	1.41 ^a	0.82 ^a	1.33 ^a	1.11 ^a
% Vol >2.0-2.5	0 ^a	0 ^a	0 ^a	0 ^a	0 ^a	0 ^a	0 ^a	0 ^a	0.106 ^a	0.13 ^a	0.30 ^a	0.42 ^a
% Vol >2.5-3.0	0 ^a	0 ^a	0 ^a	0 ^a	0 ^a	0 ^a	0 ^a	0 ^a	0 ^a	0 ^a	0 ^a	0 ^a
% Vol >3.0-3.5	0 ^a	0 ^a	0 ^a	0 ^a	0 ^a	0 ^a	0 ^a	0 ^a	0 ^a	0 ^a	0 ^a	0 ^a

*Four canola (*Brassica napus*) cultivars ('L255PC', 'Westar', 'L150' and 'Mendel') were assessed after 7, 14 and 21 days growth in a semi-hydroponic system.

2.7 Figures

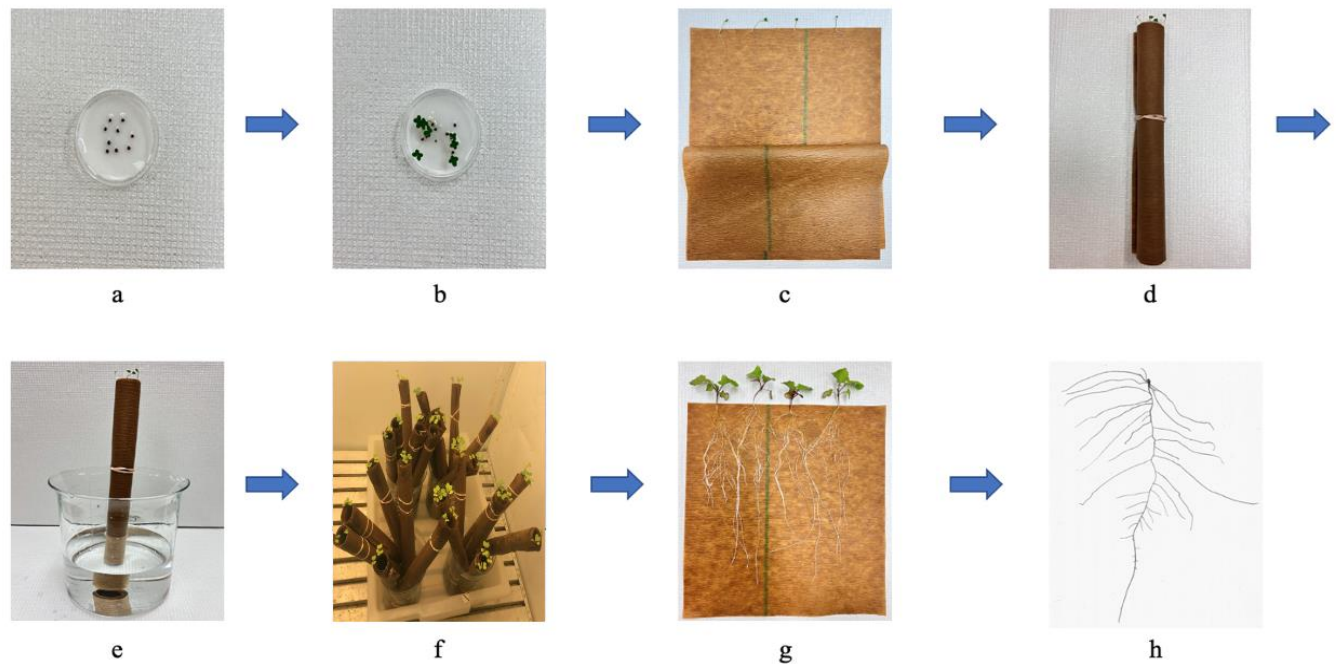


Fig 2.1 A semi-hydroponic system for evaluation of root system architecture in *Brassica napus*. (a, b) Seeds were pre-germinated on wet filter paper in Petri dishes for 7 days; (c) four pre-germinated seedlings of relatively similar vigour were placed 2 cm from the edge of each wet germination paper (approximately 25.4 cm × 30.5 cm in size); (d) the paper was rolled up and secured with rubber bands; (e) the rolls of paper were placed in a beaker containing 2 L of half-strength Hoagland's No. 2 Basal Salt Mixture solution (f) and maintained in a growth chamber under a 16 h photoperiod (20°C/18°C); (g) the paper was unrolled at the desired time-points and plants were selected at random for root phenotyping; and (h) root architecture was phenotyped on a Perfection V800 (Epson) scanner with WinRHIZO software (Regent Instruments Inc., Quebec, Canada).

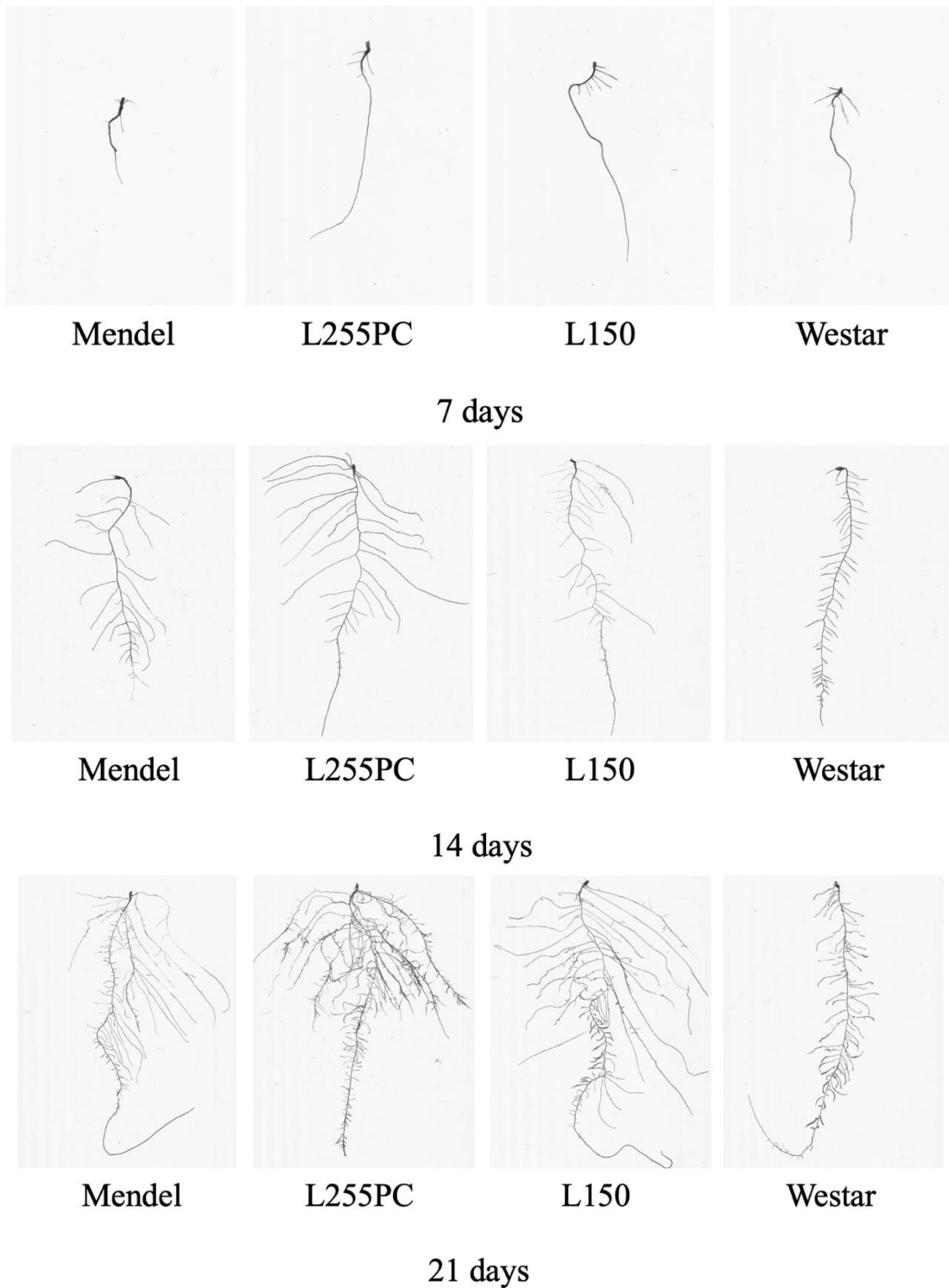


Fig 2.2 Representative roots of the *Brassica napus* cultivars ‘L255PC’, ‘Westar’, ‘L150’ and ‘Mendel’ after 7, 14 and 21 days in Hoagland’s solution. Root architecture was phenotyped in a Perfection V800 (Epson) scanner with WinRHIZO software (Regent Instruments Inc., Quebec, Canada).

Chapter 3: Genome-wide Association Studies (GWAS) of Root Architectural Traits in A Large Collection of *Brassica* Genotypes

3.1 Introduction

Roots are a fundamental component of the plant vascular system, playing a pivotal role in the plant's growth, development, and overall survival. Their primary function lies in absorbing water and nutrients from the soil, but they also serve as an anchor, firmly securing the plant to the ground and ensuring stability and support. Additionally, roots store valuable resources, safeguarding them for future use. The development of a root system is an important quantitative characteristic that determines a plant's capacity to survive across different environments. Improved understanding of the behavior of roots within natural ecosystems is of significance for enhancing crop yields, developing more resilient plant varieties, and preserving biodiversity (Griffiths et al., 2022).

The genus *Brassica* consists of 37 species including the widely cultivated *B. napus* L. (AACC, n = 19), *B. rapa* L. (AA, n = 10), *B. nigra* (L.) Koch (BB, n = 8), *B. oleracea* L. (CC, n = 9), *B. juncea* (L.) Czern & Coss (AABB, n = 18), and *B. carinata* A. Braun (BBCC, n = 17) (Branca and Cartea, 2011). Most *B. juncea* and *B. nigra* genotypes have fibrous roots (Admin, 2015), while *B. napus* (Arif et al., 2019), *B. rapa* (Admin, 2015), *B. oleracea* (Admin, 2015) and *B. carinata* (Barro and Martín, 1999) have a large taproot system with a single main root axis and hundreds of lateral roots. Several root system architecture (RSA) traits have been identified as having heritable characteristics in certain crops, suggesting the presence of genetic regulatory mechanisms that may be exploited in breeding programs (Shi et al., 2013). However, despite the apparent phenotypic differences that can make screening relatively straightforward, many of these features appear subject to complex genetic regulation with significant environmental influences (Lynch, 2007).

The use of root phenomics as a crop breeding technique is on the rise (Kuijken et al., 2015; Prince et al., 2019; Falk et al., 2020; Liu et al., 2021). Plant breeding programs that aim to alter root traits have the potential to generate *Brassica* crops with increased stress tolerance and yields, enhancing the ability of roots to explore the soil and acquire water and nutrients (Paez-Garcia et al., 2015). Despite the importance of roots, however, direct selection for optimal RSA traits has not been widely implemented (Zhu et al., 2011). The complexity of the root system has limited the scope of comparative studies that include morphological analyses of the root systems of *Brassica* crops (de Dorlodot et al., 2007; Meister et al., 2014; Ibrahim et al., 2021). By improving understanding of RSA and the underlying pathways that shape it, researchers can leverage diverse root features to help plants respond to climate change and enhance crop yields (Smith and De Smet, 2012; Ibrahim et al., 2021).

Genome-wide association mapping (GWAS) is a method that utilizes single nucleotide polymorphism (SNP) markers to analyze recombination events at the gene level in natural populations. It is based on the concept of linkage disequilibrium (LD). This approach offers notable advantages compared with traditional linkage-based association mapping (Gupta, 2016; Fredua-Agyeman et al., 2020). GWAS enables the exploration of a broader range of allelic diversity, providing enhanced resolution for analyzing various traits of interest. Moreover, it offers the opportunity to examine genotypes across different crop species, eliminating the need for ancestry or pedigree data typically required in quantitative trait locus (QTL) mapping (Fredua-Agyeman et al., 2020). However, genetic studies focusing on RSA have been relatively scarce relative to research on aboveground traits (de Dorlodot et al., 2007; Meister et al., 2014; Ibrahim et al., 2021). Most studies conducted on *Brassica* crops have emphasized the significance of root traits in nutrient uptake (Yang et al., 2010; Shi et al., 2013; Zhang et al., 2016; Ibrahim et al., 2021). For instance, chromosomal regions associated with leaf phosphorus concentration have been

identified to harbor multiple genes that influence root and root hair development (Alcock et al., 2018).

Genetic variability in plants serves as a fundamental component of biodiversity and serves as the foundation for the creation of novel and enhanced cultivars with desirable traits (Govindaraj et al., 2015; Yu et al., 2021). Increasing the genetic diversity in *Brassica* genotypes is a crucial goal in plant breeding. Considering the critical roles of root systems in plant growth and development, it is important to evaluate RSA-related traits as well as to identify the genetic regions associated with these traits. Accordingly, the objectives of this study were to (1) evaluate the RSA traits of a large collection of *Brassica* accessions representing *B. napus*, *B. juncea*, *B. carinata*, *B. oleracea*, *B. nigra* and *B. rapa*; and (2) identify the genomic regions controlling RSA via GWAS.

3.2 Materials and Methods

3.2.1. Plant Materials

Three hundred and seventy-nine genotypes comprising 68 *B. napus*, 64 *B. juncea*, 60 *B. rapa*, 66 *B. nigra*, 55 *B. oleracea* and 28 *B. carinata* accessions obtained from the Leibniz Institute of Plant Genetics and Crop Plant Research (IPK), Gatersleben, Germany (Table A1a-A1g), were included in the analysis. In addition, 25 Canadian canola (*B. napus*) cultivars and the 13 hosts of the Canadian Clubroot Differential (CCD; Strelkov et al., 2018) set were also phenotyped for RSA-related traits. The IPK accessions were multiplied under greenhouse conditions at the Crop Diversification Centre North (CDCN), Alberta Agriculture and Irrigation, Edmonton, Canada.

3.2.2. Growth Conditions and RSA Trait Phenotyping

Seven-day-old seedlings, pre-germinated in Petri dishes, were transferred to a semi-hydroponic system consisting of rolls of germination paper (Anchor Paper Company, St. Paul, USA) immersed in 2 L beakers filled with 1 L of half-strength Hoagland's No. 2 Basal Salt Mixture

solution (Sigma-Aldrich Co., Ontario, Canada) as described in Chapter 2. The seedlings were maintained in a growth chamber under a 16 h photoperiod at 20°C (day)/18°C (night) and removed from the germination paper after 14-days to measure RSA related-traits. The roots of each plant were cut, placed on a scanning tray, and spread apart with forceps. Root scanning were scanned with an EPSON Perfection V800 scanner (Epson, Markham, ON) and analyzed with WinRHIZO software (Regent Instruments Inc., Quebec, Canada) using the automatic global threshold for root and background detection method. Twenty-nine RSA-related traits were recorded per root scan, but only eight showed significant variation within and among species and hence were retained for GWAS. The eight traits included (1) total root length (TRL/cm), (2) total surface area of roots (TRSA/cm²), (3) average root diameter (RAD/cm), (4) number of tips (NTP), (5) total primary root length (TPRL/cm), (6) total lateral root length (TLRL/cm), (7) total tertiary root length (TTRL/cm) and (8) basal link length (BLL/cm) (Table 3.1). The experiment was repeated four times with four replicates per treatment.

3.2.3. Statistical Analyses

Analysis of the RSA trait data was conducted with R 4.0.2: A Language and Environment for Statistical Computing (R Foundation for Statistical Computing, Vienna, Austria). Because repetition \times treatment was not significant, the data were pooled across the four repeats for the experiment. Duncan's multiple range test (Duncan, 1955) and the bar plot of each trait were generated to test ($P \leq 0.05$) for differences in the mean root trait values among the six *Brassica* species. The Anderson-Darling test was performed to test the normality of the eight traits. The Spearman rank-based variable correlation test was conducted using the *cor* function to determine the correlation between the eight traits ($p < 0.05$). Principal component analysis (PCA) was carried out using the *prcomp* function on the eight variables. As a normal distribution is not required for PCA, no transformation of the data was performed prior to analysis (Jolliffe, 1986).

3.2.4. SNP Genotyping

SNP genotyping was performed on 313 of the 379 *Brassica* accessions (except for the 66 *B. nigra* accessions) using the *Brassica* 19K SNP array from TraitGenetics GmbH (Gatersleben, Germany) following the manufacturer's instructions. This array comprised 9,310 SNP markers on the A-genome, 8,072 SNP markers on the C-genome and 1,154 SNP markers on scaffolds. None of SNP markers on the array was from the B-genome. Therefore, the *B. nigra* accessions were not genotyped. After discarding monomorphic, low coverage site markers, markers with $MAF \leq 0.05$ and those missing data for $> 5\%$ of the accessions, 6,213 SNP markers, comprising 5,103 A-genome and 1,110 C-genome markers were used for GWAS analyses. The average inter-SNP marker distance was determined for each chromosome (Table 3.3).

3.2.5. Linkage Disequilibrium Estimation

The genetic basis of the diversity among the RSA related-traits detected as linkage disequilibrium (LD) between allelic values at two loci was estimated using Pearson's squared correlation coefficient (r^2) statistic with TASSEL 5 v5.2.2.5 (Bradbury et al., 2007). The decay and extent of LD was determined by calculating the Chi-square (χ^2) statistic for each SNP pair following Fredua-Agyeman et al. (2020). In brief, the r^2 -values of significant (p -value < 0.001) SNP marker pairs was plotted against the physical distance (in Mb) for each chromosome using the PROC GPLOT procedure in SAS v. 9.4 (SAS Institute, Cary NC, North Carolina, U.S.). The PROC TRANSREG function in SAS was then used to obtain a LD decay curve for each chromosome. Additionally, the intersection between the fitted curve and the r^2 threshold line was determined and projected onto the physical distance axis to obtain the average extent of LD for each chromosome (Breseghello and Sorrells, 2006; Bellucci et al., 2015) (Table 3.3, Figure A3).

3.2.6. Bayesian Population Structure Analysis

Population structure (Θ) was determined using the admixture and allele frequency correlated models and burn-in lengths from 5,000 to 100,000 iterations and Markov Chain Monte Carlo (MCMC) run lengths from 5,000 to 100,000 permutations using *STRUCTURE* v2.3.4 (Pritchard et al., 2000). Runs for each cluster ($K = 1-10$) were replicated 10 times. The number of clusters was determined using the ΔK statistics of Evanno et al. (Evanno et al., 2005) and the MedMedK, MedMeaK, MaxMedK and MaxMeaK statistics of Puechmaille (Puechmaille, 2016) and Li and Liu (Li and Liu, 2018). The many *STRUCTURE* runs were required to reach the convergence necessary for accurate determination of the population structure in the GWAS.

3.2.7. Genome-wide Association Studies

Two general linear models (GLM) and four mixed linear models (MLM) implemented in TASSEL 5.0 (Bradbury et al., 2007) were tested in the marker-trait association studies using the 6,213 SNP marker data and the mean ID values of each of the eight RSA related-traits. For each model, quality marker-RSA related-trait associations (Table 3.4) were determined only if the observed quantile-quantile (Q-Q) plot showed the least amount of deviation from the expected $-\log_{10}P$ -value (Figure 3.7, Figure A1). Manhattan plots were generated to represent (MTAs) (Figure 3.8, Figure A2). Significant SNP markers associated with the RSA related-traits were identified using the Bonferroni correction, i.e., p -value cut-off at $0.05/\text{total number of markers}$ (Benjamini and Hochberg, 1995). Stable MTAs detected by the different models and pleiotropic SNPs associated with the different RSA traits were considered credible.

3.2.8. Identification of Candidate Genes

To identify candidate genes associated with significant SNP markers, the SNP sequences were used in BLASTN searches of *B. rapa* (AA), *B. oleracea* (CC), *B. napus* (AACC), and *Arabidopsis thaliana* genome assemblies in the EnsemblPlants

(<https://plants.ensembl.org/Multi/Tools/Blast>) and National Centre for Biotechnology Information (<https://blast.ncbi.nlm.nih.gov/Blast.cgi>) databases. The physical locations of genes meeting an E -value $\leq 1e^{-20}$ and a percentage identity of $\geq 95\%$ were mapped to the reference genomes.

3.3 Results

3.3.1 Phenotypic Variation for RSA Traits

The phenotypic variation in the eight RSA-related traits is presented in Table 3.1. Based on the measurements, the eight RSA-related traits were significantly different ($P < 0.05$) among the *Brassica* genotypes tested. For example, TTRL ranged from 0.35 cm per plant for accession FG1063 (*B. juncea*) to 123.69 cm per plant for FG 643 (*B. oleracea*), while NTP ranged from 20 per plant for accession FG1063 (*B. juncea*) to 2,753 per plant for L345PC (a commercial canola cultivar). The coefficients of variation for TTRL, NTP, TRSA, TLRL, TRL, BLL, TPRL and RAD were 124.55%, 92.26%, 70.54%, 70.13%, 65.52%, 62.01%, 39.30% and 33.25%, respectively.

The 379 *Brassica* genotypes in this study were divided into three groups based on their root sizes according to the criteria of Liu et al. (2021). Based on a median TRL value of 137.52 cm per plant ± 2 standard errors (SE) of 7.53, genotypes with large-sized roots (TRL >130.52 cm) included 177 accessions, medium-sized root genotypes (TRL ranging from 115.45 to 130.52 cm) included 29 accessions, while small-sized root genotypes (TRL <115.45 cm) included 173 genotypes (Table A1).

3.3.2 Correlation Analysis Between Selected RSA Traits

The Anderson-Darling test showed that all eight parameters were not normally distributed ($P < 2.2e^{-16}$). A Spearman rank-based variable correlation test (Figure 3.1) indicated that TRL,

TRSA and TLRL were highly and positively correlated with each other, with coefficient values ranging from 0.80 to 0.96 ($P < 0.05$). Relatively high positive correlations were also observed among TRL, TRSA, TLRL, TTRL and NTP, with coefficients ranging from 0.52 to 0.76 ($P < 0.05$), while moderate positive correlations existed among TPRL, TTRL and NTP (coefficients = 0.4 to 0.47, $P < 0.05$).

3.3.3 Comparisons of RSA Traits Within and Among Species

3.3.3.1 Comparisons Among the Six *Brassica* Species

The PCA indicated that TRL, TRSA, TLRL and TPRL accounted for 70.5% (PC1 = 53.0% and PC2 = 17.5%) of total genotypic variation for all RSA-related traits (Figure 3.2). A biplot of the PCA indicated that TRL was the most important trait, followed by TRSA, TLRL and TPRL (Figure 3.3).

The distribution of the six *Brassica* species based on the contribution coefficient of the eight traits is illustrated in the biplot of the PCA (Figure 3.4). *B. oleracea* showed the greatest variation in the eight RSA related-traits relative to the other species. As a result, the *B. oleracea* accessions were widely dispersed in the biplot of the PCA (Figure 3.4). Nonetheless, most of the *B. oleracea* accessions were located on the right side PCA biplot (Figure 3.4). Similarly, most of the *B. napus* accessions were located on the right side of the biplot, indicating large RSA-related trait variations comparable with those observed in the *B. oleracea* accessions (Figure 3.4). Most of the *B. juncea*, *B. nigra*, *B. rapa* and *B. carinata* accessions were located on the left side of the biplot of the PCA (Figure 3.4). This suggests that *B. juncea*, *B. nigra*, *B. rapa* and *B. carinata* have comparable RSA-related traits and complexity. Therefore, *B. napus* and *B. oleracea* possessed the largest and most complex root systems among the six *Brassica* species.

Duncan's test of the eight RSA-related traits led to conclusions similar to the findings in the PCA biplot (Table 3.2 and Figure 3.4). *B. napus* and *B. oleracea* exhibited relatively greater

values of TRL, TRSA, NTP, TPRL, TLRL, and TTRL (Table 3.2, Figure 3.6), indicating they had larger and more complex root systems than the other species. *Brassica juncea* and *B. carinata* did not show significant differences for seven out of eight parameters (except for NTP). In addition, *B. juncea* and *B. carinata* had the largest RAD compared with the other species (Table 3.2, Figure 3.6), indicating that their roots were thicker, possibly due to their lower numbers of fine roots (root diameter < 0.2 cm). Among all species, *B. nigra* had the lowest values for six of the eight RSA traits examined (the only exceptions being NTP and BLL), suggesting that it had the smallest root system. There were no significant differences observed for BLL in *B. juncea*, *B. napus*, *B. rapa*, *B. carinata*, or *B. nigra*, while this trait was lowest in *B. oleracea* (Table 3.2, Figure 3.6).

3.3.3.2 Comparisons Within the Six *Brassica* Species

Based on TRL, the root sizes of the six *Brassica* species were of the order: *B. napus* (87% large, 5% medium and 8% small) (Figure 3.5a) > *B. oleracea* (63% large, 9% medium and 28% small) (Figure 3.5e) > *B. rapa* (40% large, 11% medium and 49% small) (Figure 3.5c) > *B. juncea* (24% large, 6% medium and 70% small) (Figure 3.5b) > *B. carinata* (14% large, 14% medium and 72% small) (Figure 3.5f) > *B. nigra* (12% large, 6% medium and 82% small) (Figure 3.5d). These results were consistent with the PCA described above.

3.3.4. SNP Genome Coverage and Marker Density

The mean number of filtered SNP markers was 510.3 ± 152.5 (range of 359 to 808) on the A-genome and 123.3 ± 34.0 (range of 88 to 190) on the C-genome. The filtered set of 5,103 and 1,110 markers covered 302.5 Mb and 452.8 Mb of the A- and C-genomes, respectively (Table 3.3). The mean inter-SNP marker distance or density for the A-genome was 62.9 ± 20.1 Kb (range of 38.1 to 106.8), while for the C-genome it was 426.3 ± 106.9 Kb (range 324.4 to 663.5) (Table 3.3). Thus, the marker density on the A-genome was about 7× higher than on the C-genome.

3.3.5. Estimation of Linkage Disequilibrium

The average values of r^2 and the schematic representation of decay for all chromosomes are presented in Table 3.3. Significant variation in the LD among chromosomes and between the A- and C-genomes was observed. The mean r^2 value was 0.1762 ± 0.0168 (range of 0.1456 to 0.2002) for the A-genome and 0.2126 ± 0.0213 (range 0.1901 to 0.2461) for the C-genome (Table 3.3). The average r^2 for the entire genome was 0.1830. Similarly, the estimated mean LD decay for the A-genome was 691.4 ± 283.6 (range of 440 to 1,400), while for the C-genome it was $4,705.0 \pm 2,331.8$ (range of 2,500 to 9,100); the mean LD decay was 850 for the entire genome (Table 3.3). Thus, the LD decay for the A-genome was in the hundreds of kilobases, while it persisted for several thousands of kilobases for the C-genome.

3.3.6 Population Structure

STRUCTURE analyses were carried out to understand the population stratification for the GWAS study. The ΔK statistic values for *STRUCTURE* runs below 10,000 burn-in iterations and 10,000 MCMC lengths suggested that the *Brassica* accessions could be grouped into three or six clusters, while the runs at 20,000, 50,000 and 100,000 burn-in iterations and MCMC lengths indicated three clusters. The population structure determined with the Puechmaille (2016) and Li and Liu (2018) alternative statistics (MedMedK, MedMeaK, MaxMedK and MaxMeaK) indicated three clusters for all *STRUCTURE* runs (Figure 3.9).

3.3.7. Marker-RSA Trait Associations (MTA)

Based on Manhattan plots of the six models (Supplementary Figure A2), 79 significant SNP markers were detected for the eight RSA-related traits. These comprised 6, 9, 26, 16, 12 and 6 SNP markers that were significantly associated with TRL, TRSA, RAD, TPRL, TTRL and BLL, respectively (Table 3.4). No SNP markers were associated with NTP or TLRL. The significant

MTA markers were distributed on all 19 chromosomes of *B. napus*. Sixty-nine of the MTA were located on the A-genome, while 16 were located on the C-genome.

3.3.8. Functions of Proteins Encoded by Significant Sequences

The identified sequences encoded proteins associated with functions in various cellular and biochemical processes, including ATP binding, lipid binding, ribosome binding, DNA binding, mRNA binding, RNA binding, metal ion binding, ATPase activity, ATP hydrolysis activity, kinase activity, lipase activity, transferase activity, transcription and translation factor activity, substrate selectivity, catalytic activity and carbohydrate metabolism (Table 3.4). More importantly, other proteins were involved in cell wall synthesis, cell growth, organ morphogenesis, transmembrane transporter activity, sugar-phosphatase activity and vesicle fusion, which are associated with basic biological and physiological process involved in root growth and development. Some other sequences encoded stress tolerance and disease resistance proteins, like NAC domain containing 35, ARM repeat superfamily protein, DEA(D/H)-box RNA helicase family protein, LRR and NB-ARC domains. Proteins of unknown molecular functions were also detected (Table 3.4).

3.4 Discussion

Root system architectural traits are critical to the plant's ability to absorb water and nutrients from the soil (Zobel et al., 2007; Lynch, 2019; Wen et al., 2019; Sun et al., 2021; Liu et al., 2021). The response of crops to abiotic stresses is influenced by their RSA. Since roots grow underground, they serve as the first line of defense in detecting stress signals and adapting their genetic program for post-embryonic growth to cope effectively with these challenges (Lynch, 1995). Morphological variations often correspond to physiological or functional variations (de Dorlodot et al., 2007). In this study, a highly positive correlation was observed for seven of the eight RSA-related traits evaluated in 379 *Brassica* genotypes. These parameters also showed a

positive correlation in an earlier study of 388 *B. napus* accessions conducted by Ibrahim et al. (2021).

Individual root tips that develop in the soil provide strong anchorage, which facilitates deeper penetration of roots into the soil (Bengough et al., 2016). In this study, large NTP per plant could improve the anchorage of *B. napus* and *B. oleracea* in the soil. Longer primary roots (Wasson et al., 2012), a larger root diameter (Uga et al., 2013), and abundant and steeper lateral roots (Lynch, 2013) can lead to a deeper and more resilient root system with increased radial hydraulic conductivity at depth and decreased metabolic costs for drought adaptation (Khan et al., 2016). The aforementioned root traits can also increase the efficiency of exudation of organic anions (Lynch, 2015) and enhance interactions with microbes (Walch-Liu et al., 2006), resulting in a high tolerance to deficiencies in nutrients such as nitrogen (N) and phosphate (P) (Khan et al., 2016).

Genotypes of *B. napus* and *B. oleracea* that were found to have relatively larger root systems with larger root surface areas, and longer and more vigorous roots, would be expected to provide good anchorage and penetration into the soil. This suggests high developmental plasticity in case of drought and nutrient deficiency (Choi and Cho, 2019). Akhtar and Banga (2015) reported a positive association between seed yield and root length in *B. juncea* under irrigated conditions, providing evidence that those *B. juncea* plants with longer TRL might attain higher yields. In addition, research has shown that genotypes of *B. oleracea* with high phosphorus absorption efficiency, characterized by more and longer lateral roots, have significantly increased yields, independent of external phosphorus concentrations (Hammond et al., 2009; Pongrac et al., 2020). Thus, in this study, genotypes of *B. oleracea* with large TLRL and high P absorption efficiency likely have the potential for higher yields. However, the efficiency of nutrient use is

determined by physiological traits specific to each species or genotype (Pongrac et al., 2020), and further research is needed to explore this possibility more fully.

Compared with other species, *B. juncea* and *B. carinata*, with the largest RAD, might be better at surviving in dry and compacted soil given their relatively thick and stronger roots. As for salinity, reducing main root elongation (Munns and Tester, 2008) to limit the transport of sodium ions from roots to shoots (Rus et al., 2006; Katori et al., 2010) and compartmentalizing sodium ions into root vacuoles and steles (Gupta and Huang, 2014) can increase the efficiency of water extraction and ion exclusion for salinity tolerance (Khan et al., 2016). As such, *B. nigra* and *B. rapa*, which had shorter primary roots (Table 3.2), might show greater tolerance to salinity. The mean BLL values were similar across all six species examined (Table 3.2), indicating that the potential growth of the roots of these species is quite similar.

Infection by soilborne pathogens can destroy the roots, reduce root density and diminish the functional effectiveness of the surviving infected roots (Román-Avilés et al., 2004). Therefore, promoting the growth of adventitious and lateral roots could help plants survive when roots are infected by pathogens (Snapp et al., 2003). Additionally, most *Brassica* species can produce chemical substances from roots that might suppress soilborne pathogens and pests such as nematodes, fungi, and certain weeds (Admin, 2015).

Root architectural traits below the ground can serve as a focal point for enhancement and optimization, tailored to meet the specific requirements dictated by the soil conditions (Arifuzzaman and Rahman, 2017). For example, Thomas et al. (Thomas et al., 2016) examined the root structure of various growth types of *B. napus* and determined that root morphology has the potential to enhance crop yield, provided that appropriate genetic markers associated with agronomic traits can be identified (Arifuzzaman and Rahman, 2017). The findings from this study revealed that root growth dynamics were significantly influenced by the genotype and species,

highlighting the significant role of genetic factors in this aspect, which can provide criteria for breeding selection. The presence of shared quantitative trait loci (QTL) between root characteristics and productivity measures such as yield, water usage, or nutrient acquisition suggests that the former contributes to determining the latter in numerous instances (Steele et al., 2006; Ibrahim et al., 2021). One instance of this is the utilization of the QTL *DROI*, which governs both root growth angle and root depth in rice, improving the root traits of an Indian upland rice variety through marker-assisted selection to enhance water efficiency (Steele et al., 2006; Ibrahim et al., 2021). In the case of *Brassica* crops, additional studies regarding the relationship between root-related traits and productivity or nutrient and water use efficiency are needed.

In this GWAS, 6,213 SNP markers were used to measure RSA related-traits, including 5,103 A-genome and 1,110 C-genome markers. Comparative genomic studies on *Brassica* genomes have reported that 1 cM on genetic maps corresponds to ~500 kb (Suwabe et al., 2006; Ecke et al., 2010; Delourme et al., 2013). Therefore, the 302.5 Mb marker coverage estimated in this study for the A-genome and 452.8 Mb for the C-genome corresponded to ~605 cM and ~905 cM, respectively. As such, the 6,213 SNP markers covered a total of ~1510 cM, which is about 60% of the estimated 2,500 cM *B. napus* genome. The determined genome coverage was comparable with the value of ~645 Mb obtained in studies that used the *Brassica* 60K array (Qian et al., 2014; Qu et al., 2017) and Specific-Locus Amplified Fragment Sequencing (SLAF) technology (Zhou et al., 2017). In comparison, the filtered set of 6,213 markers on the *Brassica* 19K SNP array provided about 3× more coverage than the *Brassica* 13.2K SNP array from the same company used in a previous study (Fredua-Agyeman et al., 2020).

In the current study, the mean marker density using the *Brassica* 19K SNP array was 62.9 ± 20.1 (8.43 SNP markers/cM) on the A-genome, 426.3 ± 106.9 (1.22 SNP markers/cM) on the C-genome, and 235.0 ± 200.1 (4.1 SNP markers/cM) on the entire genome. In comparison, the mean

marker density using the *Brassica* 13.2K SNP array was 63.4 ± 21.9 (8.46 SNP markers/cM) for the A-genome, 15.0 ± 8.4 (44.3 SNP markers/cM) for the C-genome, and 40.5 ± 29.8 (11.8 SNP markers/cM) for the entire *B. napus* genome (Fredua-Agyeman et al., 2020). Thus, the marker density was the same for the A-genome but about 2-3 \times less on the C-genome when genotyping was conducted with the *Brassica* 19K vs. 13.2K SNP arrays. This was expected, because the 1,110 filtered set of SNP markers on the C-genome was distributed over 302.5 Mb or 905.5 cM of the 19K array, compared with 2,367 markers on the C-genome spread over 26.7 Mb or 53.4 cM on the 13.2K array.

Linkage disequilibrium, which is the non-random association between alleles at different loci, determines the power and precision of association mapping studies using molecular markers and unobserved QTL (Goddard and Hayes, 2009; Qu et al., 2020). Determination of the extent of LD is essential for making of inferences about the genetic forces shaping a population (Qanbari, 2019). The extent of LD reported by Fredua-Agyeman et al. (2020) using the *Brassica* 13.2K SNP array varied from 1,100 to 2,300 kb for the A-genome and from 200 to 1,500 kb for the C-genome. In this study, using the *Brassica* 19K SNP array, LD varied from 440 to 1,400 Kb for the A-genome and 2,500 to 9,100 for the C-genome. The difference in LD values obtained with the two *Brassica* arrays could reflect the different marker densities. The low marker density on the C-genome might be responsible for the extended ranges of the LD decay. However, the LD values for the A-genome and C-genome were consistent with those reported in other studies (Wu et al., 2016; Qu et al., 2017; Zhou et al., 2017). Based on the minimum LD decay (440 Kb or 0.88 cM), a minimum of 3,200 markers was needed to perform the GWAS studies. Therefore, the 6,213 SNP markers used for this GWAS represented approximately twice the number needed to perform the analysis.

The current GWAS study identified three genomic regions on chromosomes A02, A03 and A06 that were associated with RSA-traits. In the case of the A02 chromosome, the SNP marker Bn_A02_p5571981 overlapped with a histone deacetylase HDT2-like protein. This protein negatively regulates GIBBERELLIN 2-OXIDASE2 (GA2oxs2) expression, which determines the cell number in the Arabidopsis root meristem and elongation zone (Li et al., 2017a). The increased expression of GA2ox2 in HDT1/2 was reported to cause a decrease in GAs levels, leading to an earlier transition from cell division to the expansion phase of transit-amplifying cells (Li et al., 2017a). On chromosome A03, a histidine kinase 2 (AHK2) encoded by genes that overlap SNP marker Bn_A03_p19974784 can positively regulate the level of cytokinin, which negatively regulates root development in Arabidopsis (Nishimura et al., 2004; Riefler et al., 2006). In Arabidopsis, histidine kinase homologs function as receptors for cytokinin and play an overlapping role in regulating the growth of shoots and roots (Nishimura et al., 2004). Root hair specific 17, encoded by genes associated with SNP marker Bn_A06_p26219274 on chromosome A06, is an expressed protein controlling root hair cell expression for regulating the root growth of Arabidopsis (Won et al., 2009).

3.5 Conclusion

The growth rate, spacing, and location of roots can be influenced by plant species and environmental cues such as nutrients, water, temperature, microbial activity, soil pH and the presence of specific chemicals or pests, all of which can dramatically influence the final RSA of plants (Ingram and Malamy, 2010). The results of this study showed that significant variation occurs in the root architectural traits of different *Brassica* species under controlled environmental conditions. The results also indicated correlations between specific RSA traits; genotypes with RSA traits (TRL, TRSA, TPRL, TLRL) showing strong correlations could be used for additional studies of stress tolerance in the field or under other adverse environmental conditions. Seventy-

nine SNP markers associated with root traits and three candidate genes related to root growth on chromosomes A02, A03 and A06 were also identified. Identification of the genomic regions and genetic mechanisms affecting RSA traits will be useful in *Brassica* breeding programs.

3.6 Tables

Table 3.1 Summary and phenotypic variations of eight root system architectural traits in a collection of 379 *Brassica* genotypes representing *B. napus*, *B. oleracea*, *B. rapa*, *B. nigra*, *B. carinata* and *B. juncea*.

RSA traits (per plant)	Abbreviation/Unit	Min	Max	Mean	SD	CV (%)	p-value
Total root length	TRL/cm	18.46	414.51	137.51	90.10	65.52	<2e ⁻¹⁶ ***
Total surface area of roots	TRSA/ cm ²	2.32	60.11	16.86	11.89	70.54	<2e ⁻¹⁶ ***
Average root diameter	RAD/cm	0.20	0.76	0.35	0.12	33.25	<2e ⁻¹⁶ ***
Number of tips	NTP	20.00	2753.00	461.30	425.58	92.26	<2e ⁻¹⁶ ***
Total primary root length	TPRL/cm	8.77	46.73	24.92	9.79	39.30	<2e ⁻¹⁶ ***
Total lateral root length	TLRL/cm	9.34	249.93	83.40	58.49	70.13	<2e ⁻¹⁶ ***
Total tertiary root length	TTRL/cm	0.35	123.69	25.24	31.44	124.55	<2e ⁻¹⁶ ***
Basal link length	BLL/cm	0.66	4.35	1.71	1.06	62.01	4.7e ⁻¹² ***

Probability values (p-values) were generated through an ANOVA test of the 379 *Brassica* genotypes.

Table 3.2 Least square means of eight root system architectural traits among six the *Brassica* species *B. napus*, *B. oleracea*, *B. rapa*, *B. nigra*, *B. carinata* and *B. juncea* based on Duncan's test. Traits examined included total root length (TRL/cm), total surface area of roots (TRSA/cm²), average root diameter (RAD/cm), number of tips (NTP), total primary root length (TPRL/cm), total lateral root length (TLRL/cm), total tertiary root length (TTRL/cm) and basal link length (BLL/cm).

Species	TRL	TRSA	RAD	NTP	TPRL	TLRL	TTRL	BLL
<i>B.juncea</i>	99.58 ^a	14.00 ^a	0.41 ^a	322.93 ^a	23.45 ^{ad}	63.57 ^a	9.29 ^a	1.85 ^a
<i>B.napus</i>	201.64 ^b	21.80 ^b	0.32 ^b	596.84 ^b	29.21 ^b	113.81 ^b	45.35 ^b	1.76 ^{ab}
<i>B.rapa</i>	120.43 ^c	15.79 ^c	0.36 ^c	378.51 ^c	21.43 ^c	77.92 ^c	20.21 ^c	1.69 ^b
<i>B.carinata</i>	95.07 ^a	13.49 ^a	0.41 ^a	378.55 ^c	24.30 ^d	61.49 ^a	9.29 ^{ac}	1.75 ^{ab}
<i>B.oleracea</i>	167.93 ^d	22.00 ^b	0.36 ^c	645.14 ^b	25.83 ^e	102.64 ^d	37.82 ^d	1.49 ^c
<i>B.nigra</i>	82.98 ^c	9.99 ^d	0.32 ^b	340.12 ^{ac}	22.45 ^{ac}	53.45 ^c	7.09 ^e	1.69 ^b

Means followed by different letters in the same column are significantly different (p-value < 0.05) from each other.

Table 3.3 SNP marker density and extent of intra-chromosomal linkage disequilibrium in *Brassica napus*, *B. rapa* and *B. juncea* accessions used in genome-wide association studies for the determination of root architectural traits

Linkage group or Chromosome	Total # of SNP markers	# Filtered SNP markers	Length covered (kb)	Average inter-SNP marker distance (kb)	Pairwise comparisons of all linked SNP markers	Number (%) of SNP pairs in significant LD [‡]	Average r ² value/ chromosome	Estimated LD decay (Mb) [‡]
A01	800	379	29044.5	76.6	17675	8203 (46.4%)	0.1456	599
A02	728	403	29846.5	74.1	18806	10438 (55.5%)	0.1712	920
A03	1458	808	37644.0	46.6	38868	19811 (51.0%)	0.1597	440
A04	909	498	22049.4	44.3	23394	12495 (53.4%)	0.1688	580
A05	916	498	29217.3	58.7	23625	12540 (53.1%)	0.1801	725
A06	1024	595	31714.7	53.3	28475	16609 (58.3%)	0.2002	600
A07	1298	722	27503.6	38.1	34825	17494 (50.2%)	0.1738	450
A08	633	359	21731.4	60.5	16675	9615 (57.7%)	0.1801	620
A09	757	404	43128.3	106.8	18925	10092 (53.3%)	0.1986	1400
A10	787	437	30624.6	70.1	20575	11452 (55.7%)	0.1876	580
C01	797	108	43764.1	405.2	4125	2754 (66.8%)	0.2284	9100
C02	820	113	54608.9	483.3	4375	2752 (62.9%)	0.2047	4000
C03	1598	190	61643.2	324.4	7740	4945 (63.9%)	0.2155	3100
C04	1224	168	55831.3	332.3	7125	4421 (62.0%)	0.1901	3160
C05	591	96	45327.5	472.2	3345	2188 (65.4%)	0.1996	4600
C06	874	103	44201.4	429.1	3601	2086 (57.9%)	0.1923	3185
C07	904	116	38338.5	330.5	4400	2785 (63.3%)	0.1981	2500
C08	755	128	50664.9	395.8	4668	3248 (69.6%)	0.2426	4600
C09	518	88	58383.8	663.5	3123	2295 (73.5%)	0.2461	8100
A-genome	9310	5103	302504.3	62.9 ±20.1	251738	134687 (53.5%)	0.1762	660
C-genome	8072	1110	452763.7	426.3 ±106.9	45441	27474 (60.5%)	0.2126	4000
AC-genome	17382	6213	755267.9	235.0±200.1	224259	169182 (75.4%)	0.1830	850

* One thousand one hundred and fifty-four SNP markers located on scaffolds or which could not be located were excluded from the analysis. [‡] The number and percentage of SNP pairs in significant LD were determined from Chi-squared tests at p-value < 0.001.

[‡] The extent of LD decay was estimated from the projection of the intersection between the fitted curve of the data points and the 95th percentile of unlinked r² threshold line (background LD) onto the physical distance axis.

Table 3.4 SNP markers in the *Brassica* species *B. napus*, *B. rapa* and *B. juncea*, including their chromosomal location and linkage association with root architectural traits

⁰ Model Used	Trait(s)	¹ SNP Marker	² Marker Position		³ Linkage Group	Description
			Start	End		
PCA/Q+K/PCA+D/PCA+K	TRSA	Bn_scaff_17036_1_p157245	243316	243334	A01	AFG1-like ATPase family protein
PCA/Q+K/PCA+D/PCA+K	TRSA	Bn_A03_p4123164	28467	28487	A03	ABC1 family protein
PCA/Q+K/PCA+D/PCA+K	TRSA	Bn_A03_p9765420	55863	55931	A03	Eukaryotic translation initiation factor 2 subunit 1
PCA/Q+K/PCA+D/PCA+K	TRSA	Bn_A09_p30678275	28355	28373	A09	AGC kinase 1.7
PCA/Q+K/PCA+D/PCA+K	TRSA	Bn_scaff_17566_1_p21523	541373	541673	C02	Calcium-dependent lipid-binding (CaLB domain) family protein
PCA/Q+K/PCA+D/PCA+K	TRSA	Bn_scaff_16445_1_p82664	105905	106136	C08	D-ribose-binding periplasmic protein
PCA/PCA+D/PCA+K	TRSA	Bn_A02_p5571981	1914669	1914789	A02	histone deacetylase HDT2-like (LOC103851751)
PCA/Q/Q+K/PCA+K	RAD	Bn_A09_p1011107	2194	2259	C08	GDSL-like lipase/acylhydrolase superfamily protein
PCA/Q/Q+K/PCA+D/PCA+K	RAD	Bn_Scaffold000164_p174512	82582	82882	A01	Tetratricopeptide repeat (TPR)-like superfamily protein
PCA	RAD	Bn_A02_p5574727	1914669	1914789	A02	DNA repair protein Rad4 family
PCA/Q/Q+D/Q+K/PCA+K	RAD	Bn_A03_p19973423	1051672	1051972	A03	zinc-dependent activator protein-1
PCA/Q/Q+D	RAD	Bn_A06_p21098677	976034	976334	A06	40S ribosomal protein S27
PCA/Q+D	RAD	Bn_A06_p26219274	4063	4263	A06	root hair specific 17
PCA/Q+K/PCA+K	RAD	Bn_A07_p11698185	545848	546047	A07	Ribosomal protein L17 family protein
PCA/PCA+D	TPRL	Bn_A03_p7058001	11959	11976	A03	GDSL-like Lipase/Acylhydrolase superfamily protein
PCA/PCA+D/PCA+K	TPRL	Bn_A04_p7442353	327569	327586	A04	transferases, transferring acyl groups
PCA/PCA+D/PCA+K	TPRL	Bn_A04_p7442886	1537209	1537329	A04	ransmembrane protein
PCA/PCA+D/PCA+K	TPRL	Bn_A04_p7443395	1317835	1317852	A04	hydroxymethylglutaryl-CoA synthase / HMG-CoA synthase
PCA/PCA+D/PCA+K	TPRL	Bn_A05_p19554281	1256900	1257100	A05	tRNase Z4
PCA/Q+K/PCA+D/PCA+K	TPRL	Bn_A06_p2619089	972332	972452	A06	exocyst subunit exo70 family protein
PCA/PCA+D/PCA+K	TPRL	Bn_A07_p3921656	174533	174552	A07	Nucleotide-sugar transporter family protein
PCA/Q+K/PCA+D/PCA+K	TPRL	Bn_A09_p7560188	192457	192577	A09	exocyst complex component sec3A

Table 3.4 (continued) SNP markers in the *Brassica* species *B. napus*, *B. rapa* and *B. juncea*, including their chromosomal location and linkage association with root architectural traits.

^a Model Used	Trait(s)	^a SNP Marker	^b Marker Position		^b Linkage Group	Description
			Start	End		
PCA/PCA+D/PCA+K	TPRL/TRL	Bn_scaff_16414_1_p539478	559675	559847	C05	protein SULFUR DEFICIENCY-INDUCED 2-like
PCA/PCA+K	TPRL/TRL	Bn_scaff_16514_1_p41089	1732209	1732509	C07	serine/threonine-protein kinase STY13-like
PCA/Q+K/PCA+D/PCA+K	TPRL	Bn_scaff_17487_1_p1782181	305799	305999	C09	hydroxyproline-rich glycoprotein family protein
Q/Q+D/Q+K/PCA+K	RAD	Bn_A04_p5183306	493479	493599	A04	Uncharacterized
Q	RAD	Bn_A08_p20968239	565906	566106	A08	phospholipase A1-IIalpha
Q+D/Q+K/PCA+K	RAD	Bn_A01_p6482543	947870	947909	A01	Homeodomain-like superfamily protein
Q+D	RAD	Bn_A02_p5516551	260256	260376	A02	cytochrome P450, family 735, subfamily A, polypeptide 2
Q+D	RAD	Bn_A02_p15693192	28725	28807	A02	Transducin/WD40 repeat-like superfamily protein
Q+D	RAD	Bn_A06_p5280225	62713	62741	A04	phosphoglycolate phosphatase
Q+D	RAD	Bn_scaff_23293_1_p25406	376195	376495	A09	NAC domain containing protein 35
Q+D	RAD	Bn_A01_p7942548	394003	394162	C01	DNA repair protein Rad4 family
Q+K	TRSA	Bn_A08_p12599446	55394	55594	A08	methylcrotonoyl-CoA carboxylase beta chain, mitochondrial
Q+K	TRSA	Bn_Scaffold000172_p99636	93776	93813	A05	ARM repeat superfamily protein
Q+K	TPRL	Bn_A02_p10126530	346076	346196	A02	Plant self-incompatibility protein S1 family
Q+K	TPRL	Bn_A09_p24564546	4286	4302	A09	<i>Brassica napus</i> genome assembly, chromosome: A09
Q+K/PCA+K	TTRL/TRL	Bn_A03_p5039586	3568080	3568097	A03	temperature-induced lipocalin-1
Q+K	TTRL	Bn_A03_p6744274	429097	429121	A03	putative defensin-like protein 225
Q+K	TTRL	Bn_A03_p19974784	1053033	1053333	A03	histidine kinase 2
Q+K/PCA+K	TTRL/TRL	Bn_A06_p17049401	43512	43640	A06	receptor-like kinase TMK2
Q+K	TTRL	Bn_scaff_18100_1_p593993	299324	299431	A09	malate dehydrogenase 1, cytoplasmic

Table 3.4 (continued) SNP markers in the *Brassica* species *B. napus*, *B. rapa* and *B. juncea*, including their chromosomal location and linkage association with root architectural traits.

^α Model Used	Trait(s)	^α SNP Marker	^β Marker Position		^β Linkage Group	Description
			Start	End		
Q+K	TTRL	Bn_A09_p13729175	142766	142782	A09	disease resistance protein TAO1
Q+K	TTRL	Bn_A09_p16833397	67051	67275	A09	protein ENHANCED DISEASE RESISTANCE 2-like
Q+K	TTRL	Bn_A09_p19872952	41038	41054	A09	alcohol dehydrogenase-like 3
Q+K	TTRL	Bn_A09_p19865476	743365	743382	A09	DEA(D/H)-box RNA helicase family protein
Q+K	TTRL	Bn_A09_p33660289	7754	7954	A09	CDP-diacylglycerol--serine O-phosphatidyltransferase 1
Q+K	TTRL	Bn_A10_p4624712	1352963	1353083	A10	equilibrative nucleoside transporter 7
Q+K	TTRL	Bn_A10_p4622209	34449	34569	A10	S-adenosyl-L-methionine-dependent methyltransferases superfamily protein
Q+K	TTRL	Bn_scaff_17440_1_p268977	101613	101813	C03	phosphatidylinositol 4-phosphate 5-kinase MSS4-like protein
Q+K	TTRL	Bn_scaff_22481_1_p200007	624510	624630	C09	Haloacid dehalogenase-like hydrolase (HAD) superfamily protein
PCA+D	RAD	Bn_A01_p5335218	66516	66534	A01	abscisic acid 8'-hydroxylase 1
PCA+D	RAD	Bn_A01_p10945930	11035	11052	A01	LRR and NB-ARC domains-containing disease resistance protein
PCA+D	RAD	Bn_A02_p10781906	44741	44765	A02	lariat debranching enzyme
PCA+D	RAD	Bn_A02_p19704677	2839848	2839865	A02	U-box domain-containing protein 37
PCA+D	RAD	Bn_A04_p16313477	354946	355064	A04	Ribosomal S17 family protein
PCA+D	RAD	Bn_A04_p18562244	188942	189242	A04	4-hydroxy-tetrahydronicotinate synthase 2, chloroplastic
PCA+D	RAD	Bn_A06_p24156940	360125	360145	A06	Disease resistance protein (TIR-NBS-LRR class) family
PCA+D	RAD	Bn_A10_p12072657	43451	43632	A07	ubiquitin family protein
PCA+D	RAD	Bn_A07_p6501207	9193	9381	A07	GDSL-like Lipase/Acylhydrolase superfamily protein
PCA+D	RAD	Bn_A02_p709952	1015827	1015844	A07	Peroxidase superfamily protein
PCA+D	RAD	Bn_A09_p14282683	37874	38166	A09	Uncharacterized

Table 3.4 (continued) SNP markers in the *Brassica* species *B. napus*, *B. rapa* and *B. juncea*, including their chromosomal location and linkage association with root architectural traits.

^a Model Used	Trait(s)	^a SNP Marker	^b Marker Position		^b Linkage Group	Description
			Start	End		
PCA+D	TPRL	Bn_A03_p7110332	1001573	1001590	A03	transducin family protein / WD-40 repeat family protein
PCA+D	TPRL	Bn_A08_p20546110	342771	342891	A08	myosin-binding protein 1
PCA+D	TPRL	Bn_scaff_17807_1_p98331	103262	103462	C02	LEAF RUST 10 DISEASE-RESISTANCE LOCUS RECEPTOR-LIKE PROTEIN KINASE-like 2.7
PCA+D	TPRL	Bn_scaff_16759_1_p264813	1114468	1114528	C04	chloride channel D
PCA+D	TPRL	Bn_C13729753_p243	858575	858775	C05	Integrase-type DNA-binding superfamily protein
PCA+K	TRL	Bn_A06_p17452087	979492	979792	A06	Polynucleotidyl transferase
PCA+K	TRL	Bn_A06_p17176086	709607	709869	A06	TCV-interacting protein
PCA+K	TRL	Bn_A01_p22999151	637603	637625	A01	SsrA-binding protein
PCA+K	TRL	Bn_scaff_17522_1_p1724143	2404	2524	A02	Tetratricopeptide repeat (TPR)-like superfamily protein
PCA+K	TRL	Bn_scaff_21861_1_p33827	717915	718115	C02	cytochrome P450, family 72, subfamily A, polypeptide 11
PCA+K	TRL	Bn_scaff_16445_1_p894350	245816	246116	C08	cytochrome P450, family 87, subfamily A, polypeptide 2
PCA+K	BLL	Bn_A03_p7178917	1429677	1429797	A03	cysteine-rich RLK (RECEPTOR-like protein kinase) 27
PCA+K	BLL	Bn_scaff_26139_1_p313572	539325	539438	A04	Inosine triphosphate pyrophosphatase family protein
PCA+K	BLL	Bn_A06_p3839293	53144	53444	A06	phosphatidylinositol 4-phosphate 5-kinase 7
PCA+K	BLL	Bn_scaff_17821_1_p119310	541935	542135	A08	V-type proton ATPase subunit c"2
PCA+K	BLL	Bn_A08_p16632230	489602	489630	A08	<i>Brassica napus</i> genome assembly
PCA+K	BLL	Bn_A09_p9101925	533420	533437	A09	SNARE associated Golgi protein family
PCA+D	RAD	Bn_A07_p6501207	9193	9381	A07	GDSL-like Lipase/Acylhydrolase superfamily protein
PCA+D	RAD	Bn_A02_p709952	1015827	1015844	A07	Peroxidase superfamily protein
PCA+D	RAD	Bn_A09_p14282683	37874	38166	A09	Uncharacterized

^aMixed Linear Model (MLM) designations: PCA, principal component analysis; Q, population structure; K, Kinship. ^aSNP markers denoted with the same superscript letter mapped to multiple chromosomes on the reference genomes. The type of PCR-based markers showing trait association has been specified. ^bLinkage groups A1-A10 = *Brassica rapa* and C1-C9 = *Brassica oleracea*. UPutative functions are based on matching entries in the *EnsemblPlants* and NCBI GenBank databases.

3.7 Figures

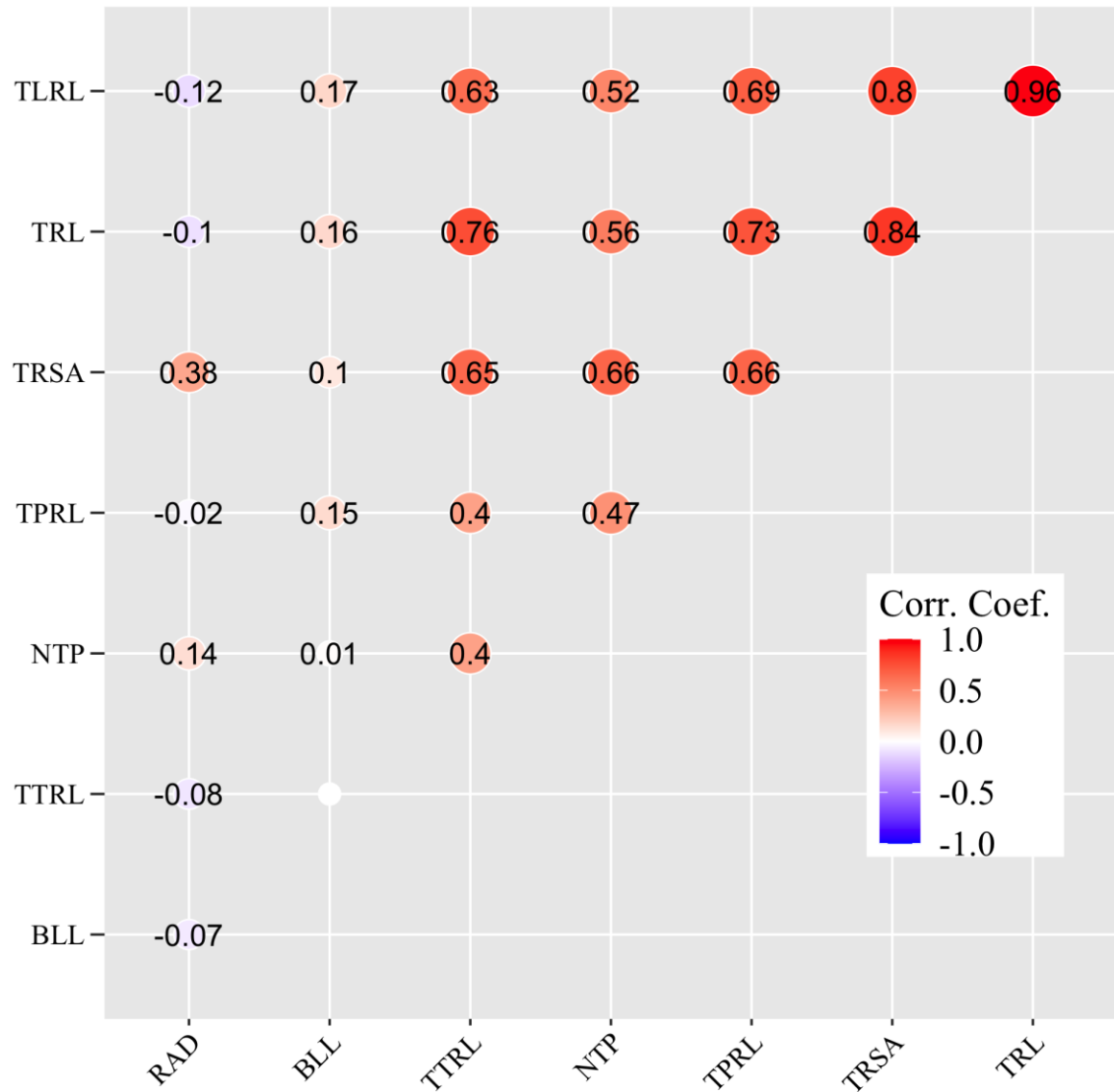


Figure 3.1 Correlation analysis between eight root system architecture (RSA) traits as determined by a Spearman rank-based variable correlation test. Total root length (TRL/cm), total surface area of roots (TRSA/cm²), average root diameter (RAD/cm), number of tips (NTP), total primary root length (TPRL/cm), total lateral root length (TLRL/cm), total tertiary root length (TTRL/cm) and basal link length (BLL/cm). ‘Corr’ showed the coefficient values of the correlation, and the strength of correlation is described with different colors. ‘0.0’ means no significant correlation (p-value >0.05).

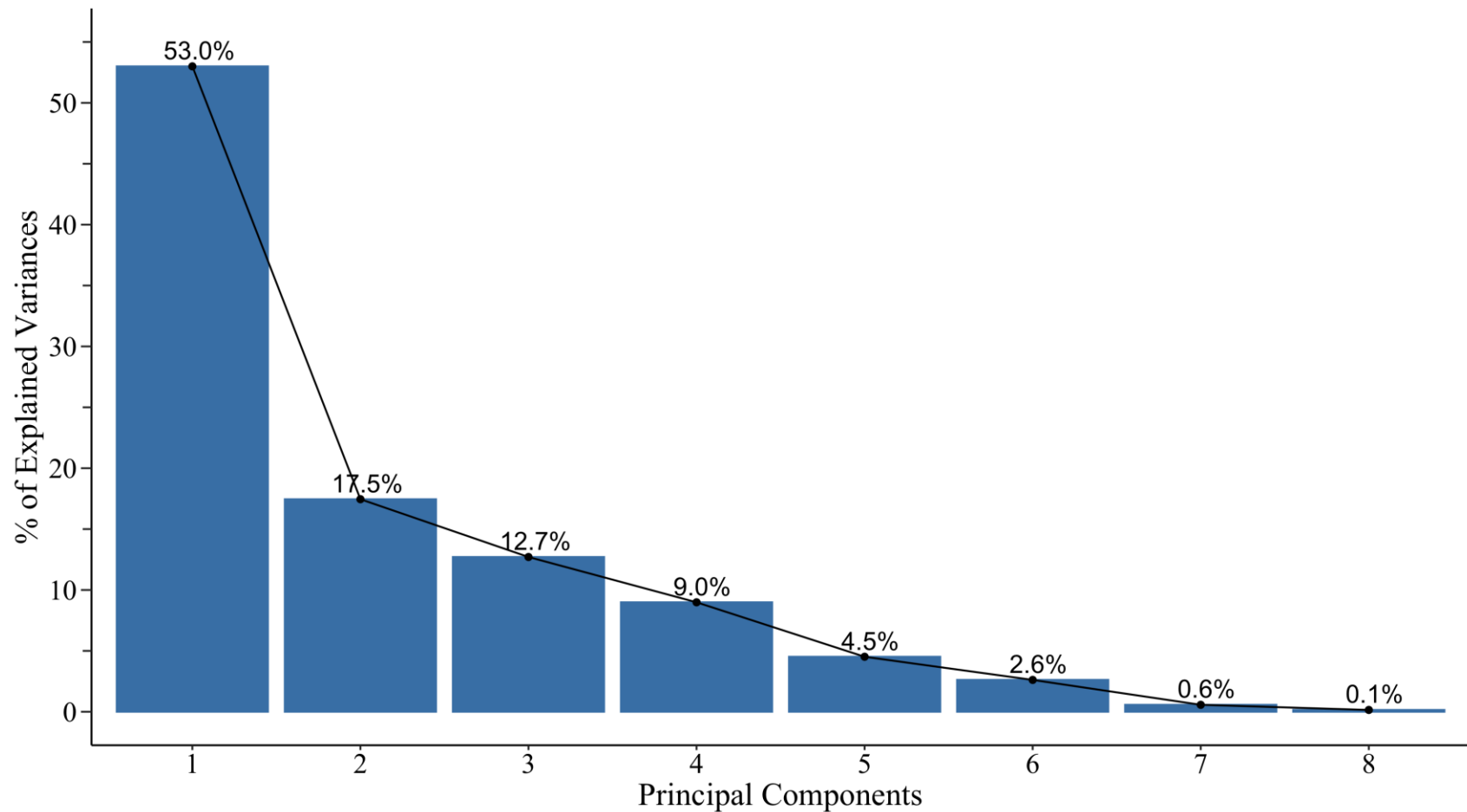


Figure 3.2 Scree plot explaining cumulative variance of the principal components. PC 1 and PC 2 explained 53% and 17.5% of the cumulative variance in the dataset, respectively, which accounted for 70.5% of total genotypic variation among all root system architecture (RSA) traits. Traits include total root length (TRL/cm), total surface area of roots (TRSA/cm²), average root diameter (RAD/cm), number of tips (NTP), total primary root length (TPRL/cm), total lateral root length (TLRL/cm), total tertiary root length (TTRL/cm) and basal link length (BLL/cm).

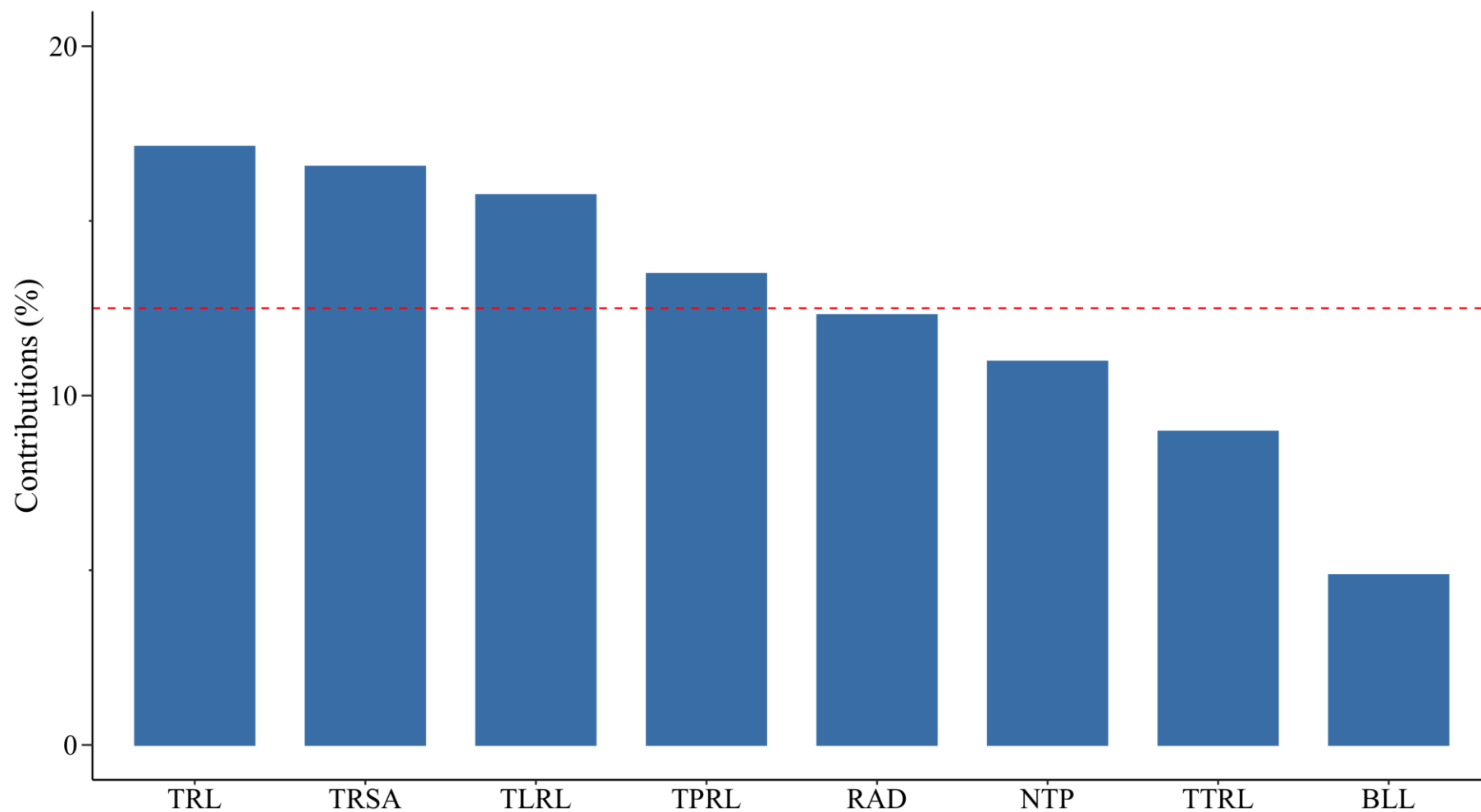


Figure 3.3 Scree plot for all variables of principal components 1 and 2. The red line indicates the average contribution. Total surface area of roots (TRSA/cm²), total root length (TRL/cm), total lateral root length (TLRL/cm) and total primary root length (TPRL/cm) made the greatest contributions, followed by average root diameter (RAD/cm), number of tips (NTP), total tertiary root length (TTRL/cm) and basal link length (BLL/cm).

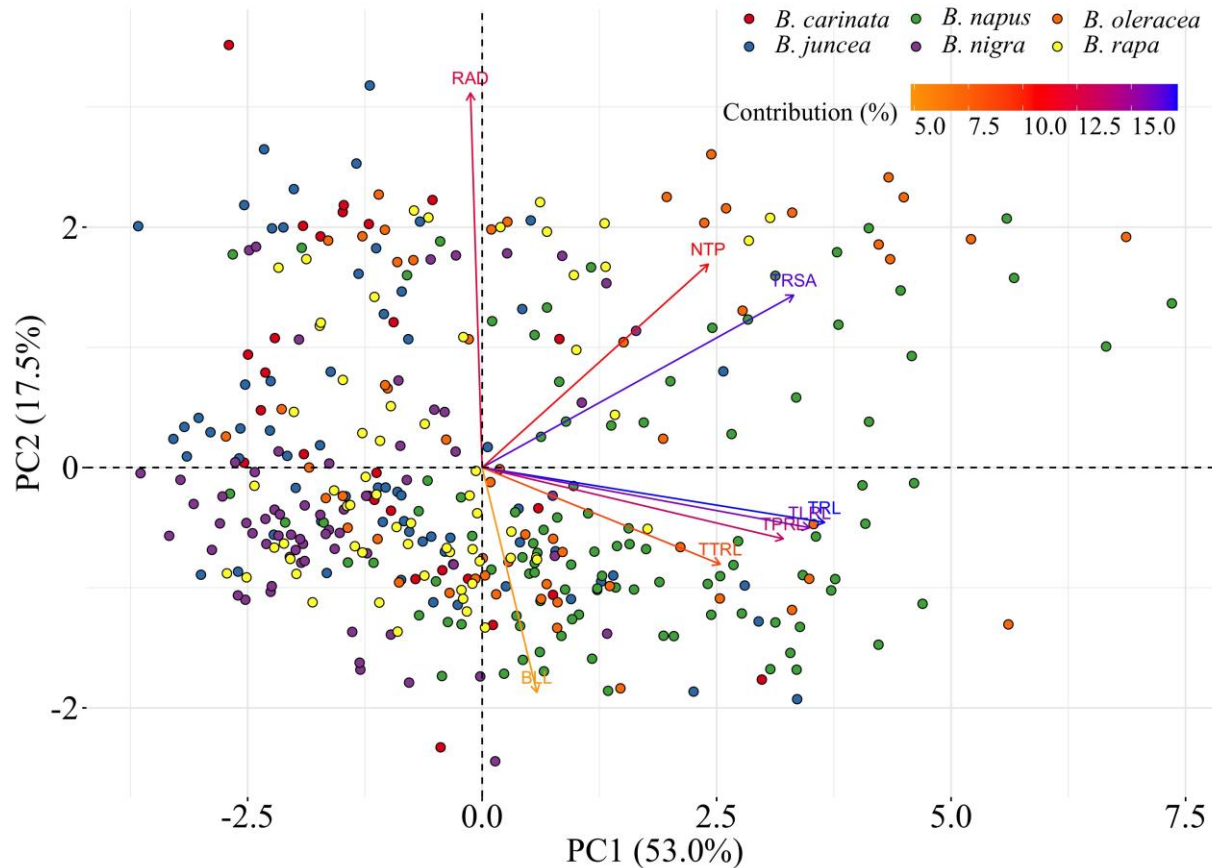


Figure 3.4 Principal components analysis (PCA) biplot among six *Brassica* species including *B. napus*, *B. oleracea*, *B. rapa*, *B. nigra*, *B. carinata* and *B. juncea*. Traits include total root length (TRL/cm), total surface area of roots (TRSA/cm²), average root diameter (RAD/cm), number of tips (NTP), total primary root length (TPRL/cm), total lateral root length (TLRL/cm), total tertiary root length (TTRL/cm) and basal link length (BLL/cm). The different species are indicated by different colors. With the increase of PC1, most of the values of the root system architecture (RSA) traits increased, except for RAD. With the increase of PC2, RAD, NTP and TRSA increased, while values of other traits decreased. Most of the *B. juncea*, *B. nigra*, *B. rapa* and *B. carinata* genotypes are located in a cloud on the left side of the biplot, while most *B. napus* and *B. oleracea* genotypes are located on the right side of the biplot with relatively larger values for the root traits. This suggests that *B. napus* and *B. oleracea* have relatively larger root systems.

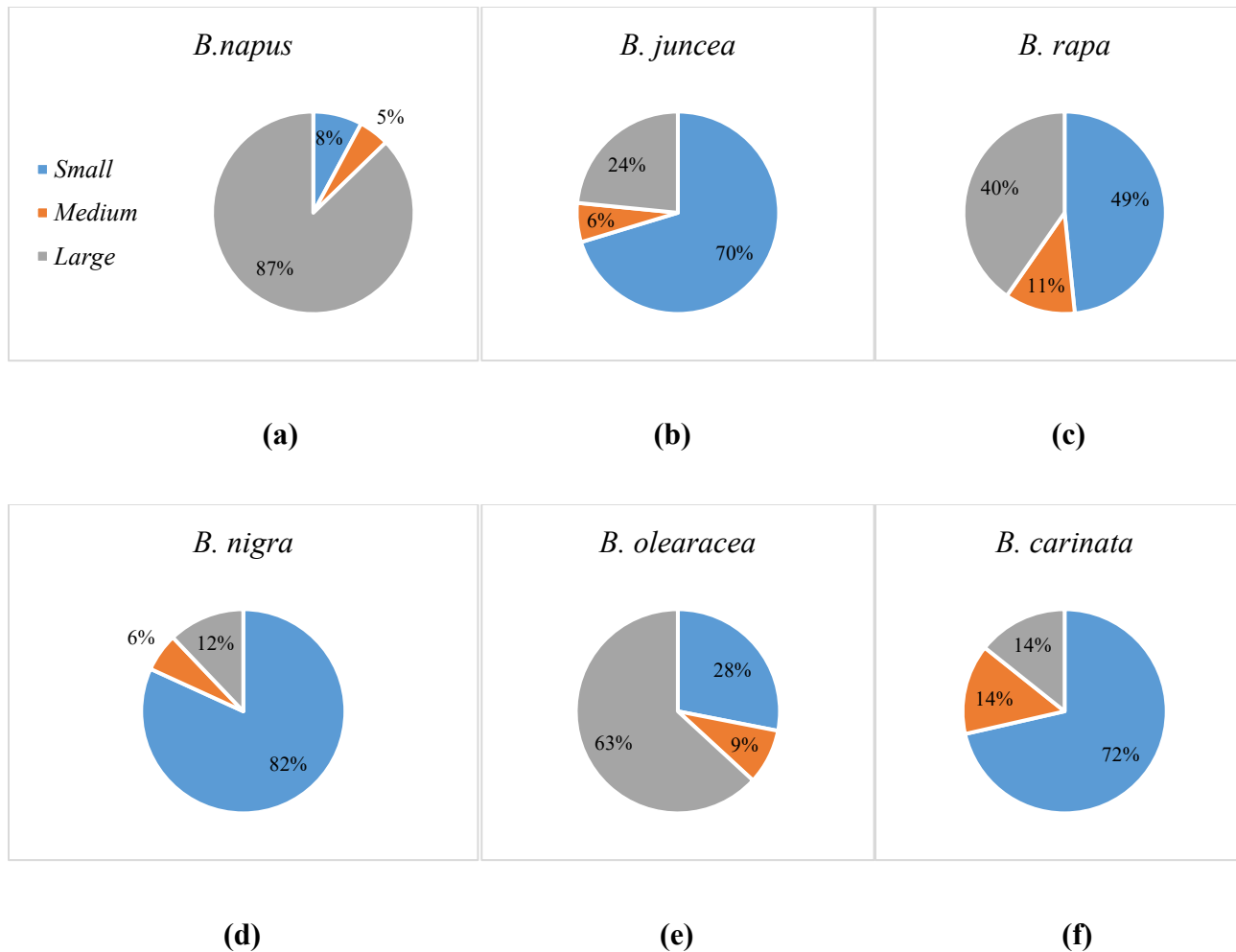


Figure 3.5 Percentage of genotypes with small, medium, or large sized root systems in six *Brassica* species – *B. napus* (a), *B. juncea* (b), *B. rapa* (c), *B. nigra* (d), *B. oleracea* (e) and *B. carinata* (f). Most *B. napus* and *B. oleracea* genotypes had larger-sized root systems, while most *B. juncea*, *B. rapa*, *B. nigra* and *B. carinata* genotypes had smaller-sized root systems. Genotypes with medium-sized root system represented the smallest percentage for all of the species.

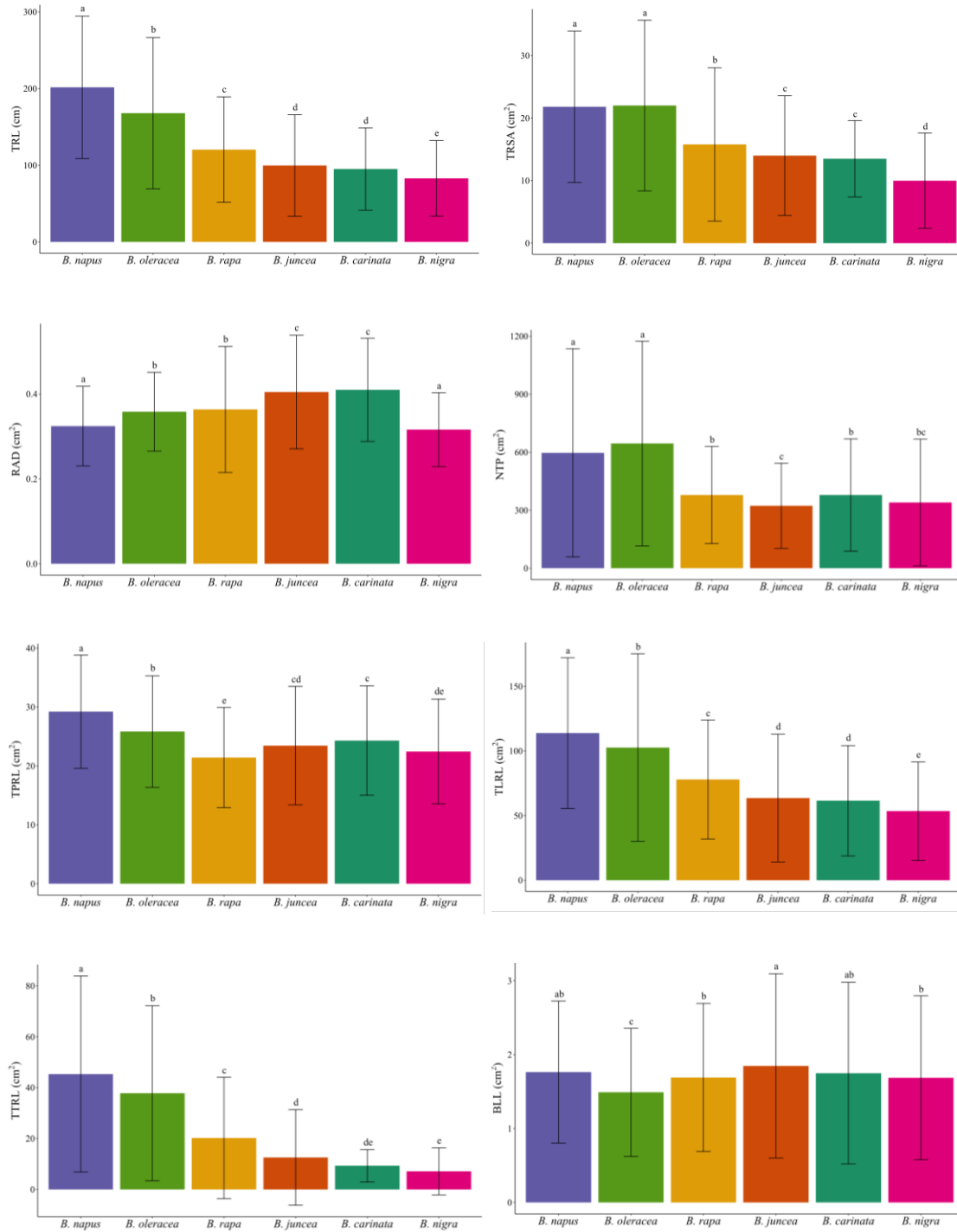
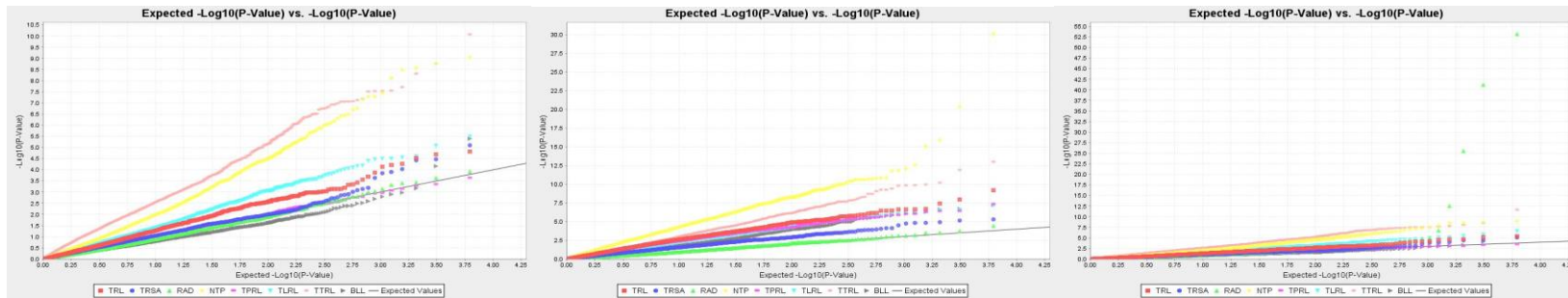


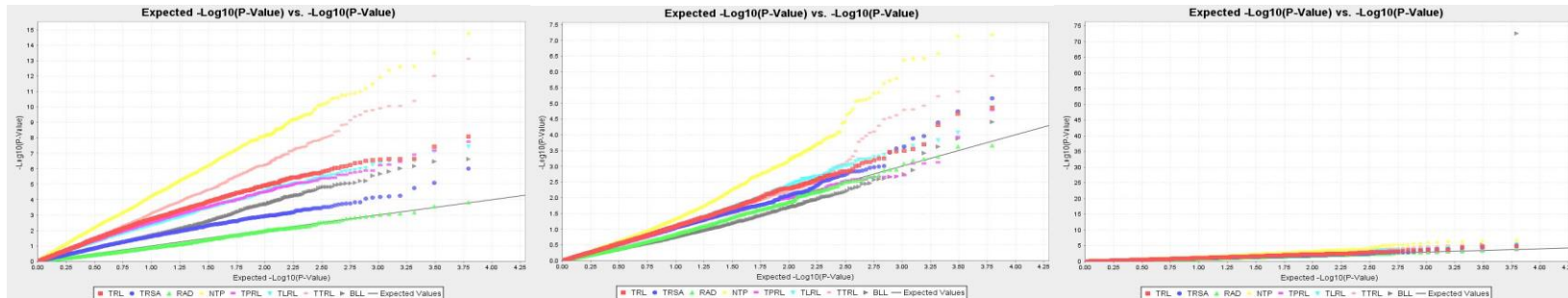
Figure 3.6 Bar plot of eight root system architecture (RSA) traits among six *Brassica* species. *B. napus* and *B. oleracea* had a relatively greater total root length (TRL/cm), total surface area of roots (TRSA/cm²), number of tips (NTP), total primary root length (TPRL/cm), total lateral root length (TLRL/cm) and total tertiary root length (TTRL/cm). In general, values for six of the eight traits (with the exception of NTP and basal link length (BLL/cm)) were lowest in *B. nigra*.



(a)

(c)

(e)



(b)

(d)

(f)

Figure 3.7 Quantile-Quantile comparison of six GWAS models for identifying loci associated with root architecture (RSA) traits in 313 *Brassica* accessions representing five species, including *B. napus*, *B. oleracea*, *B. rapa*, *B. carinata* and *B. juncea*. The two general linear models (GLM) tested comprised the principal coordinate analysis (PCA)-only (a) and the population structure (Q)-only (b). The four mixed linear models (MLM) tested comprised the Q + D (c), Q + K (d), PCA + D (e), PCA + K (f) models, where D and K are the Distance and Kinship Matrices, respectively. The black line is the expected $-\log_{10} P$ distribution, while the colored lines are the observed $-\log_{10} P$ distribution for each of the eight RSA traits.

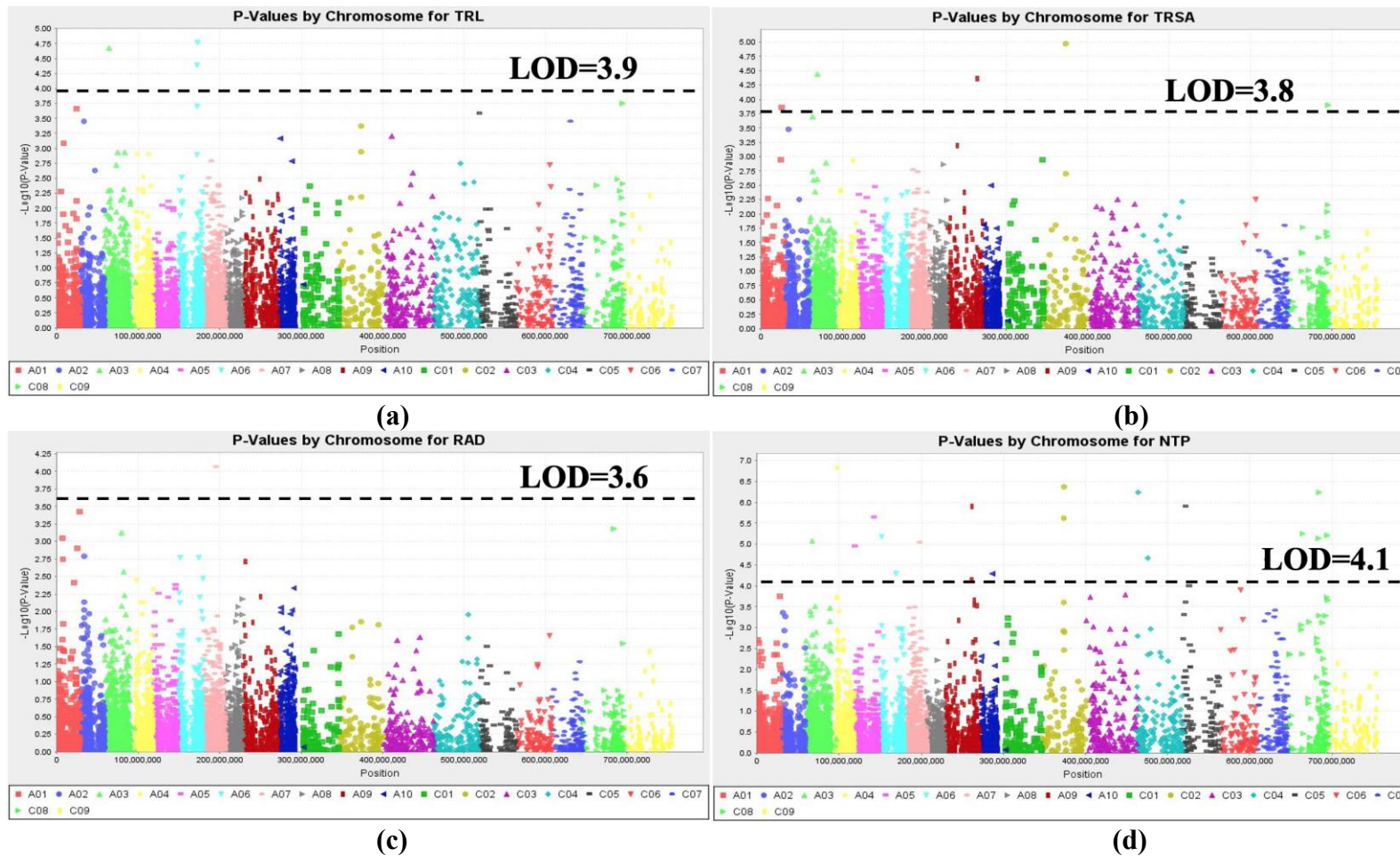


Figure 3.8 Manhattan plots of the PCA + K MLM models for identifying root system architecture (RSA) trait loci in 313 *Brassica* accessions representing five species, including *B. napus*, *B. oleracea*, *B. rapa*, *B. carinata* and *B. juncea*. The dashed horizontal lines indicate the Bonferroni-adjusted significance threshold (“logarithm-of-odds” (LOD) score). The dots above the significance threshold indicate SNPs associated with each trait.

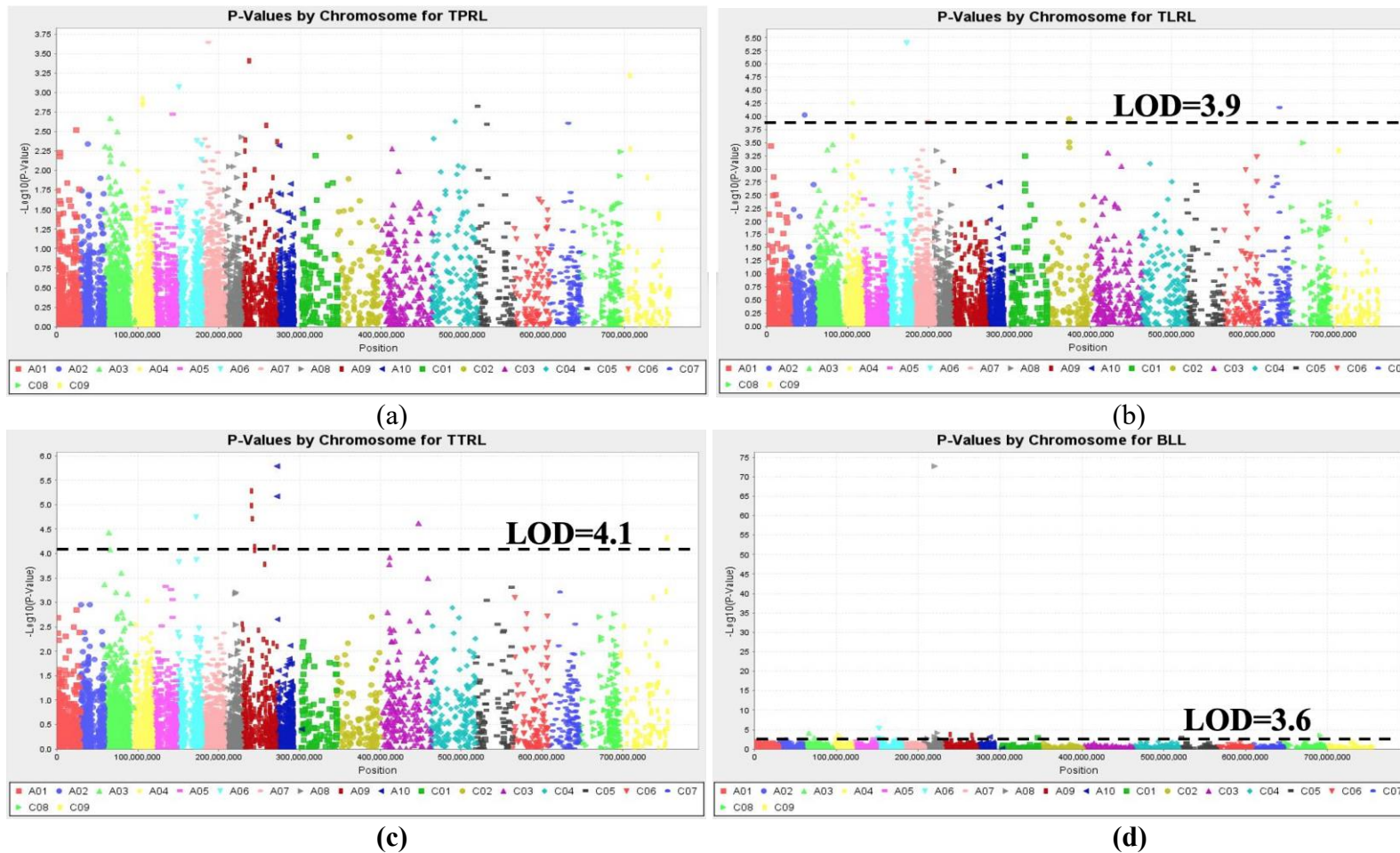


Figure 3.8 (continued) Manhattan plots of the PCA + K MLM models for identifying root system architecture (RSA) trait loci in 313 *Brassica* accessions representing five species, including *B. napus*, *B. oleracea*, *B. rapa*, *B. carinata*, and *B. juncea*. The dashed horizontal lines indicate the Bonferroni-adjusted significance threshold (“logarithm-of-odds” (LOD) score). The dots above the significance threshold indicate SNPs associated with each trait.

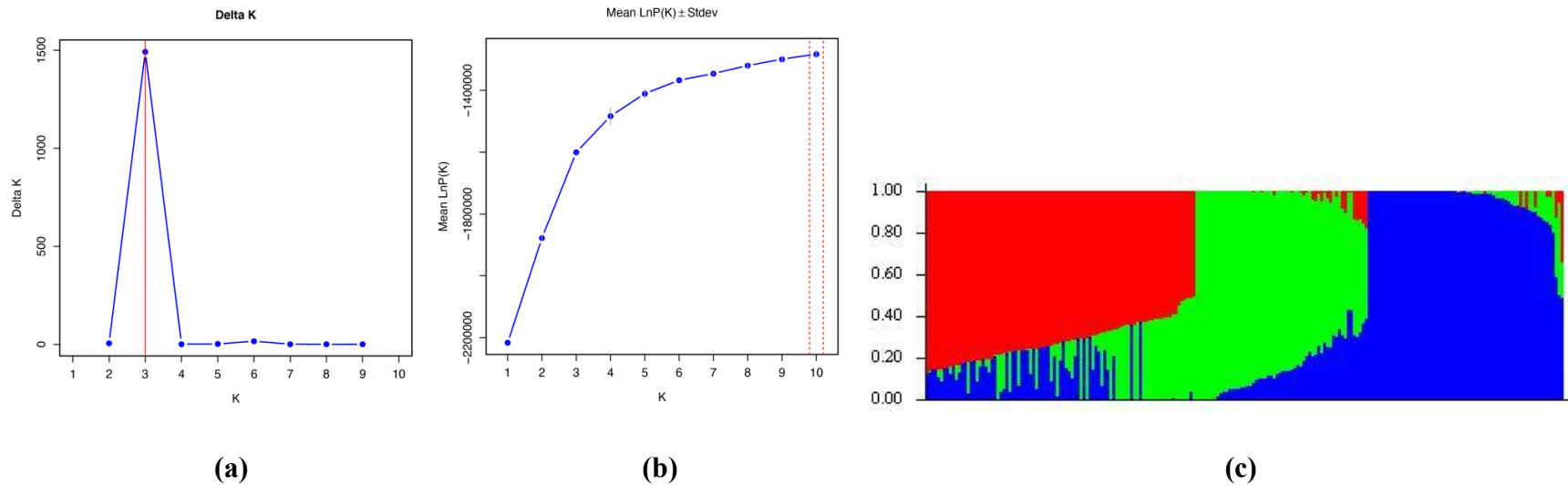


Figure 3.9 Bayesian cluster analysis of 313 *Brassica* accessions representing five species, including *B. napus*, *B. oleracea*, *B. rapa*, *B. carinata* and *B. juncea*, estimated with STRUCTURE based on 6,213 SNP markers using 50,000 burn-in iterations and Markov Chain Monte Carlo (MCMC) lengths. The value of K, determined following Evanno et al. (2005), and the population structure determined with the Puechmaille (2016) and Li and Liu (2018) alternative, indicated three clusters for all runs (a & b). Detailed Bayesian clustering of the 313 accessions is shown in (c), with each colour represents one ancestry component. The simplified view suggests three ancestral populations.

Chapter 4: Conclusions

4.1 Introduction

The genus *Brassica* comprises many agriculturally important crops, including *B. napus* L., *B. rapa* L., *B. nigra* (L.) Koch, *B. oleracea* L., *B. juncea* (L.) Czern & Coss, and *B. carinata* A. Braun (Branca and Cartea, 2011). *Brassica* species exhibit significant adaptability and resilience, and are able to grow under many conditions. Nonetheless, there is the potential for further improvement to enhance *Brassica* stress tolerance, traits of agronomic significance, and seed and oil quality (Sharma et al., 2022). One approach that can contribute to achieving these improvements is to target the root system architecture (RSA). The objectives of this thesis were to increase knowledge of *Brassica* root systems by evaluating RSA traits in a large collection of genotypes, and to identify genomic regions controlling these traits.

4.2 Optimizing the Evaluation of *Brassica* Root System Architectural Traits

In Chapter 2, a semi-hydroponic system was developed to determine the optimal timing for assessing root traits. Seedlings representing four *B. napus* genotypes were grown in rolls of germination paper in half-strength Hoagland's No. 2 Basal Salt Mixture (Sigma-Aldrich Co., Ontario, Canada) solution, with a suite of RSA traits assessed after 7, 14, and 21 days using WinRHIZO (Régent Instruments Inc., Quebec, Canada). At the 7-day mark, there were no notable disparities in root morphology among the *B. napus* cultivars, as the seedlings were still in their early stages of growth and lacked significant development. However, by day 14, the root systems had undergone substantial growth, displaying enhanced complexity and thereby enabling better differentiation between cultivars. By day 21, the root systems had matured further, but extracting the roots without overlap posed a challenge due to the large amounts of tissue. Consequently, the assessment of roots after 14 days in the Hoagland's solution was deemed as a reliable approach

that yielded accurate results within a reasonable timeframe. This methodology served as the basis for phenotyping *Brassica* roots in Chapter 3.

4.3 Evaluation of Root Architectural Traits in A Collection of *Brassica* Genotypes

In Chapter 3, the RSA traits of 379 *Brassica* genotypes were examined, including 68 *B. napus*, 64 *B. juncea*, 60 *B. rapa*, 66 *B. nigra*, 57 *B. oleracea*, and 28 *B. carinata* accessions. In addition, 25 Canadian canola (*B. napus*) cultivars and 13 hosts of the Canadian Clubroot Differential set (Strelkov et al., 2018) were also compared. Eight fundamental parameters related to root architecture were quantified, including total root length (TRL/cm per plant), total root surface area (TRSA/cm² per plant), average root diameter (RAD/mm per plant), number of tips (NTP per plant), total primary root length (TPRL/cm per plant), total lateral root length (TLRT/cm per plant), total tertiary root length (TTRL/cm per plant), and basal link length (BLL/cm per plant). Analysis of the phenotypic data indicated that among the studied species, *B. napus* and *B. oleracea* developed the most intricate and expansive root systems, showing higher values for six of the eight measured traits. In contrast, *B. nigra* possessed the smallest root systems. The two species *B. juncea* and *B. carinata* shared comparable root system complexity and had the largest average root diameter (RAD) compared with the other *Brassica* species, indicating the presence of thicker root systems. This comprehensive examination improved understanding of the diversity within *Brassica* root systems and laid a foundation for conducting genome-wide association studies (GWAS).

Single nucleotide polymorphism (SNP) genotyping was carried out on 313 of the *Brassica* accessions (the 66 *B. nigra* accessions were excluded, as explained in Chapter 3). After data filtering, a set of 6,213 SNP markers was employed to conduct the GWAS. This marker set encompassed 5,103 markers on the A-genome and 1,110 markers on the C-genome, effectively

covering a genomic region of 302.5 Mb for the A-genome and 452.8 Mb for the C-genome. The GWAS identified 79 significant SNP markers associated with the eight root-related traits under investigation. These markers were distributed across the 18 chromosomes of *B. napus*, excluding chromosome C06. Among these markers, 65 were located on the A-genome, while 14 were found on the C-genome. Six markers were related to TRL, 9 to TRSA, 26 to RAD, 16 to TPRL, 12 to TTRL, 6 to BLL, 2 to TPRL/TRL and 2 to TTRL/TRL. No markers were associated with the number of tips (NTP) or total lateral root length (TLRL).

Further analysis indicated the presence of two pleiotropic SNP markers, Bn_scaff_1_p539478 and Bn_scaff_1_p41089, which exhibited associations with both TPRL and total root length (TRL), along with Bn_A03_p5039586 and Bn_A06_p17049401, which were linked to TTRL and TRL. The investigation of these SNP markers led to the identification of potential candidate genes, encompassing not only genes encoding proteins involved in plant root growth, such as cell wall synthesis, vesicle fusion, and cell growth, but also proteins associated with fundamental biological processes in plant development, including ATP binding, DNA binding, and mRNA binding. Furthermore, the analysis identified three genomic regions on chromosomes A03, A02, and A06 as hotspots harboring genes closely related to root traits, thereby opening up new avenues for further research and exploration.

4.4 Future studies

The findings derived from this research demonstrated significant variation in RSA traits among *Brassica* species, and enabled the detection of multiple markers associated with these traits. Nonetheless, these experiments were conducted under controlled conditions, which may not entirely reflect 'real-world' scenarios, and the SNP array utilized was limited to the A- and C-genomes. Consequently, further investigations integrating both morphological and genetic

analyses of root architecture in the *Brassicas*, which incorporate their responses to diverse stress conditions, are necessary. These studies would contribute to establishing the fundamental principles governing root traits in specific *Brassica* subspecies or for cultivar development. Such invaluable insights would facilitate a more targeted breeding approach based on RSA traits, facilitating the development of improved *Brassica* cultivars and contributing to future food security.

References

- Abdirad, S., Ghaffari, M. R., Majd, A., Irian, S., Soleymaniniya, A., Daryani, P., et al. (2022). Genome-wide expression analysis of root tips in contrasting rice genotypes revealed novel candidate genes for water stress adaptation. *Frontiers in Plant Science* 13, 792079. doi: 10.3389/fpls.2022.792079.
- Acinas, S. G., Sarma-Rupavtarm, R., Klepac-Ceraj, V., and Polz, M. F. (2005). PCR-induced sequence artifacts and bias: insights from comparison of two 16S rRNA clone libraries constructed from the same sample. *Applied and Environmental Microbiology* 71, 8966–8969. doi: 10.1128/AEM.71.12.8966-8969.2005.
- Admin (2015). Cover Crops, *Brassicas*. *Center for Agriculture, Food, and the Environment*. Available at: <https://ag.umass.edu/vegetable/fact-sheets/cover-crops-brassicas>.
- Akhtar, J., and Banga, S. S. (2015). Genome-wide association mapping for grain yield components and root traits in *Brassica juncea* (L.) Czern & Coss. *Molecular Breeding* 35, 48. doi: 10.1007/s11032-015-0230-8.
- Albery, W. J., Haggett, B. G. D., and Svanberg, L. R. (1985). The development of sensors for hydroponics. *Biosensors* 1, 369–397. doi: 10.1016/0265-928X(85)80006-7.
- Alcock, T. D., Havlickova, L., He, Z., Wilson, L., Bancroft, I., White, P. J., et al. (2018). Species-wide variation in shoot nitrate concentration, and genetic loci controlling nitrate, phosphorus and potassium accumulation in *Brassica napus* L. *Frontiers in Plant Science* 9. doi: 10.3389/fpls.2018.01487.
- Alvarez, S., Berla, B. M., Sheffield, J., Cahoon, R. E., Jez, J. M., and Hicks, L. M. (2009). Comprehensive analysis of the *Brassica juncea* root proteome in response to cadmium exposure by complementary proteomic approaches. *Proteomics* 9, 2419–2431. doi: 10.1002/pmic.200800478.
- Arif, M. R., Islam, M. T., and Robin, A. H. K. (2019). Salinity stress alters root morphology and root hair traits in *Brassica napus*. *Plants* 8, 192. doi: 10.3390/plants8070192.
- Arifuzzaman, M., Mamidi, S., McClean, P., and Rahman, M. (2016). QTL mapping for root vigor and days to flowering in *Brassica napus* L. *Canadian Journal of Plant Science*, CJPS-2016-0048. doi: 10.1139/CJPS-2016-0048.
- Arifuzzaman, M., Oladzadabbasabadi, A., McClean, P., and Rahman, M. (2019). Shovelomics for phenotyping root architectural traits of rapeseed/canola (*Brassica napus* L.) and genome-wide association mapping. *Molecular Genetics and Genomics* 294, 985–1000. doi: 10.1007/s00438-019-01563-x.
- Arifuzzaman, M., and Rahman, M. (2017). A Comparative study on root traits of spring and winter canola (*Brassica napus* L.) under controlled and water stressed conditions. *Journal of Agricultural Science* 9, 58. doi: 10.5539/jas.v9n7p58.

- Armengaud, P., Zambaux, K., Hills, A., Sulpice, R., Pattison, R. J., Blatt, M. R., et al. (2009). EZ-Rhizo: Integrated software for the fast and accurate measurement of root system architecture. *The Plant Journal* 57, 945–956. doi: 10.1111/j.1365-313X.2008.03739.x.
- Arnaud, C., Bonnot, C., Desnos, T., and Nussaume, L. (2010). The root cap at the forefront. *Comptes Rendus Biologies* 333, 335–343. doi: 10.1016/j.crvi.2010.01.011.
- Arsenault, J.-L., Poulcur, S., Messier, C., and Guay, R. (1995). WinRHIZO™, a root-measuring system with a unique overlap correction method. *HortScience* 30, 906D – 906. doi: 10.21273/HORTSCI.30.4.906D.
- Ashraf, M., and McNeilly, T. (2004). Salinity tolerance in *Brassica* oilseeds. *Critical Reviews in Plant Sciences* 23, 157–174. doi: 10.1080/07352680490433286.
- Ayele, M., Haas, B. J., Kumar, N., Wu, H., Xiao, Y., Van Aken, S., et al. (2005). Whole genome shotgun sequencing of *Brassica oleracea* and its application to gene discovery and annotation in *Arabidopsis*. *Genome Research* 15, 487–495. doi: 10.1101/gr.3176505.
- Bailey, P. H. J., Currey, J. D., and Fitter, A. H. (2002). The role of root system architecture and root hairs in promoting anchorage against uprooting forces in *Allium cepa* and root mutants of *Arabidopsis thaliana*. *Journal of Experimental Botany* 53, 333–340. doi: 10.1093/jexbot/53.367.333.
- Barber, S. A. (1995). Soil nutrient bioavailability: a mechanistic approach. *Soil Science* 161, 140-141. doi:10.1097/00010694-199602000-00012.
- Barro, F., and Martín, A. (1999). Response of different genotypes of *Brassica carinata* to microspore culture. *Plant Breeding* 118, 79–81. doi: 10.1046/j.1439-0523.1999.118001079.x.
- Baskin, T. I., Preston, S., Zelinsky, E., Yang, X., Elmali, M., Bellos, D., et al. (2020). Positioning the root elongation zone is saltatory and receives input from the shoot. *iScience* 23, 101309. doi: 10.1016/j.isci.2020.101309.
- Basu, P., Brown, K. M., and Pal, A. (2011). Detailed quantitative analysis of architectural traits of basal roots of young seedlings of bean in response to auxin and ethylene1. *Plant Physiology* 155, 2056–2065. doi: 10.1104/pp.110.168229.
- Basu, P., and Pal, A. (2011). Spatio-temporal analysis of development of basal roots of common bean (*Phaseolus vulgaris* L.). *Plant Signaling & Behavior* 6, 982–985. doi: 10.4161/psb.6.7.15460.
- Basu, P., and Pal, A. (2012). A new tool for analysis of root growth in the spatio-temporal continuum. *New Phytologist* 195, 264–274. doi: 10.1111/j.1469-8137.2012.04149.x.
- Basu, P., Zhang, Y.-J., Lynch, J. P., Brown, K. M., Basu, P., Zhang, Y.-J., et al. (2007). Ethylene modulates genetic, positional, and nutritional regulation of root plagiogravitropism. *Functional Plant Biology* 34, 41–51. doi: 10.1071/FP06209.

- Becker, H. C., Engqvist, G. M., and Karlsson, B. (1995). Comparison of rapeseed cultivars and resynthesized lines based on allozyme and RFLP markers. *Theoretical & Applied Genetics* 91, 62–67. doi: 10.1007/BF00220859.
- Bellucci, R., Martin, A., Bommarito, D., Wang, K., Hansen, S. H., Freeman, G. J., et al. (2015). Interferon- γ -induced activation of JAK1 and JAK2 suppresses tumor cell susceptibility to NK cells through upregulation of PD-L1 expression. *Oncoimmunology* 4, e1008824. doi: 10.1080/2162402X.2015.1008824.
- Bengough, A. G., Loades, K., and McKenzie, B. M. (2016). Root hairs aid soil penetration by anchoring the root surface to pore walls. *Journal of Experimental Botany* 67, 1071–1078. doi: 10.1093/jxb/erv560.
- Benjamini, Y., and Hochberg, Y. (1995). Controlling the false discovery rate: A practical and powerful approach to multiple testing. *Journal of the Royal Statistical Society: Series B (Methodological)* 57, 289–300. doi: 10.1111/j.2517-6161.1995.tb02031.x.
- Bingham, I. J., and Bengough, A. G. (2003). Morphological plasticity of wheat and barley roots in response to spatial variation in soil strength. *Plant and Soil* 250, 273–282. doi: 10.1023/A:1022891519039.
- Bouma, T. J., Nielsen, K. L., and Koutstaal, B. (2000). Sample preparation and scanning protocol for computerised analysis of root length and diameter. *Plant and Soil* 218, 185–196. doi: 10.1023/A:1014905104017.
- Brachi, B., Morris, G. P., and Borevitz, J. O. (2011). Genome-wide association studies in plants: the missing heritability is in the field. *Genome Biology* 12, 232. doi: 10.1186/gb-2011-12-10-232.
- Bradbury, P. J., Zhang, Z., Kroon, D. E., Casstevens, T. M., Ramdoss, Y., and Buckler, E. S. (2007). TASSEL: Software for association mapping of complex traits in diverse samples. *Bioinformatics* 23, 2633–2635. doi: 10.1093/bioinformatics/btm308.
- Brakenhoff, R. H., Schoenmakers, J. G. G., and Lubsen, N. H. (1991). Chimeric cDNA clones: A novel PCR artifact. *Nucleic Acids Research* 19, 1949. doi: 10.1093/nar/19.8.1949.
- Branca, F., and Cartea, E. (2011). “*Brassica*,” in *Wild Crop Relatives: Genomic and Breeding Resources*, ed. C. Kole (Berlin, Heidelberg: Springer Berlin Heidelberg), 17–36. doi: 10.1007/978-3-642-14871-2_2.
- Breseghele, F., and Sorrells, M. E. (2006). Association mapping of kernel size and milling quality in wheat (*Triticum aestivum* L.) cultivars. *Genetics* 172, 1165–1177. doi: 10.1534/genetics.105.044586.
- Burton, A. L., Williams, M., Lynch, J. P., and Brown, K. M. (2012). RootScan: Software for high-throughput analysis of root anatomical traits. *Plant Soil* 357, 189–203. doi: 10.1007/s11104-012-1138-2.

- Cajero Sánchez, W., García-Ponce, B., Sánchez, M. de la P., Álvarez-Buylla, E. R., and Garay-Arroyo, A. (2018). Identifying the transition to the maturation zone in three ecotypes of *Arabidopsis thaliana* roots. *Communicative & Integrative Biology* 11, e1395993. doi: 10.1080/19420889.2017.1395993.
- Cardone, M., Mazzoncini, M., Menini, S., Rocco, V., Senatore, A., Seggiani, M., et al. (2003). *Brassica carinata* as an alternative oil crop for the production of biodiesel in Italy: agronomic evaluation, fuel production by transesterification and characterization. *Biomass and Bioenergy* 25, 623–636. doi: 10.1016/S0961-9534(03)00058-8.
- Cardoza, V., and Stewart, C. N. (2004). *Brassica* biotechnology: Progress in cellular and molecular biology. *In Vitro Cellular & Developmental Biology - Plant* 40, 542–551. doi: 10.1079/IVP2004568.
- Chalhoub, B., Denoeud, F., Liu, S., Parkin, I. A. P., Tang, H., Wang, X., et al. (2014). Early allopolyploid evolution in the post-Neolithic *Brassica napus* oilseed genome. *Science* 345, 950–953. doi: 10.1126/science.1253435.
- Chen, Y., Ghanem, M. E., and Siddique, K. H. (2017). Characterising root trait variability in chickpea (*Cicer arietinum* L.) germplasm. *Journal of Experimental Botany* 68, 1987–1999. doi: 10.1093/jxb/erw368.
- Chen, Y. L., Dunbabin, V. M., Diggle, A. J., Siddique, K. H. M., and Rengel, Z. (2012). Assessing variability in root traits of wild *Lupinus angustifolius* germplasm: Basis for modelling root system structure. *Plant Soil* 354, 141–155. doi: 10.1007/s11104-011-1050-1.
- Chen, Y. L., Dunbabin, V. M., Postma, J. A., Diggle, A. J., Palta, J. A., Lynch, J. P., et al. (2011). Phenotypic variability and modelling of root structure of wild *Lupinus angustifolius* genotypes. *Plant Soil* 348, 345–364. doi: 10.1007/s11104-011-0939-z.
- Chen, Y., Palta, J., Prasad, P. V. V., and Siddique, K. H. M. (2020). Phenotypic variability in bread wheat root systems at the early vegetative stage. *BMC Plant Biology* 20, 185. doi: 10.1186/s12870-020-02390-8.
- Chen, Y., Shan, F., Nelson, M. N., Siddique, K. H., and Rengel, Z. (2016). Root trait diversity, molecular marker diversity, and trait-marker associations in a core collection of *Lupinus angustifolius*. *Journal of Experimental Botany* 67, 3683–3697. doi: 10.1093/jxb/erw127.
- Choi, H.-S., and Cho, H.-T. (2019). Root hairs enhance *Arabidopsis* seedling survival upon soil disruption. *Scientific Reports* 9, 11181. doi: 10.1038/s41598-019-47733-0.
- Cichy, K. A., Snapp, S. S., and Kirk, W. W. (2007). Fusarium root rot incidence and root system architecture in grafted common bean lines. *Plant Soil* 300, 233–244. doi: 10.1007/s11104-007-9408-0.
- Clark, R. T., Famoso, A. N., Zhao, K., Shaff, J. E., Craft, E. J., Bustamante, C. D., et al. (2013). High-throughput two-dimensional root system phenotyping platform facilitates genetic

- analysis of root growth and development. *Plant Cell & Environment* 36, 454–466. doi: 10.1111/j.1365-3040.2012.02587.x.
- Clark, R. T., MacCurdy, R. B., Jung, J. K., Shaff, J. E., McCouch, S. R., Aneshansley, D. J., et al. (2011). Three-dimensional root phenotyping with a novel imaging and software platform. *Plant Physiology* 156, 455–465. doi: 10.1104/pp.110.169102.
- Clarke, W. E., Higgins, E. E., Plieske, J., Wieseke, R., Sidebottom, C., Khedikar, Y., et al. (2016). A high-density SNP genotyping array for *Brassica napus* and its ancestral diploid species based on optimised selection of single-locus markers in the allotetraploid genome. *Theoretical & Applied Genetics* 129, 1887–1899. doi: 10.1007/s00122-016-2746-7.
- Cline, J., Braman, J. C., and Hogrefe, H. H. (1996). PCR fidelity of Pfu DNA polymerase and other thermostable DNA polymerases. *Nucleic Acids Research* 24, 3546–3551. doi: 10.1093/nar/24.18.3546.
- Collard, B. C. Y., and Mackill, D. J. (2008). Marker-assisted selection: an approach for precision plant breeding in the twenty-first century. *Philosophical Transactions of the Royal Society B: Biological Sciences* 363, 557–572. doi: 10.1098/rstb.2007.2170.
- Comas, L., Becker, S., Cruz, V. M., Byrne, P. F., and Dierig, D. A. (2013). Root traits contributing to plant productivity under drought. *Frontiers in Plant Science* 4, 442. doi: 10.3389/fpls.2013.00442.
- Courtois, B., Audebert, A., Dardou, A., Roques, S., Herrera, T. G., Droc, G., et al. (2013). Genome-wide association mapping of root traits in a Japonica rice panel. *PLoS ONE* 8, e78037. doi: 10.1371/journal.pone.0078037.
- Davydenko, K., Nowakowska, J., Kaluski, T., Gawlak, M., Sadowska, K., García, J., et al. (2018). A Comparative study of the pathogenicity of *Fusarium circinatum* and other *Fusarium* species in Polish provenances of *P. sylvestris* L. *Forests* 9, 560. doi: 10.3390/f9090560.
- de Dorlodot, S., Forster, B., Pagès, L., Price, A., Tuberosa, R., and Draye, X. (2007). Root system architecture: opportunities and constraints for genetic improvement of crops. *Trends in Plant Science* 12, 474–481. doi: 10.1016/j.tplants.2007.08.012.
- Deak, K. I., and Malamy, J. (2005). Osmotic regulation of root system architecture. *The Plant Journal* 43, 17–28. doi: 10.1111/j.1365-313X.2005.02425.x.
- Delourme, R., Falentin, C., Fomeju, B. F., Boillot, M., Lassalle, G., André, I., et al. (2013). High-density SNP-based genetic map development and linkage disequilibrium assessment in *Brassica napus* L. *BMC Genomics* 14, 120. doi: 10.1186/1471-2164-14-120.
- Desgroux, A., Baudais, V. N., Aubert, V., Le Roy, G., de Larambergue, H., Miteul, H., et al. (2018). Comparative genome-wide-association mapping identifies common loci

- controlling root system architecture and resistance to *Aphanomyces euteiches* in Pea. *Frontiers in Plant Science* 8, 2195. doi:10.3389/fpls.2017.02195.
- Diers, B. W., and Osborn, T. C. (1994). Genetic diversity of oilseed *Brassica napus* germ plasm based on restriction fragment length polymorphisms. *Theoretical & Applied Genetics* 88, 662–668. doi: 10.1007/BF01253968.
- Diggle, A. J. (1988). ROOTMAP—a model in three-dimensional coordinates of the growth and structure of fibrous root systems. *Plant Soil* 105, 169–178. doi: 10.1007/BF02376780.
- Dixon, G. R. (2006). “Origins and diversity of *Brassica* and its relatives,” in *Vegetable brassicas and related crucifers*, ed. G. R. Dixon (Wallingford: CABI), 1–33. doi: 10.1079/9780851993959.0001.
- Dun, X., Tao, Z., Wang, J., Wang, X., Liu, G., and Wang, H. (2016). Comparative Transcriptome Analysis of Primary Roots of *Brassica napus* Seedlings with Extremely Different Primary Root Lengths Using RNA Sequencing. *Frontiers in Plant Science* 7. doi: 10.3389/fpls.2016.01238.
- Duncan, D. B. (1955). Multiple Range and Multiple F Tests. *Biometrics* 11, 1–42. doi: 10.2307/3001478.
- Ecke, W., Clemens, R., Honsdorf, N., and Becker, H. C. (2010). Extent and structure of linkage disequilibrium in canola quality winter rapeseed (*Brassica napus* L.). *Theoretical & Applied Genetics* 120, 921–931. doi: 10.1007/s00122-009-1221-0.
- Engels, C., and Marschner, H. (1992). Adaptation of potassium translocation into the shoot of maize (*Zea mays*) to shoot demand: Evidence for xylem loading as a regulating step. *Physiologia Plantarum* 86, 263–268. doi: 10.1034/j.1399-3054.1992.860211.x.
- Evanno, G., Regnaut, S., and Goudet, J. (2005). Detecting the number of clusters of individuals using the software structure: a simulation study. *Molecular Ecology* 14, 2611–2620. doi: 10.1111/j.1365-294X.2005.02553.x.
- Falk, K. G., Jubery, T. Z., O’Rourke, J. A., Singh, A., Sarkar, S., Ganapathysubramanian, B., et al. (2020). Soybean root system architecture trait study through genotypic, phenotypic, and shape-based clusters. *Plant Phenomics* 2020, 2020/1925495. doi: 10.34133/2020/1925495.
- Ferreira, M. E., Satagopan, J., Yandell, B. S., Williams, P. H., and Osborn, T. C. (1995). Mapping loci controlling vernalization requirement and flowering time in *Brassica napus*. *Theoretical & Applied Genetics* 90, 727–732. doi: 10.1007/BF00222140.
- Fletcher, R. S., Herrmann, D., Mullen, J. L., Li, Q., Schrider, D. R., Price, N., et al. (2016). Identification of polymorphisms associated with drought adaptation QTL in *Brassica napus* by resequencing. *G3 (Bethesda, Md.)* 6, 793–803. doi: 10.1534/g3.115.021279.

- Flint-Garcia, S., Thornsberry, J., and Buckler, E. (2003). Structure of linkage disequilibrium in plants. *Annual review of plant biology* 54, 357–74. doi: 10.1146/annurev.arplant.54.031902.134907.
- Forde, B. G. (2014). Nitrogen signalling pathways shaping root system architecture: an update. *Current Opinion in Plant Biology* 21, 30–36. doi: 10.1016/j.pbi.2014.06.004.
- Fredua-Agyeman, R., Yu, Z., Hwang, S.-F., and Strelkov, S. E. (2020). Genome-wide mapping of loci associated with resistance to clubroot in *Brassica napus* ssp. *napobrassica* (Rutabaga) accessions from Nordic countries. *Frontiers in Plant Science*. 11, 742. doi: 10.3389/fpls.2020.00742.
- French, A., Ubeda-Tomás, S., Holman, T. J., Bennett, M. J., and Pridmore, T. (2009). High-throughput quantification of root growth using a novel image-analysis tool. *Plant Physiology* 150, 1784–1795. doi: 10.1104/pp.109.140558.
- Fritsche-Neto, R., and Borém, A. eds. (2015). *Phenomics*. Cham: Springer International Publishing doi: 10.1007/978-3-319-13677-6.
- Gabelman, W. H., Gerloff, G. C., Schettini, T., and Coltman, R. (1986). Genetic variability in root systems associated with nutrient acquisition and use. *HortScience* 21, 971–973. doi: 10.21273/HORTSCI.21.4.971.
- Galkovskyi, T., Mileyko, Y., Bucksch, A., Moore, B., Symonova, O., Price, C. A., et al. (2012). GiA Roots: software for the high throughput analysis of plant root system architecture. *BMC Plant Biology* 12, 116. doi: 10.1186/1471-2229-12-116.
- Gallardo, M., Jackson, L. e., and Thompson, R. b. (1996). Shoot and root physiological responses to localized zones of soil moisture in cultivated and wild lettuce (*Lactuca* spp.). *Plant, Cell & Environment* 19, 1169–1178. doi: 10.1111/j.1365-3040.1996.tb00432.x.
- Ganal, M. W., Polley, A., Graner, E.-M., Plieske, J., Wieseke, R., Luerssen, H., et al. (2012). Large SNP arrays for genotyping in crop plants. *Journal of Biosciences* 37, 821–828. doi: 10.1007/s12038-012-9225-3.
- Goddard, M. E., and Hayes, B. J. (2009). Mapping genes for complex traits in domestic animals and their use in breeding programmes. *Nature Reviews. Genetics* 10, 381–391. doi: 10.1038/nrg2575.
- Gorim, L. Y., and Vandenberg, A. (2017). Root traits, nodulation and root distribution in soil for five wild lentil species and *Lens culinaris* (Medik.) grown under well-watered conditions. *Frontiers in Plant Science*. 8, 1632. doi: 10.3389/fpls.2017.01632.
- Govindaraj, M., Vetriventhan, M., and Srinivasan, M. (2015). Importance of genetic diversity assessment in crop plants and its recent advances: An overview of its analytical perspectives. *Genetics Research International* 2015, e431487. doi: 10.1155/2015/431487.

- Grierson, C., Nielsen, E., Ketelaarc, T., and Schiefelbein, J. (2014). Root hairs. *The Arabidopsis Book* 12, e0172. doi: 10.1199/tab.0172.
- Griffiths, M., Delory, B. M., Jawahir, V., Wong, K. M., Bagnall, G. C., Dowd, T. G., et al. (2022). Optimisation of root traits to provide enhanced ecosystem services in agricultural systems: A focus on cover crops. *Plant, Cell & Environment* 45, 751–770. doi: 10.1111/pce.14247.
- Gruber, B. D., Giehl, R. F. H., Friedel, S., and von Wirén, N. (2013). Plasticity of the Arabidopsis root system under nutrient deficiencies. *Plant Physiology* 163, 161–179. doi: 10.1104/pp.113.218453.
- Gu, R., Chen, F., Long, L., Cai, H., Liu, Z., Yang, J., et al. (2016). Enhancing phosphorus uptake efficiency through QTL-based selection for root system architecture in maize. *Journal of Genetics and Genomics* 43, 663–672. doi: 10.1016/j.jgg.2016.11.002.
- Gupta, B., and Huang, B. (2014). Mechanism of salinity tolerance in plants: Physiological, biochemical, and molecular characterization. *International Journal of Genomics* 2014, e701596. doi: 10.1155/2014/701596.
- Gupta, S. K. (2016). “Chapter 3 - Brassicas,” in *Breeding Oilseed Crops for Sustainable Production*, ed. S. K. Gupta (San Diego: Academic Press), 33–53. doi: 10.1016/B978-0-12-801309-0.00003-3.
- Hagerty, C. H., Cuesta-Marcos, A., Cregan, P. B., Song, Q., McClean, P., Noffsinger, S., et al. (2015). Mapping *Fusarium solani* and *Aphanomyces euteiches* root rot resistance and root architecture quantitative trait loci in common bean. *Crop Science* 55, 1969–1977. doi: 10.2135/cropsci2014.11.0805.
- Halder, T., Liu, H., Chen, Y., Yan, G., and Siddique, K. H. M. (2021). Identification of candidate genes for root traits using genotype–phenotype association analysis of near-isogenic lines in hexaploid wheat (*Triticum aestivum* L.). *International Journal of Molecular Sciences* 22, 3579. doi: 10.3390/ijms22073579.
- Hammond, J. P., Broadley, M. R., and White, P. J. (2004). Genetic responses to phosphorus deficiency. *Annals of Botany* 94, 323–332. doi: 10.1093/aob/mch156.
- Hammond, J. P., Broadley, M. R., White, P. J., King, G. J., Bowen, H. C., Hayden, R., et al. (2009). Shoot yield drives phosphorus use efficiency in *Brassica oleracea* and correlates with root architecture traits. *Journal of Experimental Botany* 60, 1953–1968. doi: 10.1093/jxb/erp083.
- Hasan, M. J., and Rahman, H. (2016). Genetics and molecular mapping of resistance to *Plasmodiophora brassicae* pathotypes 2, 3, 5, 6, and 8 in rutabaga (*Brassica napus* var. *napobrassica*). *Genome* 59, 805–815. doi: 10.1139/gen-2016-0034.
- Heinisch, O. (1962). Steel, R. G. D., and J. H. Torrie: principles and procedures of Sstatistics (with special reference to the biological sciences.) McGraw-Hill Book Company, New

- York, Toronto, London 1960, 481 S., 15 Abb.; 81 s 6 d. *Biometrische Zeitschrift* 4, 207–208. doi: 10.1002/bimj.19620040313.
- Hodge, A. (2004). The plastic plant: root responses to heterogeneous supplies of nutrients. *New Phytologist* 162, 9–24. doi: 10.1111/j.1469-8137.2004.01015.x.
- Hodge, A., Berta, G., Doussan, C., Merchan, F., and Crespi, M. (2009a). Plant root growth, architecture and function. *Plant Soil* 321, 153–187. doi: 10.1007/s11104-009-9929-9.
- Hodge, A., Berta, G., Doussan, C., Merchan, F., and Crespi, M. (2009b). Plant root growth, architecture and function. *Plant Soil* 321, 153–187. doi: 10.1007/s11104-009-9929-9.
- Hunter, P., Teakle, G., and Bending, G. (2014). Root traits and microbial community interactions in relation to phosphorus availability and acquisition, with particular reference to *Brassica*. *Frontiers in Plant Science* 5. doi: 10.3389/fpls.2014.00027.
- Ibrahim, S., Li, K., Ahmad, N., Kuang, L., Sadau, S. B., Tian, Z., et al. (2021). Genetic dissection of mature root characteristics by genome-wide association studies in rapeseed (*Brassica napus* L.). *Plants* 10, 2569. doi: 10.3390/plants10122569.
- Ingram, P. A., and Malamy, J. E. (2010). “Chapter 2 - Root system architecture,” in *Advances in Botanical Research*, eds. J.-C. Kader and M. Delseny (Academic Press), 75–117. doi: 10.1016/B978-0-12-380868-4.00002-8.
- Ito, O. (1996). Roots and nitrogen in cropping systems of the semi-arid tropics. *Japanese Journal of Soil Science & Plant Nutrition* 68.
- Jackson, L. E. (1995). Root architecture in cultivated and wild lettuce (*Lactuca* spp.). *Plant, Cell & Environment* 18, 885–894. doi: 10.1111/j.1365-3040.1995.tb00597.x.
- Jakobsen, B. F., and Dexter, A. R. (1987). Effect of soil structure on wheat root growth, water uptake and grain yield. A computer simulation model. *Soil and Tillage Research* 10, 331–345. doi: 10.1016/0167-1987(87)90022-5.
- Jannink, J.-L., Bink, M. C. A. M., and Jansen, R. C. (2001). Using complex plant pedigrees to map valuable genes. *Trends in Plant Science* 6, 337–342. doi: 10.1016/S1360-1385(01)02017-9.
- Jolliffe, I. T. (1986). *Principal Component Analysis*. New York, NY: Springer New York doi: 10.1007/978-1-4757-1904-8.
- Katori, T., Ikeda, A., Iuchi, S., Kobayashi, M., Shinozaki, K., Maehashi, K., et al. (2010). Dissecting the genetic control of natural variation in salt tolerance of *Arabidopsis thaliana* accessions. *Journal of Experimental Botany* 61, 1125–1138. doi: 10.1093/jxb/erp376.

- Kebede, B., Thiagarajah, M., Zimmerli, C., and Rahman, M. H. (2010). Improvement of open-pollinated spring rapeseed (*Brassica napus* L.) through introgression of genetic diversity from winter rapeseed. *Crop Science* 50, 1236–1243. doi: 10.2135/cropsci2009.06.0352.
- Khan, M. A., Gemenet, D. C., and Villordon, A. (2016). Root system architecture and abiotic stress tolerance: Current knowledge in root and tuber crops. *Frontiers in Plant Science* 7. doi: 10.3389/fpls.2016.01584.
- Kraft, J. M., and Boge, W. (2001). Root characteristics in pea in relation to compaction and Fusarium root rot. *Plant Disease* 85, 936–940. doi: 10.1094/PDIS.2001.85.9.936.
- Kuijken, R. C. P., van Eeuwijk, Fred. A., Marcelis, L. F. M., and Bouwmeester, H. J. (2015). Root phenotyping: From component trait in the lab to breeding: Table 1. *Journal of Experimental Botany* 66, 5389–5401. doi: 10.1093/jxb/erv239.
- Kulibaba, R. A., and Liashenko, Y. V. (2016). Influence of the PCR artifacts on the genotyping efficiency by the microsatellite loci using native polyacrylamide gel electrophoresis. *Cytology Genetics* 50, 162–167. doi: 10.3103/S0095452716030087.
- Kumar, V., Thakur, A. K., Barothia, N. D., and Chatterjee, S. S. (2011). Therapeutic potentials of *Brassica juncea*: An overview. *Tang [Humanitas Medicine]* 1, 2.1-2.16. doi: 10.5667/TANG.2011.0005.
- Landry, B. S., Hubert, N., Crete, R., Chang, M. S., Lincoln, S. E., and Etoh, T. (1992). A genetic map for *Brassica oleracea* based on RFLP markers detected with expressed DNA sequences and mapping of resistance genes to race 2 of *Plasmodiophora brassicae* (Woronin). *Genome* 35, 409–420. doi: 10.1139/g92-061.
- Le Bot, J., Serra, V., Fabre, J., Draye, X., Adamowicz, S., and Pagès, L. (2010). DART: a software to analyse root system architecture and development from captured images. *Plant Soil* 326, 261–273. doi: 10.1007/s11104-009-0005-2.
- Leitner, D., Felderer, B., Vontobel, P., and Schnepf, A. (2014). Recovering root system traits using image analysis exemplified by two-dimensional neutron radiography images of lupine. *Plant Physiology* 164, 24–35. doi: 10.1104/pp.113.227892.
- Leskovar, D. I., and Stoffella, P. J. (1995). Vegetable seedling root systems: Morphology, development, and importance. *HortSci* 30, 1153–1159. doi: 10.21273/HORTSCI.30.6.1153.
- Li, H., Torres-Garcia, J., Latrasse, D., Benhamed, M., Schilderink, S., Zhou, W., et al. (2017a). Plant-specific histone deacetylases HDT1/2 regulate GIBBERELLIN 2-OXIDASE2 expression to control Arabidopsis root meristem cell number. *The Plant Cell* 29, 2183–2196. doi: 10.1105/tpc.17.00366.
- Li, J., Han, Y., Liu, L., Chen, Y., Du, Y., Zhang, J., et al. (2015). qRT9, a quantitative trait locus controlling root thickness and root length in upland rice. *Journal of Experimental Botany* 66, 2723–2732. doi: 10.1093/jxb/erv076.

- Li, M., Naeem, M. S., Ali, S., Zhang, L., Liu, L., Ma, N., et al. (2017b). Leaf senescence, root morphology, and seed yield of winter oilseed rape (*Brassica napus* L.) at varying plant densities. *BioMed Research International* 2017, e8581072. doi: 10.1155/2017/8581072.
- Li, Y.-L., and Liu, J.-X. (2018). StructureSelector: A web-based software to select and visualize the optimal number of clusters using multiple methods. *Molecular Ecology Resources* 18, 176–177. doi: 10.1111/1755-0998.12719.
- Liu, L., Gan, Y., Bueckert, R., Van Rees, K., and Warkentin, T. (2010). Fine root distributions in oilseed and pulse crops. *Crop Science* 50, 222–226. doi: 10.2135/cropsci2009.03.0156.
- Liu, S., Begum, N., An, T., Zhao, T., Xu, B., Zhang, S., et al. (2021). Characterization of root system architecture traits in diverse soybean genotypes using a semi-hydroponic system. *Plants* 10, 2781. doi: 10.3390/plants10122781.
- Liu, S., Liu, Y., Yang, X., Tong, C., Edwards, D., Parkin, I. A. P., et al. (2014). The *Brassica oleracea* genome reveals the asymmetrical evolution of polyploid genomes. *Nature Communications* 5, 3930. doi: 10.1038/ncomms4930.
- Luc, J. E., Crow, W. T., Stimac, J. L., Sartain, J. B., and Giblin-Davis, R. M. (2006). Influence of *Belonolaimus longicaudatus* on nitrate leaching in Turf. *Journal of nematology* 38, 461–465. PMID: 19259464; PMCID: PMC2586471.
- Lynch, J. (1995). Root architecture and plant productivity. *Plant Physiology* 109, 7–13. doi: 10.1104/pp.109.1.7.
- Lynch, J. P. (2007). Roots of the second green revolution. *Australian Journal of Botany* 55, 493. doi: 10.1071/BT06118.
- Lynch, J. P. (2013). Steep, cheap and deep: An ideotype to optimize water and N acquisition by maize root systems. *Annals of Botany* 112, 347–357. doi: 10.1093/aob/mcs293.
- Lynch, J. P. (2015). Root phenes that reduce the metabolic costs of soil exploration: Opportunities for 21st century agriculture. *Plant, Cell & Environment* 38, 1775–1784. doi: 10.1111/pce.12451.
- Lynch, J. P. (2019). Root phenotypes for improved nutrient capture: An underexploited opportunity for global agriculture. *New Phytologist* 223, 548–564. doi: 10.1111/nph.15738.
- Lynch, J. P., and Brown, K. M. (2001). Topsoil foraging – an architectural adaptation of plants to low phosphorus availability. *Plant and Soil* 237, 225–237. doi: 10.1023/A:1013324727040.
- Lynch, J. P., and Wojciechowski, T. (2015). Opportunities and challenges in the subsoil: pathways to deeper rooted crops. *Journal of Experimental Botany* 66, 2199–2210. doi: 10.1093/jxb/eru508.

- Lynch, J., and van Beem, J. J. (1993). Growth and architecture of seedling roots of common bean genotypes. *Crop Science* 33, crops1993.0011183X003300060028x. doi: 10.2135/crops1993.0011183X003300060028x.
- Maggio, A., De Pascale, S., Ruggiero, C., and Barbieri, G. (2005). Physiological response of field-grown cabbage to salinity and drought stress. *European Journal of Agronomy* 23, 57–67. doi: 10.1016/j.eja.2004.09.004.
- Mairhofer, S., Zappala, S., Tracy, S. R., Sturrock, C., Bennett, M., Mooney, S. J., et al. (2012). RooTrak: automated recovery of three-dimensional plant root architecture in soil from X-ray microcomputed tomography images using visual tracking. *Plant Physiology* 158, 561–569. doi: 10.1104/pp.111.186221.
- Malamy, J. E. (2005). Intrinsic and environmental response pathways that regulate root system architecture. *Plant, Cell & Environment* 28, 67–77. doi: 10.1111/j.1365-3040.2005.01306.x.
- Marschner, P., Solaiman, Z., and Rengel, Z. (2007). *Brassica* genotypes differ in growth, phosphorus uptake and rhizosphere properties under P-limiting conditions. *Soil Biology and Biochemistry* 39, 87–98. doi: 10.1016/j.soilbio.2006.06.014.
- Mason, A. S., Higgins, E. E., Snowdon, R. J., Batley, J., Stein, A., Werner, C., et al. (2017). A user guide to the Brassica 60K Illumina Infinium™ SNP genotyping array. *Theoretical & Applied Genetics* 130, 621–633. doi: 10.1007/s00122-016-2849-1.
- Meister, R., Rajani, M. S., Ruzicka, D., and Schachtman, D. P. (2014). Challenges of modifying root traits in crops for agriculture. *Trends in Plant Science* 19, 779–788. doi: 10.1016/j.tplants.2014.08.005.
- Miguel, M. A., Widrig, A., Vieira, R. F., Brown, K. M., and Lynch, J. P. (2013). Basal root whorl number: A modulator of phosphorus acquisition in common bean (*Phaseolus vulgaris*). *Annals of Botany* 112, 973–982. doi: 10.1093/aob/mct164.
- Munns, R., and Tester, M. (2008). Mechanisms of salinity tolerance. *Annual Review of Plant Biology* 59, 651–681. doi: 10.1146/annurev.arplant.59.032607.092911.
- Neik, T. X., Barbetti, M. J., and Batley, J. (2017). Current status and challenges in identifying disease resistance genes in *Brassica napus*. *Frontiers in Plant Science* 8, 1788. doi: 10.3389/fpls.2017.01788.
- Nesi, N., Delourme, R., Brégeon, M., Falentin, C., and Renard, M. (2008). Genetic and molecular approaches to improve nutritional value of *Brassica napus* L. seed. *Comptes Rendus Biologies* 331, 763–771. doi: 10.1016/j.crv.2008.07.018.
- Nguyen, N. T., McInturf, S. A., and Mendoza-Cózatl, D. G. (2016). Hydroponics: A versatile system to study nutrient allocation and plant responses to nutrient availability and exposure to toxic elements. *Journal of Visualized Experiments*, e54317. doi: 10.3791/54317.

- Nishimura, C., Ohashi, Y., Sato, S., Kato, T., Tabata, S., and Ueguchi, C. (2004). Histidine kinase homologs that act as cytokinin receptors possess overlapping functions in the regulation of shoot and root growth in *Arabidopsis*. *The Plant Cell* 16, 1365–1377. doi: 10.1105/tpc.021477.
- Obayuwana, E., and Obayuwana, M. O. (2022). Ameliorative effects of aqueous extract of *Brassica nigra* on phenylhydrazine-induced liver toxicity in wistar rats. *Journal of Applied Sciences & Environmental Management* 26, 661–666. doi: 10.4314/jasem.v26i4.14.
- Paez-Garcia, A., Motes, C., Scheible, W.-R., Chen, R., Blancaflor, E., and Monteros, M. (2015). Root traits and phenotyping strategies for plant improvement. *Plants* 4, 334–355. doi: 10.3390/plants4020334.
- Pagès, L., Bécel, C., Boukcim, H., Moreau, D., Nguyen, C., and Voisin, A.-S. (2014). Calibration and evaluation of ArchiSimple, a simple model of root system architecture. *Ecological Modelling* 290, 76–84. doi: 10.1016/j.ecolmodel.2013.11.014.
- Pagès, L., Vercambre, G., Drouet, J.-L., Lecompte, F., Collet, C., and Le Bot, J. (2004). Root Typ: A generic model to depict and analyse the root system architecture. *Plant and Soil* 258, 103–119. doi: 10.1023/B:PLSO.0000016540.47134.03.
- Pang, W., Crow, W. T., Luc, J. E., McSorley, R., Giblin-Davis, R. M., Kenworthy, K. E., et al. (2011). Comparison of water displacement and WinRHIZO software for plant root parameter assessment. *Plant Disease* 95, 1308–1310. doi: 10.1094/PDIS-01-11-0026.
- Panjabi, P., Yadava, S. K., Kumar, N., Bangkim, R., and Ramchiary, N. (2019). “Breeding *Brassica juncea* and *B. rapa* for sustainable oilseed production in the changing climate: progress and prospects,” in *Genomic Designing of Climate-Smart Oilseed Crops*, ed. C. Kole (Cham: Springer International Publishing), 275–369. doi: 10.1007/978-3-319-93536-2_6.
- Perilli, S., Di Mambro, R., and Sabatini, S. (2012). Growth and development of the root apical meristem. *Current Opinion in Plant Biology* 15, 17–23. doi: 10.1016/j.pbi.2011.10.006.
- Piao, Z. Y., Deng, Y. Q., Choi, S. R., Park, Y. J., and Lim, Y. P. (2004). SCAR and CAPS mapping of CRb, a gene conferring resistance to *Plasmodiophora brassicae* in Chinese cabbage (*Brassica rapa* ssp. *pekinensis*). *Theoretical & Applied Genetics* 108, 1458–1465. doi: 10.1007/s00122-003-1577-5.
- Pierret, A., Gonkhamdee, S., Jourdan, C., and Maeght, J.-L. (2013). IJ_Rhizo: an open-source software to measure scanned images of root samples. *Plant Soil* 373, 531–539. doi: 10.1007/s11104-013-1795-9.
- Pongrac, P., Castillo-Michel, H., Reyes-Herrera, J., Hancock, R. D., Fischer, S., Kelemen, M., et al. (2020). Effect of phosphorus supply on root traits of two *Brassica oleracea* L. genotypes. *BMC Plant Biol* 20, 368. doi: 10.1186/s12870-020-02558-2.

- Postma, J. A., Dathe, A., and Lynch, J. P. (2014). The optimal lateral root branching density for maize depends on nitrogen and phosphorus availability. *Plant Physiology* 166, 590–602. doi: 10.1104/pp.113.233916.
- Postma, J. A., and Lynch, J. P. (2011). Root cortical aerenchyma enhances the growth of maize on soils with suboptimal availability of nitrogen, phosphorus, and potassium. *Plant Physiology* 156, 1190–1201. doi: 10.1104/pp.111.175489.
- Pound, M. P., French, A. P., Atkinson, J. A., Wells, D. M., Bennett, M. J., and Pridmore, T. (2013). RootNav: Navigating images of complex root architectures. *Plant Physiology* 162, 1802–1814. doi: 10.1104/pp.113.221531.
- Prince, S. J., Valliyodan, B., Ye, H., Yang, M., Tai, S., Hu, W., et al. (2019). Understanding genetic control of root system architecture in soybean: Insights into the genetic basis of lateral root number. *Plant, Cell & Environment* 42, 212–229. doi: 10.1111/pce.13333.
- Pritchard, J. K., Stephens, M., and Donnelly, P. (2000). Inference of Population Structure Using Multilocus Genotype Data. *Genetics* 155, 945–959. doi: 10.1093/genetics/155.2.945.
- Puechmaille, S. J. (2016). The program structure does not reliably recover the correct population structure when sampling is uneven: Subsampling and new estimators alleviate the problem. *Molecular Ecology Resources* 16, 608–627. doi: 10.1111/1755-0998.12512.
- Qanbari, S. (2019). On the extent of linkage disequilibrium in the genome of farm animals. *Frontiers in Genetics* 10, 1304. doi: 10.3389/fgene.2019.01304.
- Qian, L., Qian, W., and Snowdon, R. J. (2014). Sub-genomic selection patterns as a signature of breeding in the allopolyploid *Brassica napus* genome. *BMC Genomics* 15, 1170. doi: 10.1186/1471-2164-15-1170.
- Qiao, S., Fang, Y., Wu, A., Xu, B., Zhang, S., Deng, X., et al. (2019). Dissecting root trait variability in maize genotypes using the semi-hydroponic phenotyping platform. *Plant Soil* 439, 75–90. doi: 10.1007/s11104-018-3803-6.
- Qu, C., Jia, L., Fu, F., Zhao, H., Lu, K., Wei, L., et al. (2017). Genome-wide association mapping and identification of candidate genes for fatty acid composition in *Brassica napus* L. using SNP markers. *BMC Genomics* 18, 232. doi: 10.1186/s12864-017-3607-8.
- Qu, J., Kachman, S. D., Garrick, D., Fernando, R. L., and Cheng, H. (2020). Exact distribution of linkage disequilibrium in the presence of mutation, selection, or minor allele frequency filtering. *Frontiers in Genetics* 11. doi: 10.3389/fgene.2020.00362.
- Rahman, M., and McClean, P. (2013a). Genetic analysis on flowering time and root system in *Brassica napus* L. *Crop Science* 53, 141–147. doi: 10.2135/cropsci2012.02.0095.
- Rahman, M., and McClean, P. (2013b). Genetic analysis on flowering time and root system in *Brassica napus* L. *Crop Science* 53, 141–147. doi: 10.2135/cropsci2012.02.0095.

- Rakow, G. (2004). "Species origin and economic importance of *Brassica*," in *Brassica biotechnology in agriculture and forestry.*, eds. E.-C. Pua and C. J. Douglas (Berlin, Heidelberg: Springer), 3–11. doi: 10.1007/978-3-662-06164-0_1.
- Rangarajan, H., Postma, J. A., and Lynch, J. P. (2018). Co-optimization of axial root phenotypes for nitrogen and phosphorus acquisition in common bean. *Annals of Botany* 122, 485–499. doi: 10.1093/aob/mcy092.
- Raymer, P. L. (2002). Canola: an emerging oilseed crop. *In Trends in New Crops and New Uses* (ASHS Press), 122–126.
- Richardson, A. E., Hocking, P. J., Simpson, R. J., and George, T. S. (2009). Plant mechanisms to optimise access to soil phosphorus. *Crop Pasture Sci.* 60, 124. doi: 10.1071/CP07125.
- Riefler, M., Novak, O., Strnad, M., and Schmülling, T. (2006). Arabidopsis cytokinin receptor mutants reveal functions in shoot growth, leaf senescence, seed size, germination, root development, and cytokinin metabolism. *Plant Cell* 18, 40–54. doi: 10.1105/tpc.105.037796.
- Robinson, H., Kelly, A., Fox, G., Franckowiak, J., Borrell, A., and Hickey, L. (2018). Root architectural traits and yield: exploring the relationship in barley breeding trials. *Euphytica* 214, 151. doi: 10.1007/s10681-018-2219-y.
- Román-Avilés, B., Snapp, S. S., and Kelly, J. D. (2004). Assessing root traits associated with root rot resistance in common bean. *Field Crops Research* 86, 147–156. doi: 10.1016/j.fcr.2003.08.001.
- Rus, A., Baxter, I., Muthukumar, B., Gustin, J., Lahner, B., Yakubova, E., et al. (2006). Natural variants of AtHKT1 enhance Na⁺ accumulation in two wild populations of Arabidopsis. *PLoS Genetics* 2, e210. doi: 10.1371/journal.pgen.0020210.
- Saito, M., Kubo, N., Matsumoto, S., Suwabe, K., Tsukada, M., and Hirai, M. (2006). Fine mapping of the clubroot resistance gene, *Crr3*, in *Brassica rapa*. *Theoretical & Applied Genetics* 114, 81–91. doi: 10.1007/s00122-006-0412-1.
- Sanchez, A. c., Brar, D. s., Huang, N., Li, Z., and Khush, G. s. (2000). Sequence tagged site marker-assisted selection for three bacterial blight resistance genes in rice. *Crop Science* 40, 792–797. doi: 10.2135/cropsci2000.403792x.
- Saraswathi, D., Manibharathy, P., Gokulnath, R., Sureshkumar, E., and Karthikeyan, K. (2018). Automation of hydroponics green house farming using IOT. *IEEE International Conference on System, Computation, Automation and Networking (ICSCA)*, 1–4. doi: 10.1109/ICSCAN.2018.8541251.
- Schaal, B. A., Hayworth, D. A., Olsen, K. M., Rauscher, J. T., and Smith, W. A. (1998). Phylogeographic studies in plants: problems and prospects. *Molecular Ecology* 7, 465–474. doi: 10.1046/j.1365-294x.1998.00318.x.

- Schnepf, A., Leitner, D., Landl, M., Lobet, G., Mai, T. H., Morandage, S., et al. (2018). CRootBox: a structural–functional modelling framework for root systems. *Annals of Botany* 121, 1033–1053. doi: 10.1093/aob/mcx221.
- Schwartz, B. M., Kenworthy, K. E., Crow, W. T., Ferrell, J. A., Miller, G. L., and Quesenberry, K. H. (2010). Variable responses of zoysiagrass genotypes to the sting nematode. *Crop Science* 50, 723–729. doi: 10.2135/cropsci2008.11.0672.
- Shan, X., Blake, T. K., and Talbert, L. E. (1999). Conversion of AFLP markers to sequence-specific PCR markers in barley and wheat. *Theoretical & Applied Genetics* 98, 1072–1078. doi: 10.1007/s001220051169.
- Sharma, H. K., Singh, V. V., Kumar, A., Meena, H. S., Sharma, P., and Rai, P. K. (2022). “Genepools of *Brassica*,” in *The Brassica juncea genome compendium of plant genomes.*, eds. C. Kole and T. Mohapatra (Cham: Springer International Publishing), 57–72. doi: 10.1007/978-3-030-91507-0_4.
- Sharp, P. J., Johnston, S., Brown, G., McIntosh, R. A., Pallotta, M., Carter, M., et al. (2001). Validation of molecular markers for wheat breeding. *Aust. J. Agric. Res.* 52, 1357–1366. doi: 10.1071/ar01052.
- Shekhawat, K., Rathore, S. S., Premi, O. P., Kandpal, B. K., and Chauhan, J. S. (2012). Advances in agronomic management of Indian mustard (*Brassica juncea* (L.) Czernj. Cosson): An overview. *International Journal of Agronomy* 2012, 1–14. doi: 10.1155/2012/408284.
- Shi, L., Shi, T., Broadley, M. R., White, P. J., Long, Y., Meng, J., et al. (2013). High-throughput root phenotyping screens identify genetic loci associated with root architectural traits in *Brassica napus* under contrasting phosphate availabilities. *Annals of Botany* 112, 381–389. doi: 10.1093/aob/mcs245.
- Smith, A. G., Petersen, J., Selvan, R., and Rasmussen, C. R. (2020). Segmentation of roots in soil with U-Net. *Plant Methods* 16, 13. doi: 10.1186/s13007-020-0563-0.
- Smith, S., and De Smet, I. (2012). Root system architecture: insights from *Arabidopsis* and cereal crops. *Philosophical Transactions of the Royal Society B: Biological Sciences* 367, 1441–1452. doi: 10.1098/rstb.2011.0234.
- Snapp, S., Kirk, W., Román-Avilés, B., and Kelly, J. (2003). Root traits play a role in integrated management of Fusarium root rot in snap beans. *HortSci* 38, 187–191. doi: 10.21273/HORTSCI.38.2.187.
- Snapp, S., Koide, R., and Lynch, J. (1995). Exploitation of localized phosphorus-patches by common bean roots. *Plant Soil* 177, 211–218. doi: 10.1007/BF00010127.
- So, K. K. Y., and Duncan, R. W. (2021). Breeding canola (*Brassica napus* L.) for protein in feed and food. *Plants* 10, 2220. doi: 10.3390/plants10102220.

- Steele, K. A., Price, A. H., Shashidhar, H. E., and Witcombe, J. R. (2006). Marker-assisted selection to introgress rice QTLs controlling root traits into an Indian upland rice variety. *Theoretical & Applied Genetics* 112, 208–221. doi: 10.1007/s00122-005-0110-4.
- Strelkov, S. E., Hwang, S.-F., Manolii, V. P., Cao, T., Fredua-Agyeman, R., Harding, M. W., et al. (2018). Virulence and pathotype classification of *Plasmodiophora brassicae* populations collected from clubroot resistant canola (*Brassica napus*) in Canada. *Canadian Journal of Plant Pathology* 40, 284–298. doi: 10.1080/07060661.2018.1459851.
- Sun, X., Ren, W., Wang, P., Chen, F., Yuan, L., Pan, Q., et al. (2021). Evaluation of maize root growth and genome-wide association studies of root traits in response to low nitrogen supply at seedling emergence. *The Crop Journal* 9, 794–804. doi: 10.1016/j.cj.2020.09.011.
- Suwabe, K., Tsukazaki, H., Iketani, H., Hatakeyama, K., Kondo, M., Fujimura, M., et al. (2006). Simple sequence repeat-based comparative genomics between *Brassica rapa* and *Arabidopsis thaliana*: The genetic origin of clubroot resistance. *Genetics* 173, 309–319. doi: 10.1534/genetics.104.038968.
- Svistoonoff, S., Creff, A., Reymond, M., Sigoillot-Claude, C., Ricaud, L., Blanchet, A., et al. (2007). Root tip contact with low-phosphate media reprograms plant root architecture. *Nature Genetics* 39, 792–796. doi: 10.1038/ng2041.
- Syvänen, A.-C. (2001). Accessing genetic variation: genotyping single nucleotide polymorphisms. *Nature Reviews Genetics* 2, 930–942. doi: 10.1038/35103535.
- Tanaka, N., Kato, M., Tomioka, R., Kurata, R., Fukao, Y., Aoyama, T., et al. (2014). Characteristics of a root hair-less line of *Arabidopsis thaliana* under physiological stresses. *Journal of Experimental Botany* 65, 1497–1512. doi: 10.1093/jxb/eru014.
- Tennant, D. (1975). A test of a modified line intersect method of estimating root length. *Journal of Ecology* 63, 995–1001. doi: 10.2307/2258617.
- Thomas, C. L., Alcock, T. D., Graham, N. S., Hayden, R., Matterson, S., Wilson, L., et al. (2016). Root morphology and seed and leaf ionic traits in a *Brassica napus* L. diversity panel show wide phenotypic variation and are characteristic of crop habit. *BMC Plant Biol* 16, 214. doi: 10.1186/s12870-016-0902-5.
- Tong, J., Walk, T. C., Han, P., Chen, L., Shen, X., Li, Y., et al. (2020). Genome-wide identification and analysis of high-affinity nitrate transporter 2 (NRT2) family genes in rapeseed (*Brassica napus* L.) and their responses to various stresses. *BMC Plant Biology* 20, 464. doi: 10.1186/s12870-020-02648-1.
- Ueno, H., Matsumoto, E., Aruga, D., Kitagawa, S., Matsumura, H., and Hayashida, N. (2012). Molecular characterization of the CRA gene conferring clubroot resistance in *Brassica rapa*. *Plant Mol Biol* 80, 621–629. doi: 10.1007/s11103-012-9971-5.

- Uga, Y., Sugimoto, K., Ogawa, S., Rane, J., Ishitani, M., Hara, N., et al. (2013). Control of root system architecture by DEEPER ROOTING 1 increases rice yield under drought conditions. *Nature Genetics* 45, 1097–1102. doi: 10.1038/ng.2725.
- Vercambre, G., Pagès, L., Doussan, C., and Habib, R. (2003). Architectural analysis and synthesis of the plum tree root system in an orchard using a quantitative modelling approach. *Plant and Soil* 251, 1–11. doi: 10.1023/A:1022961513239.
- Voorrips, R. E., and Visser, D. L. (1993). Examination of resistance to clubroot in accessions of *Brassica oleracea* using a glasshouse seedling test. *Netherlands Journal of Plant Pathology* 99, 269–276. doi: 10.1007/BF01974308.
- Waisel, Y., Eshel, A., and Kafkafi, U. eds. (2002). *Plant roots: the hidden half*. 3rd ed., rev.expanded. New York: M. Dekker.
- Walch-Liu, P., Ivanov, I. I., Filleur, S., Gan, Y., Remans, T., and Forde, B. G. (2006). Nitrogen regulation of root branching. *Annals of Botany* 97, 875–881. doi: 10.1093/aob/mcj601.
- Wang, H., Inukai, Y., and Yamauchi, A. (2006). Root development and nutrient uptake. *Critical Reviews in Plant Sciences* 25, 279–301. doi: 10.1080/07352680600709917.
- Wang, J., Chen, Y., Zhang, Y., Zhang, Y., Ai, Y., Feng, Y., et al. (2021). Phenotyping and validation of root morphological traits in barley (*Hordeum vulgare* L.). *Agronomy* 11, 1583. doi: 10.3390/agronomy11081583.
- Wang, J., Kuang, L., Wang, X., Liu, G., Dun, X., and Wang, H. (2019). Temporal genetic patterns of root growth in *Brassica napus* L. revealed by a low-cost, high-efficiency hydroponic system. *Theoretical & Applied Genetics* 132, 2309–2323. doi: 10.1007/s00122-019-03356-7.
- Wang, M.-B., and Zhang, Q. (2009). Issues in using the WinRHIZO system to determine physical characteristics of plant fine roots. *Acta Ecologica Sinica* 29, 136–138. doi: 10.1016/j.chnaes.2009.05.007.
- Wang, X., Chen, Y., Thomas, C. L., Ding, G., Xu, P., Shi, D., et al. (2017). Genetic variants associated with the root system architecture of oilseed rape (*Brassica napus* L.) under contrasting phosphate supply. *DNA Research* 24, 407–417. doi: 10.1093/dnares/dsx013.
- Wang, X., Torres, M. J., Pierce, G., Lemke, C., Nelson, L. K., Yuksel, B., et al. (2011). A physical map of *Brassica oleracea* shows complexity of chromosomal changes following recursive paleopolyploidizations. *BMC Genomics* 12, 470. doi: 10.1186/1471-2164-12-470.
- Wasson, A. P., Richards, R. A., Chatrath, R., Misra, S. C., Prasad, S. V. S., Rebetzke, G. J., et al. (2012). Traits and selection strategies to improve root systems and water uptake in water-limited wheat crops. *Journal of Experimental Botany* 63, 3485–3498. doi: 10.1093/jxb/ers111.

- Wen, Z., Li, H., Shen, Q., Tang, X., Xiong, C., Li, H., et al. (2019). Tradeoffs among root morphology, exudation and mycorrhizal symbioses for phosphorus-acquisition strategies of 16 crop species. *New Phytologist* 223, 882–895. doi: 10.1111/nph.15833.
- White, P. J., George, T. S., Gregory, P. J., Bengough, A. G., Hallett, P. D., and McKenzie, B. M. (2013). Matching roots to their environment. *Annals of Botany* 112, 207–222. doi: 10.1093/aob/mct123.
- Williams, P. H., and Hill, C. B. (1986). Rapid-cycling populations of *Brassica*. *Science* 232, 1385–1389. doi: 10.1126/science.232.4756.1385.
- Won, S.-K., Lee, Y.-J., Lee, H.-Y., Heo, Y.-K., Cho, M., and Cho, H.-T. (2009). cis-Element- and transcriptome-based screening of root hair-specific genes and their functional characterization in *Arabidopsis*. *Plant Physiology* 150, 1459–1473. doi: 10.1104/pp.109.140905.
- Wu, Y., Xun, Q., Guo, Y., Zhang, J., Cheng, K., Shi, T., et al. (2016). Genome-wide expression pattern analyses of the *Arabidopsis* leucine-rich repeat receptor-like kinases. *Molecular Plant* 9, 289–300. doi: 10.1016/j.molp.2015.12.011.
- Yang, M., Ding, G., Shi, L., Feng, J., Xu, F., and Meng, J. (2010). Quantitative trait loci for root morphology in response to low phosphorus stress in *Brassica napus*. *Theoretical & Applied Genetics* 121, 181–193. doi: 10.1007/s00122-010-1301-1.
- Yu, J., Zhao, M., Wang, X., Tong, C., Huang, S., Tehrim, S., et al. (2013). Bolbase: a comprehensive genomics database for *Brassica oleracea*. *BMC Genomics* 14, 664. doi: 10.1186/1471-2164-14-664.
- Yu, Z., Fredua-Agyeman, R., Hwang, S.-F., and Strelkov, S. E. (2021). Molecular genetic diversity and population structure analyses of rutabaga accessions from Nordic countries as revealed by single nucleotide polymorphism markers. *BMC Genomics* 22, 442. doi: 10.1186/s12864-021-07762-4.
- Zhan, A., and Lynch, J. P. (2015). Reduced frequency of lateral root branching improves N capture from low-N soils in maize. *Journal of Experimental Botany* 66, 2055–2065. doi: 10.1093/jxb/erv007.
- Zhan, A., Schneider, H., and Lynch, J. P. (2015). Reduced lateral root branching density improves drought tolerance in maize. *Plant Physiology* 168, 1603–1615. doi: 10.1104/pp.15.00187.
- Zhang, T., Zhao, Z., Zhang, C., Pang, W., Choi, S. R., Lim, Y. P., et al. (2014). Fine genetic and physical mapping of the CRb gene conferring resistance to clubroot disease in *Brassica rapa*. *Molecular Breeding* 34, 1173–1183. doi: 10.1007/s11032-014-0108-1.
- Zhang, Y., Thomas, C. L., Xiang, J., Long, Y., Wang, X., Zou, J., et al. (2016). QTL meta-analysis of root traits in *Brassica napus* under contrasting phosphorus supply in two growth systems. *Scientific Reports* 6, 33113. doi: 10.1038/srep33113.

- Zhao, J., Fu, J., Liao, H., Yong, H., Hai, N., Yueming, H., et al. (2004). Characterization of root architecture in an applied core collection for phosphorus efficiency of soybean germplasm. *Scientific Reports* 49, 10. doi: 10.1360/04wc0142.
- Zhou, Q., Zhou, C., Zheng, W., Mason, A. S., Fan, S., Wu, C., et al. (2017). Genome-wide SNP markers based on SLAF-Seq uncover breeding traces in rapeseed (*Brassica napus* L.). *Frontiers in Plant Science* 8, 648. doi: 10.3389/fpls.2017.00648.
- Zhu, J., Ingram, P. A., Benfey, P. N., and Elich, T. (2011). From lab to field, new approaches to phenotyping root system architecture. *Current Opinion in Plant Biology* 14, 310–317. doi: 10.1016/j.pbi.2011.03.020.
- Zobel, R. W. (1995). Genetic and environmental aspects of roots and seedling stress. *HortSci* 30, 1189–1192. doi: 10.21273/HORTSCI.30.6.1189.
- Zobel, R. W., Kinraide, T. B., and Baligar, V. C. (2007). Fine root diameters can change in response to changes in nutrient concentrations. *Plant Soil* 297, 243–254. doi: 10.1007/s11104-007-9341-2.
- Zobel, R. W., and Waisel, Y. (2010). A plant root system architectural taxonomy: A framework for root nomenclature. *Plant Biosystems - An International Journal Dealing with all Aspects of Plant Biology* 144, 507–512. doi: 10.1080/11263501003764483.
- Zondervan, K. T., and Cardon, L. R. (2004). The complex interplay among factors that influence allelic association. *Nature Reviews Genetics* 5, 89–100. doi: 10.1038/nrg1270.

Appendix

Table A1. List of 379 genotypes of *Brassica* used in the root system architecture studies under semi-hydroponic system. Information about *Brassica* species, genotypes #, root traits including total root length (TRL/cm per plant), total surface area of roots (TRSA/cm² per plant), average root diameter (RAD/cm per plant), number of tips (NTP per plant), total primary root length (TPRL/cm per plant), total lateral root length (TLRT/cm per plant), total tertiary root length (TTRL/cm per plant), basal link length (BLL/cm per plant) and root size of small, medium and large were provided.

Table A1a. Commercial lines

Genotypes #	TRL	TRSA	RAD	NTP	TPRL	TLRL	TTRL	BLL	Root Size
5770	165.53	14.48	0.27	636.69	26.62	100.53	14.78	1.57	Large
7454	280.4	33.61	0.37	1910.06	37.21	137.97	24.48	1.3	Large
08N823R	81.76	6.24	0.25	173.25	18.18	53.63	6.32	1.16	Small
45CM39	288.97	34.49	0.38	1682.5	27.61	141.05	46.37	1.37	Large
45CS40	175.99	13.24	0.25	280.88	30.25	114.94	20.18	1.19	Large
45H26	212.85	21.63	0.32	806.75	31.1	131.74	20.33	1.27	Large
45H29	175.1	18.92	0.34	1166.44	20.62	75.51	25.8	1.32	Large
45H31	183.89	17.42	0.29	517.63	27.48	115.5	22.3	1.59	Large
45M35	296.5	39.44	0.42	1131.75	39.59	171.69	37.68	1.28	Large
6207TF	126.84	8.79	0.22	197.56	27.27	92.84	6.61	1.56	Medium
6056CR	190.34	14.03	0.23	384.38	31.24	124.84	23.53	1.4	Large
7444BL	349.98	43.65	0.39	1529.88	38.27	228.04	22.55	1.48	Large
9558C	206.9	26.49	0.4	868.06	32.27	122.62	21.15	1.75	Large
Brevant3010	279.24	35.98	0.41	1295.25	33.37	154.5	30.77	1.86	Large
Brutor	301.55	41.72	0.44	930.63	38.27	162.06	57.19	1.79	Large
BY6204	253.26	17.98	0.23	428.69	36.69	162.75	41.71	1.37	Large
CS2000	324.8	31.43	0.3	868.63	39.6	224.39	36.18	1.39	Large
CS2600	252.57	29.86	0.38	1491.5	34.25	141.72	12	1.38	Large
D3155C	242.63	26.1	0.32	1693.81	30.22	118.07	28.95	1.47	Large
DKTF98CR	266.07	19.58	0.23	484.19	42.11	189.29	22.4	1.96	Large
L150	192.27	22.43	0.37	1280.13	31.51	89.51	5.63	1.75	Large
L234PC	148.98	18.41	0.39	929.94	23.3	76.91	7.94	1.39	Large
L241	289.32	32.91	0.35	1202.69	37.18	167.02	39.67	1.89	Large
L255PC	272.69	19.5	0.23	491.44	35.91	180.24	36.46	1.47	Large
L343PC	224.92	15.16	0.21	525.75	37.14	152.95	22.05	1.65	Large
L345PC	338.73	36.79	0.35	2753.19	36.9	159.49	16.5	2.11	Large
Laurentian	170.28	10.94	0.2	628.25	30.99	104.21	22.34	1.2	Large
Mendel	388.51	44.36	0.36	1622.38	42.4	249.93	30.95	1.76	Large
P501L	414.51	52.98	0.41	1403.19	43.48	247.38	56.92	1.53	Large
WESTAR	161.06	29.86	0.59	285.44	25	90.19	24.09	2.22	Large

Table A1b. *Brassica napus*

Genotypes #	TRL	TRSA	RAD	NTP	TPRL	TLRL	TTRL	BLL	Root Size
ECD06	204.34	20.97	0.31	778.88	28.77	130.5	13.14	1.29	Large
ECD08	242.64	23.96	0.3	1074.44	34.15	143.03	26.93	1.44	Large
ECD09	186.3	12.88	0.22	399	34.64	135.9	7.73	1.61	Large
ECD10	223.13	25.17	0.36	1578.56	33.08	107.93	11.48	1.82	Large
FG001	131.86	12.67	0.29	164.38	22.52	77.33	32.01	2.71	Large
FG002	310.25	28.53	0.28	419.88	36.85	169.8	103.6	1.81	Large
FG004	266.6	23.98	0.26	403.81	38.28	151.1	77.21	1.85	Large
FG005	180.68	17.37	0.28	233.81	27.39	104.69	48.6	2.12	Large
FG007	284.23	27.62	0.28	971.13	46.73	152.63	84.87	2.08	Large
FG008	173.7	17.01	0.28	522.81	32.9	97.05	43.76	2.93	Large
FG009	47.98	10.58	0.56	246.31	12.05	29.27	6.66	1.47	Small
FG010	161.1	14.39	0.28	215.81	28.62	94.14	38.34	2.33	Large
FG011	141.59	15.11	0.3	248.06	20.19	82.13	39.27	2.45	Large
FG012	161.13	15.61	0.29	470.69	26.94	90.2	43.98	2.2	Large
FG013	159.33	14.22	0.25	308.69	27.93	93.17	38.23	1.81	Large
FG014	153.67	14.52	0.28	250.38	25.4	89.56	38.71	2.6	Large
FG015	223.39	21.92	0.32	487.25	25.07	143.4	54.93	2.21	Large
FG019	156.35	14.72	0.27	378.13	26.82	90.21	39.32	2.19	Large
FG022	103.71	10.35	0.28	447.06	16.5	58.03	29.19	2.06	Small
FG025	164.63	17	0.3	339.88	26.56	125.97	12.11	2.82	Large
FG026	158.62	32.55	0.57	418.56	27.66	116.55	14.41	1.9	Large
FG027	53.28	13.44	0.54	453.38	19.2	31.41	2.67	1.48	Small
FG029	222.22	44.42	0.58	321.88	37.74	167.08	17.39	3.07	Large
FG031	134.66	12.66	0.28	283.69	20.67	80.41	33.58	1.89	Large
FG033	147.46	22.31	0.39	468.19	27.66	80.94	38.86	1.73	Large
FG034	100.38	22.4	0.65	236.25	18.71	73.52	8.16	2.43	Small
FG035	96.01	9.72	0.3	191.06	15.57	64.57	15.87	1.62	Small
FG037	96.78	10.1	0.31	183.69	18.97	57.33	20.47	1.99	Small
FG038	61.31	6.04	0.31	94.25	13.02	36.99	11.3	1.39	Small
FG040	135.85	12.33	0.28	237.19	23.29	81.95	30.61	2.17	Large
FG041	116.1	13.85	0.34	447.88	19.64	79.24	17.23	2.11	Medium
FG042	127.31	24.53	0.48	357.19	15.86	80.73	30.72	0.86	Medium
FG665	178.79	17.9	0.31	282.56	20.54	75.36	82.89	1.5	Large
FG666	224.02	22.39	0.28	598.69	35.68	102.94	85.4	1.64	Large
FG667	191.03	20.04	0.31	469.5	23.73	92.2	75.1	1.45	Large
FG668	177.86	23.55	0.41	306.25	24.11	88.6	65.15	1.38	Large
FG670	276.35	24.48	0.26	308.31	36.58	143.35	96.42	1.8	Large

Genotypes #	TRL	TRSA	RAD	NTP	TPRL	TLRL	TTRL	BLL	Root Size
FG688	284.28	29.98	0.3	505.25	33.66	142.79	107.83	1.65	Large
FG689	249.48	25.99	0.3	606.69	23.91	102.4	123.17	1.74	Large
FG690	243.24	27.83	0.32	531.5	27.71	104.97	110.56	1.67	Large
FG691	166.12	19.37	0.33	304.5	26.94	94.99	44.19	1.75	Large
FG692	278.65	32.4	0.33	929.19	31.72	135.14	111.79	1.63	Large
FG694	268.12	26.84	0.29	651.63	32.43	132.36	103.33	1.71	Large
FG710	231.66	22.7	0.29	523.44	30.76	110.06	90.85	1.74	Large
FG723	176.26	17.54	0.29	494.94	26.97	97.65	51.64	1.85	Large
FG725	280.6	33.07	0.33	803.94	32.74	139.29	108.57	1.86	Large
FG726	252.92	30.77	0.34	748.63	35.31	137.66	79.95	2.13	Large
FG727	273	30.87	0.32	412.69	37.33	136.31	99.37	1.86	Large
FG730	269.25	24.71	0.27	371.56	33.72	139.71	95.82	1.6	Large
FG734	173.16	19.46	0.31	426.69	30.41	97.56	45.19	1.23	Large
FG735	278.41	24.76	0.27	432.69	34.57	145.98	97.86	1.65	Large
FG736	154.09	15.49	0.28	546.88	29.45	94.07	30.58	1.81	Large
FG737	159.53	16.68	0.29	259.44	29.54	88.4	41.59	1.7	Large
FG748	164.64	14.75	0.27	252.38	30.5	86.41	47.73	2.32	Large
FG750	177.34	16.43	0.26	448.69	31.39	94.04	51.91	2.33	Large
FG756	150.77	15.04	0.28	492.63	20.27	82.44	48.06	1.98	Large
FG767	201.13	19.23	0.29	380.44	28.22	109.94	62.98	1.8	Large
FG768	233.09	21.24	0.27	203.44	30.61	122.96	79.53	1.7	Large
FG769	182.09	18.46	0.28	379.44	26.56	94.82	60.71	2.08	Large
FG771	159.76	25.76	0.41	489.88	23.9	81.4	54.47	1.45	Large
FG782	129.84	13.93	0.31	462.75	25.78	63.65	40.41	1.84	Medium
FG783	187.66	19.74	0.29	390.5	29.25	94.98	63.44	1.76	Large
FG784	164.57	15.24	0.28	294.19	29.75	85.32	49.51	1.53	Large
FG818	182.81	18.4	0.29	300.31	33.38	94.58	54.85	1.71	Large
FG819	131.47	13.87	0.31	390	25.89	72.02	33.55	1.41	Large
FG820	125.24	13.28	0.31	369.63	21.78	66.43	37.03	1.29	Medium
FG821	198.5	19.93	0.29	575.69	25.19	103.51	69.8	1.7	Large
FG822	209.74	21.12	0.3	385.13	27.32	117.39	65.02	1.51	Large
FG823	185.22	21.9	0.34	265.24	29.04	106.48	49.7	1.93	Large
FG825	200.94	22.03	0.32	227.6	32.38	110.28	58.28	1.92	Large
FG826	211.97	21.81	0.32	476.63	26.47	110.86	74.65	1.8	Large
FG828	201.7	23.46	0.33	342.63	28.19	111	62.5	1.66	Large

Table A1c. *Brassica rapa*

Genotypes #	TRL	TRSA	RAD	NTP	TPRL	TLRL	TTRL	BLL	Root Size
ECD02	174.92	20.7	0.38	1097	27.52	97.55	6.17	1.7	Large
ECD05	147.98	9.97	0.21	405.94	27.06	96.48	14.43	1.64	Large
FG043	113.87	9.72	0.25	252.44	19.65	82.21	12.01	1.94	Small
FG044	166.5	15.3	0.26	442.06	22.52	106.54	37.45	1.36	Large
FG052	75.45	15.64	0.61	147	14.98	53.26	7.2	1.79	Small
FG053	88.03	8.31	0.29	260.38	13.68	65.6	8.76	2.44	Small
FG054	94.52	16.01	0.48	325.38	17.79	63.16	13.57	2.59	Small
FG056	205.9	44.49	0.55	759.19	31.62	109.91	64.37	1.6	Large
FG058	151.86	32.93	0.58	461.19	23.57	101.99	26.29	2.16	Large
FG060	72.82	6.3	0.25	234.56	15.77	52.67	4.37	1.56	Small
FG061	143.48	15.29	0.28	557.56	20.88	80.11	42.5	1.18	Large
FG062	83.92	7.29	0.26	193.25	15.69	60.74	7.48	1.81	Small
FG063	110.87	23.69	0.58	316.38	19.73	71.47	19.66	1.37	Small
FG066	118.03	10.11	0.24	269.56	20.99	86.41	10.63	2.14	Medium
FG072	139.42	12.18	0.26	342.94	25.39	101.72	12.31	1.96	Large
FG073	109.64	11.61	0.29	419.81	24.38	76.53	8.73	1.71	Small
FG080	115.55	20.74	0.48	649.44	20.36	77.11	18.08	2.01	Medium
FG082	105.39	12.44	0.34	287.88	17.31	55.36	32.72	1.13	Small
FG084	66.91	5.02	0.22	186	13.35	43.64	9.93	1.55	Small
FG085	104.04	8.93	0.26	365.5	17.11	71.8	15.13	1.66	Small
FG088	138.54	13.39	0.28	343.63	23.45	95.9	19.19	2.08	Large
FG091	89.96	17.36	0.57	186.56	22.76	61.81	5.4	1.76	Small
FG092	157.98	31.27	0.51	722	26.76	82.61	48.61	1.18	Large
FG094	109.56	17.33	0.45	223.25	25.24	73.82	10.5	1.94	Small
FG095	92.76	9.27	0.29	331.44	21.25	61.8	9.71	1.47	Small
FG096	203.71	20.53	0.26	840.31	25.12	111.09	67.51	1.64	Large
FG097	121.22	11.3	0.27	335.81	18.99	80.11	22.12	1.46	Medium
FG101	129.21	11.33	0.26	403.44	16.87	87.91	24.43	1.62	Medium
FG102	109.04	14.46	0.41	275.75	20.59	68.79	19.66	1.46	Small
FG106	164.41	12.02	0.26	339.56	21.55	118.94	23.92	1.49	Large
FG109	128.25	11.69	0.26	278.69	23.03	93.22	11.99	1.74	Medium
FG112	103.9	13.74	0.35	147.13	19.29	64.45	20.16	1.54	Small
FG113	67.59	10.51	0.4	247.56	17.91	39.86	9.82	1.54	Small
FG114	153.37	15.67	0.29	405.94	25.85	90.88	36.65	1.81	Large
FG119	86.01	6.32	0.23	160.5	16.37	58.19	11.45	1.32	Small
FG120	161.78	16.37	0.29	289.5	32.1	119.65	10.03	1.7	Large
FG121	149.89	12.28	0.23	367.38	23.97	103.84	22.08	1.55	Large

Genotypes #	TRL	TRSA	RAD	NTP	TPRL	TLRL	TTRL	BLL	Root Size
FG123	63.78	14.48	0.58	309.63	18.35	40.72	4.72	2.35	Small
FG124	118.27	30.03	0.55	817.69	26.84	81.1	10.33	2.01	Medium
FG125	85.49	9.11	0.3	362.13	22.37	55.76	7.36	1.61	Small
FG126	147.77	12.28	0.25	327.63	27	105.48	15.28	2.06	Large
FG129	125.27	27.7	0.58	418.25	23.8	68.81	32.66	1.53	Medium
FG133	51.39	5.03	0.28	210.13	12.63	34.64	4.13	2.11	Small
FG136	75.44	7.08	0.28	187.44	16.75	53.81	4.88	1.69	Small
FG137	87.33	13.89	0.42	276	18.42	54.43	14.49	1.43	Small
FG138	158.21	17.2	0.32	459.31	27.07	107.23	23.92	2.18	Large
FG142	79.64	13.31	0.41	452.31	14.59	49.48	15.57	1.1	Small
FG153	56.62	13.05	0.61	202.94	16.29	31.57	8.76	1.89	Small
FG158	85.38	8.35	0.27	396.44	20.64	57.56	7.18	1.28	Small
FG166	98.67	9.63	0.25	554	20.81	62.59	15.28	1.3	Small
FG167	108.01	10.95	0.28	302.06	16.17	79.98	11.86	1.89	Small
FG183	158.16	33.32	0.57	480.88	28.15	98.18	31.83	1.9	Large
FG184	108.66	22.76	0.59	226.75	20.06	65.4	23.2	1.22	Small
FG191	144.75	14.08	0.27	493.25	23.07	93.21	28.48	1.41	Large
FG194	130.88	12.85	0.28	460.25	22.5	87.28	21.1	1.88	Large
FG196	144.51	18.39	0.33	386	18.05	94.05	32.4	1.81	Large
FG201	175.72	22.76	0.33	782.88	29.34	105.04	41.33	1.29	Large
FG203	66.23	6.46	0.3	184.88	15.01	40.99	10.23	1.31	Small
FG211	214.14	46.48	0.63	366.19	28.23	126.37	59.54	2.08	Large
FG212	138.76	14.51	0.31	412.75	17.68	99.78	21.31	2.13	Large
FG215	139.6	30.51	0.63	250.81	28.46	78.83	32.31	1.43	Large
FG219	147.57	13.13	0.27	274.94	25.86	91.62	30.09	1.38	Large

Table A1d. *Brassica juncea*

Genotypes #	TRL	TRSA	RAD	NTP	TPRL	TLRL	TTRL	BLL	Root Size
FG402	174.76	18.63	0.3	714	27.66	126.23	20.86	2.63	Large
FG403	198.41	21.12	0.29	775.13	34.91	148.31	15.19	3.48	Large
FG404	58.61	8.15	0.38	68.19	19.87	35.91	2.83	2.29	Small
FG405	76.41	10.75	0.4	78.63	23.69	47.44	5.28	1.54	Small
FG406	233.97	24.38	0.31	768.31	33.62	176.7	23.66	2.56	Large
FG412	170.35	23.16	0.39	154.75	39.47	117.94	12.93	2.52	Large
FG429	106.15	15.68	0.42	114.94	22.9	74	9.26	2.23	Small
FG430	71.05	9.16	0.38	210.63	15.85	29.81	25.38	1.65	Small
FG431	103.13	13.66	0.35	586.94	22.12	43.05	37.96	2.49	Small
FG432	57.74	7.22	0.32	258.06	20.37	26.75	10.62	0.99	Small
FG443	44.11	6.38	0.33	278.19	18.7	18.56	6.85	1.15	Small
FG444	99.48	10.76	0.32	199.94	27.67	45.15	26.66	1.19	Small
FG449	122.98	14.02	0.33	226.38	26.08	55.45	41.45	1.88	Medium
FG450	136.92	15.37	0.31	357.75	30.11	61.41	45.4	2.11	Large
FG454	178.07	17.59	0.32	299.69	28.06	78.87	71.13	2.04	Large
FG460	147.49	17.06	0.34	232.19	31.54	72.65	43.3	1.77	Large
FG995	127.34	13.62	0.34	294	26.48	92.83	8.03	2.04	Medium
FG1003	234.13	23.53	0.3	674	39.3	178.21	16.63	2.61	Large
FG1005	107.87	12.15	0.33	414.63	22.14	74.43	11.3	1.8	Small
FG1006	49.69	5.55	0.32	219.94	14.17	31.82	3.7	2.41	Small
FG1007	99.57	10.39	0.31	432.81	22.05	71.14	6.39	1.92	Small
FG1023	92.31	21.02	0.55	447.25	18.73	66.12	7.46	2.52	Small
FG1036	35.07	4.43	0.39	19.94	12.89	21.54	0.63	1.5	Small
FG1037	35.35	4.49	0.37	38.13	15.67	18.07	1.62	1.2	Small
FG1039	98.08	10.06	0.28	474.75	22.69	69.41	5.99	1.4	Small
FG1040	86.48	20.74	0.58	464.81	19.73	53.28	13.48	2.28	Small
FG1041	53.47	12.37	0.65	136.06	21.58	30.89	1	1.66	Small
FG1042	40.67	3.7	0.27	99.44	14.66	25.1	0.9	1.89	Small
FG1043	110.83	10.55	0.29	241.44	25.34	82.1	3.38	2	Small
FG1049	52.21	7.04	0.34	380.63	15.03	28.61	8.57	0.98	Small
FG1050	59.21	14.28	0.59	362.56	16.98	34.2	8.03	1.21	Small
FG1051	65.16	7.46	0.32	280.06	21.34	37.01	6.81	1.54	Small
FG1053	50.01	5.12	0.33	115.38	14.7	28.58	6.72	0.99	Small
FG1054	50.28	12.8	0.65	252.25	17.36	26.96	5.96	1.14	Small
FG1055	76.63	19.07	0.75	121.38	28.59	40.38	7.67	1.04	Small
FG1056	42.9	11.34	0.57	325.56	15.25	21.98	5.66	1.17	Small
FG1057	139.24	15.87	0.33	470.69	26.61	81.05	31.58	1.22	Large

Genotypes #	TRL	TRSA	RAD	NTP	TPRL	TLRL	TTRL	BLL	Root Size
FG1058	83.9	19.67	0.65	178.88	20.34	48.66	14.9	1.2	Small
FG1060	52.09	12.79	0.59	272.06	16.92	29.01	6.15	1.46	Small
FG1061	41.95	4.58	0.33	106.25	12.06	24.35	5.54	1.28	Small
FG1063	18.46	4.98	0.57	190.63	8.77	9.34	0.35	1.22	Small
FG1065	81.13	7.61	0.28	218.13	22.58	54.97	3.58	1.9	Small
FG1066	139.11	18.13	0.37	289.88	33.46	94.18	11.47	1.96	Large
FG1070	70.23	10.08	0.36	528.5	21.84	38.44	9.94	1.09	Small
FG1071	82.79	9.2	0.34	183.63	20	58.67	4.12	1.92	Small
FG1072	189.26	38.61	0.59	310.69	39.99	140.62	8.65	2.81	Large
FG1077	103.74	11.06	0.3	445.25	25.75	73.48	4.51	1.9	Small
FG1081	168.53	22.89	0.4	139.56	37.43	116.29	14.81	2.66	Large
FG1082	94.7	10.58	0.3	524.94	26.76	63.75	4.18	1.9	Small
FG1083	244	29.1	0.33	475.56	39.06	168.58	36.37	3.41	Large
FG1084	103.07	11.25	0.31	438.38	28.92	67.71	6.44	2.58	Small
FG1085	161.21	17.29	0.31	420.94	31.86	107.52	21.82	1.91	Large
FG1088	120.88	27.11	0.58	435.13	29.16	84.32	7.4	2.36	Medium
FG1090	49.43	7.14	0.33	653.38	16.02	27.21	6.21	1.21	Small
FG1100	120.13	13.33	0.33	359.44	27.44	82.02	10.68	2.67	Medium
FG1101	77.83	18.02	0.63	191.44	21.92	53.08	2.83	2.11	Small
FG1102	82.97	19.55	0.6	409.31	18.91	58.54	5.52	1.98	Small
FG1103	91.02	12.25	0.32	233.38	19.14	58.51	13.36	1.64	Small
FG1104	38.91	5.56	0.39	136.13	14.07	21.49	3.34	1.43	Small
FG1105	51.41	5.36	0.31	193	18.61	29.77	3.03	1.13	Small
FG1108	83.04	18.66	0.55	422.56	20.26	54.83	7.95	2.17	Small
FG1111	90.81	22.08	0.61	402.38	24.33	59.96	6.52	1.75	Small
FG1112	114.61	11.97	0.3	390	24.97	83.65	5.99	1.92	Small
FG1113	131.72	28.37	0.58	528.63	26.24	87.85	17.63	1.63	Large

Table A1e. *Brassica oleracea*

Genotypes #	TRL	TRSA	RAD	NTP	TPRL	TLRL	TTRL	BLL	Root Size
ECD11	261.81	31.23	0.38	1924.56	30.47	126.53	16.08	1.43	Large
ECD13	155.96	11.37	0.23	243.13	32.8	113.07	4.98	1.38	Large
FG467	97.17	10.04	0.32	150.19	19.88	45.15	32.14	1.31	Small
FG485	139.19	13.19	0.29	287.69	29.59	69.69	39.91	1.55	Large
FG503	161.55	31.05	0.45	1321.13	29.31	96.33	35.91	1.19	Large
FG505	87.44	9.17	0.29	314.69	14.98	57.08	15.37	1.2	Small
FG510	128.72	13.98	0.29	639.25	20.19	82.06	26.48	1.17	Medium
FG514	161.81	16.47	0.28	287.19	29.79	74.51	57.52	1.79	Large
FG518	88.03	10.29	0.32	333.63	19.43	53.03	15.57	1.98	Small
FG533	174.92	17.4	0.28	286.38	27.8	86.72	60.4	1.82	Large
FG534	162.36	16.62	0.31	400.69	23.53	58.59	80.25	1.54	Large
FG535	150.33	13.01	0.26	298.5	25.78	72.63	51.93	1.45	Large
FG536	187.59	17.12	0.28	258.63	22.18	77.24	88.16	1.92	Large
FG538	197.75	17.25	0.27	323.56	30.76	94.58	72.4	2.38	Large
FG539	165.34	35.2	0.45	1748.5	25.14	100.46	39.75	1.5	Large
FG557	93.06	15.6	0.41	578.13	17.65	64.26	11.14	1.84	Small
FG562	201.29	36.63	0.47	1032.25	29.5	137.66	34.13	2.12	Large
FG565	161.56	26.77	0.41	948.88	29.32	108.56	23.68	1.72	Large
FG570	201.34	18.29	0.28	257.69	32.78	146.91	21.64	1.66	Large
FG577	170.14	15.11	0.26	460.63	28.05	115.04	27.06	1.81	Large
FG582	360.36	60.11	0.47	1038.31	37.64	242.91	79.81	1.23	Large
FG590	276.4	24.43	0.26	560.5	33.57	188.02	54.81	1.81	Large
FG595	124.38	13.11	0.3	274.56	25.6	49.69	49.09	2.03	Medium
FG597	149.62	16.99	0.32	258.06	25.08	65.14	59.4	1.1	Large
FG598	176.9	33.77	0.43	1448.63	32.48	120.31	24.1	1.34	Large
FG599	118.7	23.51	0.48	785.44	23.34	83.31	12.06	1.22	Medium
FG614	317.2	24.35	0.29	474.81	25.44	228.72	63.04	1.56	Large
FG616	235.26	43.35	0.43	1592.88	36.03	152.06	47.17	1.14	Large
FG621	251.29	22.04	0.27	292.31	35.66	188.02	27.61	1.58	Large
FG622	91.96	10.01	0.34	152.81	17.52	49.69	24.75	1.59	Small
FG626	270.38	47.93	0.51	898.94	35.13	175.1	60.15	1.07	Large
FG628	290.16	29.02	0.3	527.31	30.48	185.8	73.88	1.33	Large
FG633	199.33	25.66	0.42	388.44	33.58	84.36	81.39	1.44	Large
FG634	121.89	23.97	0.46	937.13	22.17	75.75	23.96	1.14	Medium
FG635	172.58	18.12	0.32	388.25	27.13	79.7	65.74	1.79	Large
FG636	105.04	18.52	0.41	1016.63	20.73	63.33	20.98	1.88	Small
FG637	63.04	6.76	0.34	149.88	10.51	40	12.53	1.2	Small

Genotypes #	TRL	TRSA	RAD	NTP	TPRL	TLRL	TTRL	BLL	Root Size
FG640	69.4	14.97	0.41	1005.56	16.16	38.83	14.42	1.03	Small
FG643	378.32	35.79	0.28	684.19	29.06	225.57	123.69	1.95	Large
FG646	245.05	44.8	0.47	1201.75	34.88	169.45	40.71	1.68	Large
FG647	282.41	48.92	0.45	1310.69	35.73	178.7	67.98	1.44	Large
FG649	154.49	19.72	0.34	302.63	21.39	72.71	60.39	1.33	Large
FG650	250.08	41.29	0.39	1475.44	33.95	156.44	59.69	1.3	Large
FG651	139.76	13.69	0.28	229.31	27.85	68.43	43.48	1.63	Large
FG653	72.1	14.16	0.49	575.44	16.3	46.33	9.46	1.14	Small
FG654	112.78	9.94	0.27	229.38	25.1	75.03	12.65	1.78	Small
FG655	173.22	16.86	0.3	265.19	20.04	118.54	34.63	1.83	Large
FG656	59.85	8.74	0.34	453.5	16.66	37.88	5.32	1.32	Small
FG657	100.78	16.86	0.43	648.69	16.74	78.48	5.56	0.66	Small
FG658	81.29	17.6	0.44	866.69	19.16	53.61	8.53	1.36	Small
FG659	176.74	32.04	0.41	1411.63	30.34	125	21.39	1.27	Large
FG660	117.92	10.53	0.28	235.38	18.49	82.41	17.02	1.55	Medium
FG661	97.11	19.55	0.5	562.19	20.7	62.98	13.42	1.38	Small
FG662	178.99	16.31	0.28	402	27.44	122.97	28.59	1.47	Large
FG663	96.14	18.8	0.52	540.63	15.92	65.62	14.6	0.94	Small
FG679	225.89	22.9	0.29	321.56	34.94	165.43	25.52	1.45	Large
FG851	87.94	12.85	0.32	771.06	20.5	53.86	13.59	1.27	Small

Table A1f. *Brassica carinata*

Genotypes #	TRL	TRSA	RAD	NTP	TPRL	TLRL	TTRL	BLL	Root Size
FG349	102.55	14.39	0.4	91.31	28.33	66.3	8.19	4.35	Small
FG350	56.48	7.33	0.36	283.63	17.94	32.47	6.08	1.21	Small
FG351	93.96	11.77	0.39	240.06	24.84	54.46	14.67	1.81	Small
FG352	91	10.55	0.34	303.38	24.52	56.07	10.41	1.72	Small
FG354	139.06	14.15	0.3	234.56	31.01	96.52	11.53	2.36	Large
FG355	118.83	13.09	0.34	246.69	30.91	80.01	7.92	2.17	Medium
FG357	56.95	14.98	0.58	383.13	21.48	28.92	6.55	1.57	Small
FG358	86.1	16.17	0.47	455.19	24.97	50.95	10.19	1.47	Small
FG360	64.87	9.05	0.4	268.63	18.01	37.67	9.19	0.82	Small
FG361	48.37	13.26	0.76	147.69	12.48	27.37	8.51	0.96	Small
FG364	54.01	15.21	0.67	315.5	18.04	29.94	6.03	2.16	Small
FG366	163.6	15.62	0.3	308	33.5	117.07	13.03	1.23	Large
FG368	51.92	6.84	0.36	144.13	17.78	30.76	3.38	1.56	Small
FG371	123.13	13.33	0.32	424.94	28.44	85.22	9.47	2.4	Medium
FG372	95.11	11.62	0.35	215.75	25.03	62.87	7.22	1.76	Small
FG373	108.88	12.04	0.34	196.19	27.52	75.68	5.68	2.33	Small
FG374	113.88	11.71	0.31	236.69	22.41	85.6	5.87	1.56	Small
FG379	71.46	16.57	0.49	805.63	18.62	44.72	8.12	1.32	Small
FG382	69.15	8.19	0.35	272.13	21.63	40.38	7.14	1.44	Small
FG383	58.41	8.12	0.4	251.69	18.39	32.07	7.95	1.12	Small
FG386	115.79	22.53	0.4	1189.81	30.35	74.15	11.28	1.99	Medium
FG388	74.13	19.16	0.45	1128.56	23.86	40.8	9.46	1.16	Small
FG390	68.18	16.96	0.55	486.63	20	39.05	9.13	1.21	Small
FG391	162.63	14.43	0.27	392.63	34.34	111.39	16.9	1.85	Large
FG393	64.13	15.22	0.53	523.94	22.66	36.08	5.4	1.09	Small
FG394	49.67	7.39	0.4	334.06	17.04	27.68	4.95	1.1	Small
FG395	115.85	13.65	0.35	356.19	25.6	76.76	13.5	2.54	Medium
FG398	243.89	24.36	0.3	362.75	40.72	180.75	22.42	2.72	Large

Table A1g. *Brassica nigra*

Genotypes #	TRL	TRSA	RAD	NTP	TPRL	TLRL	TTRL	BLL	Root Size
FG224	121.66	19.62	0.43	275.06	19.91	80.04	21.72	1.79	Medium
FG225	59.84	5.93	0.27	355.81	16.13	35.17	8.54	1.6	Small
FG227	104.73	10.73	0.29	249.13	20.71	59.82	24.19	1.22	Small
FG228	66.12	8.89	0.31	190.38	16.95	38.38	10.79	1.72	Small
FG229	122.95	13.53	0.32	354.31	18.48	87.57	16.9	1.53	Medium
FG230	153.48	23.39	0.36	831.56	28.48	111.73	13.28	1.75	Large
FG231	115.13	12.3	0.33	366.56	21.65	75.87	17.6	1.22	Small
FG234	112.63	17.64	0.35	560.88	23.09	72.87	16.68	1.48	Small
FG240	92.23	9.04	0.28	255.56	21.82	55.53	14.88	1.3	Small
FG241	71.41	7.7	0.28	340.69	19.91	43.87	7.64	1.48	Small
FG242	43.3	5.93	0.31	210	13.72	24.84	4.74	1.91	Small
FG243	54.13	5.62	0.28	419.31	19.42	30.63	4.08	1.64	Small
FG245	54.13	5.62	0.28	419.31	19.42	30.63	4.08	1.64	Small
FG246	73.82	6.64	0.28	258.94	25.63	43.95	4.24	1.33	Small
FG247	60.18	7.37	0.35	143.81	16.66	38.72	4.8	1.57	Small
FG248	54.48	11.23	0.49	306.75	14.94	32.56	6.98	0.88	Small
FG249	61.83	6.16	0.3	276.19	21.74	34.4	5.68	1	Small
FG250	55.4	4.97	0.26	257.44	16.22	34.84	4.34	0.87	Small
FG251	62.46	6.93	0.32	119.13	25.58	33.72	3.16	1.99	Small
FG252	63.84	6.13	0.27	299.19	23.81	35.64	4.39	1.8	Small
FG253	60.47	5.53	0.25	480.94	19.53	34.92	6.02	1.68	Small
FG262	53.45	5.37	0.27	250.38	20.49	29.73	3.23	2.12	Small
FG263	72.82	11.39	0.48	180.06	18.51	47.11	7.2	1.39	Small
FG265	108.08	13.25	0.32	602.25	31.03	69.65	7.4	1.43	Small
FG269	121.05	10.63	0.27	243.44	34.85	82.18	4.02	1.48	Medium
FG271	139.38	24.2	0.45	793.63	31.63	97.02	10.72	1.04	Large
FG274	77	16.47	0.39	1143.13	30.81	41.87	4.33	1.03	Small
FG276	85.62	9.39	0.31	272.88	21.07	57.44	7.11	1.21	Small
FG281	86.7	6.68	0.24	212.25	25.4	58.47	2.83	1.25	Small
FG285	186.46	18.15	0.3	369.63	33.2	138.62	14.64	2.49	Large
FG286	31.86	3.23	0.26	285.19	14.78	15.59	1.5	1.38	Small
FG287	46.58	10.82	0.59	217.5	16.41	27.77	2.4	1.58	Small
FG289	42.35	4.65	0.31	110.38	15.02	22.13	5.19	1.97	Small
FG291	97.47	19.18	0.38	1240.44	30.5	58.75	8.21	1.05	Small
FG292	75.94	7.24	0.28	174.31	17.53	51.4	7.01	1.78	Small
FG293	92.01	9.06	0.29	181.06	21.68	63.82	6.51	2.5	Small
FG294	73.15	7.67	0.3	308.56	17.36	46.05	9.73	1.94	Small

Genotypes #	TRL	TRSA	RAD	NTP	TPRL	TLRL	TTRL	BLL	Root Size
FG295	59.89	6.56	0.31	135.31	15.16	40.18	4.55	1.74	Small
FG297	52.9	5.74	0.29	133.06	16.33	33.22	3.36	2.3	Small
FG298	29.77	2.98	0.29	119.44	12.07	14.02	3.67	1.75	Small
FG299	68.04	6.22	0.26	198	16.25	44.27	7.51	1.55	Small
FG302	39.89	4.27	0.33	109.44	10.93	26.29	2.66	1.54	Small
FG305	64.33	6.05	0.26	283.94	15.69	42	6.63	2.08	Small
FG309	75.51	14.98	0.38	1051.25	29.32	42.11	4.08	0.86	Small
FG312	141.05	13.22	0.28	186.88	28.91	98.44	13.7	3.43	Large
FG316	127.58	11.88	0.28	273.75	32.77	89.82	4.99	2.71	Medium
FG317	85.2	8.72	0.31	223.94	23.31	55.64	6.24	1.75	Small
FG319	87.8	10.55	0.33	306.5	26.68	55.92	5.2	2.97	Small
FG321	167.18	18.7	0.34	367.94	30.37	125.96	10.86	1.66	Large
FG325	45.58	4.08	0.27	127.94	19.32	22.53	3.74	1.07	Small
FG331	82.58	8.56	0.28	214.38	25.73	52.11	4.75	2.78	Small
FG332	64.8	6.37	0.29	240	18.84	42.08	3.88	1.74	Small
FG333	59.32	5.27	0.25	149.44	19.04	37.65	2.62	1.29	Small
FG334	72.29	6.52	0.26	298.25	20.83	46.52	4.94	1.59	Small
FG336	27.79	2.32	0.24	100.13	10.55	16.54	0.7	0.78	Small
FG338	106.19	8.93	0.27	214.31	28.22	71.47	6.49	2.68	Small
FG339	154.75	20.62	0.37	134.88	35.74	108.17	10.85	2.21	Large
FG340	74.05	6.9	0.29	211.19	26.78	43.28	3.99	1.52	Small
FG341	149.18	25.5	0.4	1114.75	35.46	105.79	7.92	1.71	Large
FG342	53.36	4.79	0.27	109.69	16.58	32.4	4.38	2.03	Small
FG343	74.1	7.9	0.31	135.38	19.19	46.66	8.25	1.89	Small
FG344	70.36	7.01	0.27	288.25	27.49	38.81	4.05	1.43	Small
FG345	85.55	7.35	0.26	183.69	27.31	54.35	3.89	2.44	Small
FG346	79.92	11.98	0.37	117.13	28.44	48.07	3.41	2.34	Small
FG347	140.09	24.61	0.41	1184	32.44	100.01	7.64	1.48	Large
FG348	83.7	12.19	0.32	679.13	27.97	49.89	5.83	0.98	Small

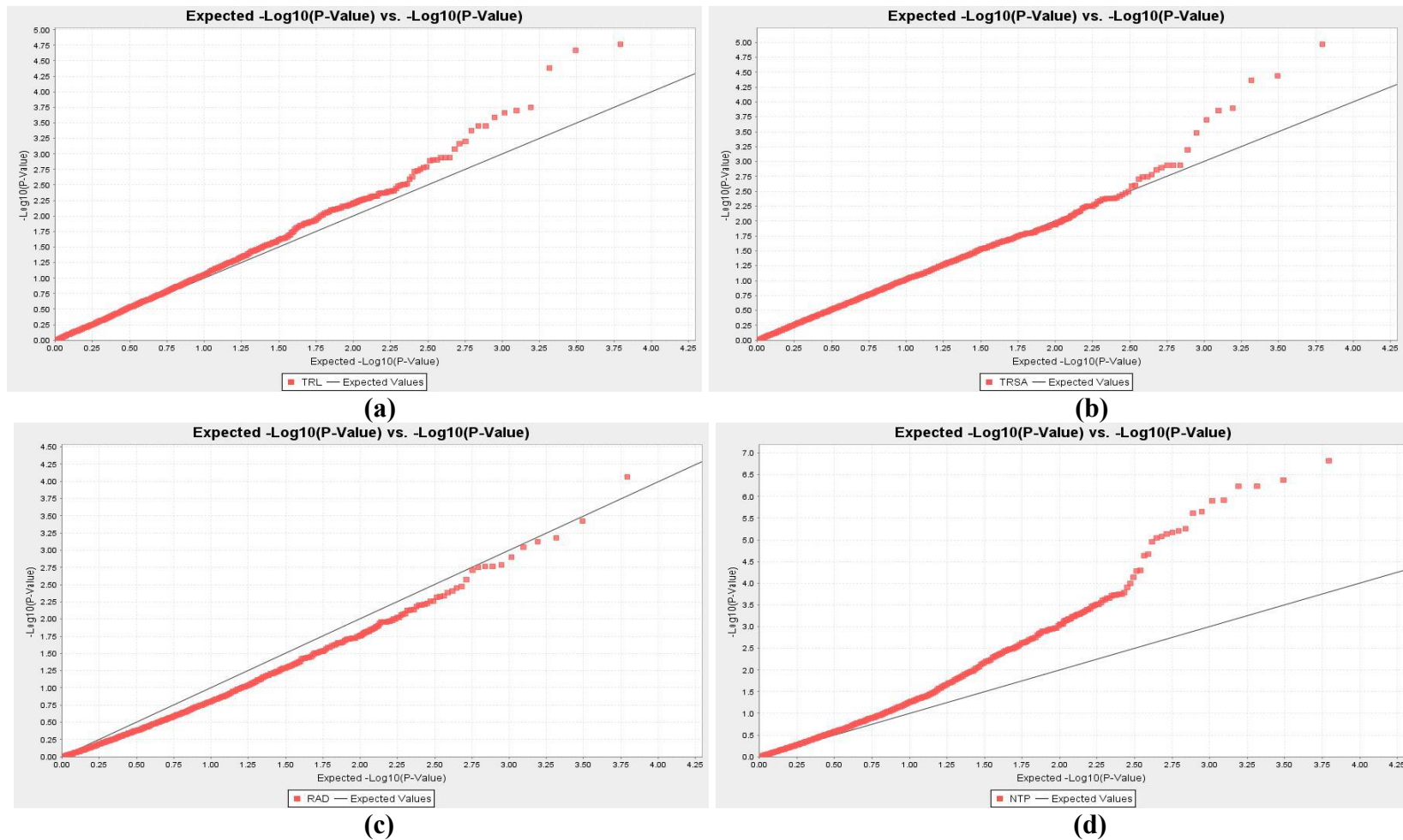
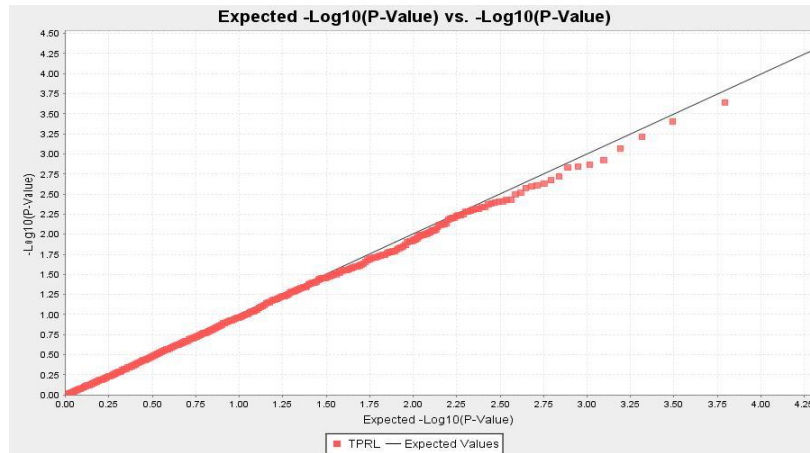
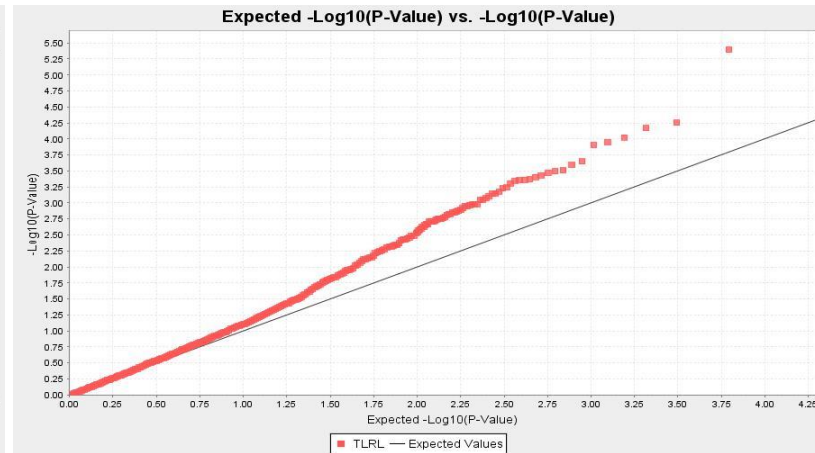


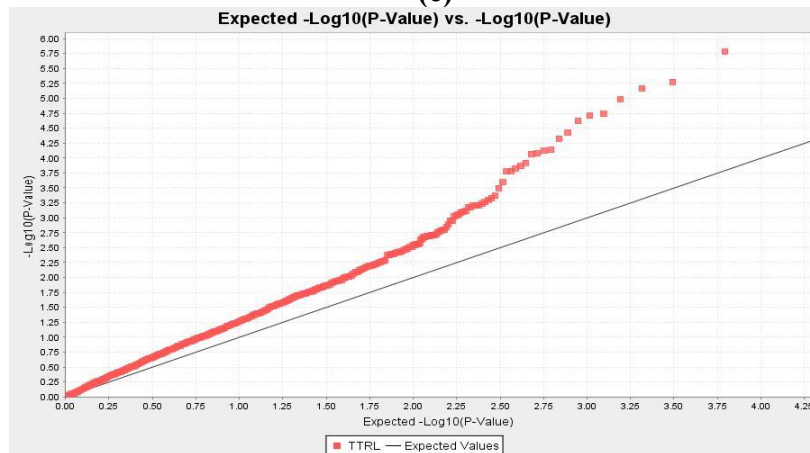
Figure A1a. Quantile-Quantile comparison of GWAS model PCA + K for identifying loci associated with eight root architectural traits in 313 *Brassica* accessions representing five species *B. napus*, *B. oleracea*, *B. rapa*, *B. carinata* and *B. juncea* except *B. nigra*. Traits include (a) total root length (TRL/cm), (b) total surface area of roots (TRSA/cm²), (c) average root diameter (RAD/cm), (d) number of tips (NTP), (e) total primary root length (TPRL/cm), (f) total lateral root length (TLRL/cm), (g) total tertiary root length (TTRL/cm) and (h) basal link length (BLL/cm). The black line is the expected $-\log_{10}P$ distribution while colored lines are the observed $-\log_{10}P$ distribution for each of the eight root architectural traits.



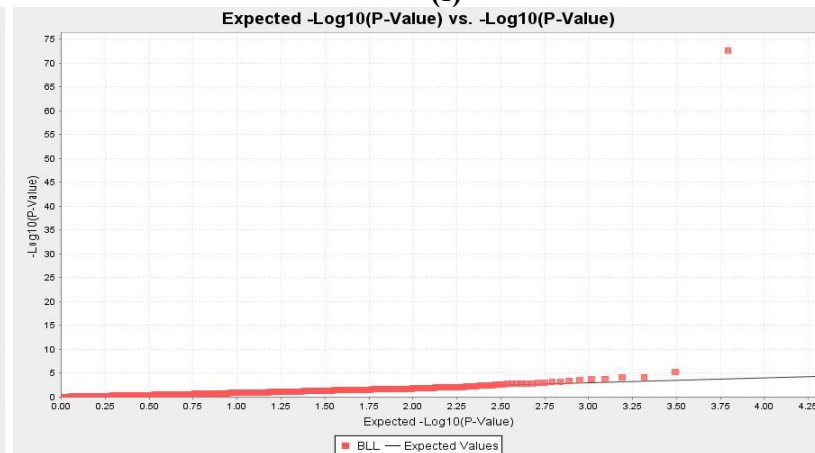
(e)



(f)

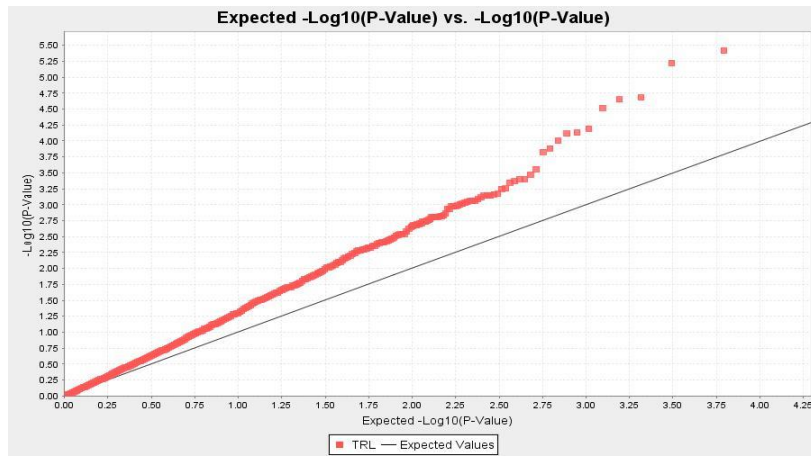


(g)

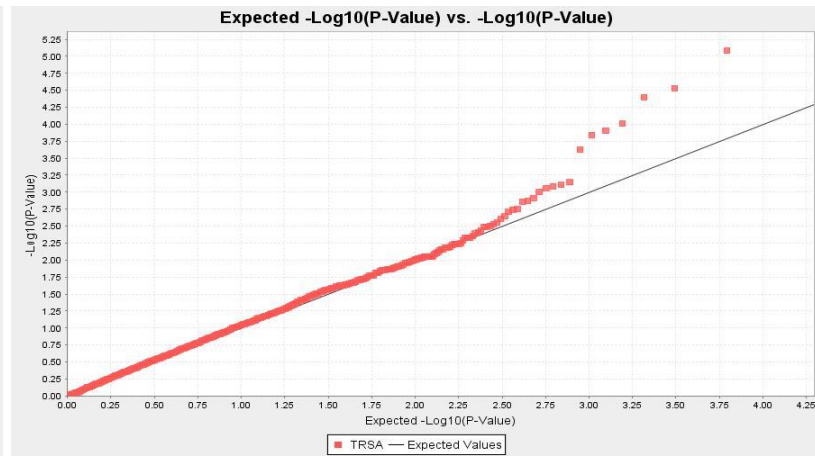


(h)

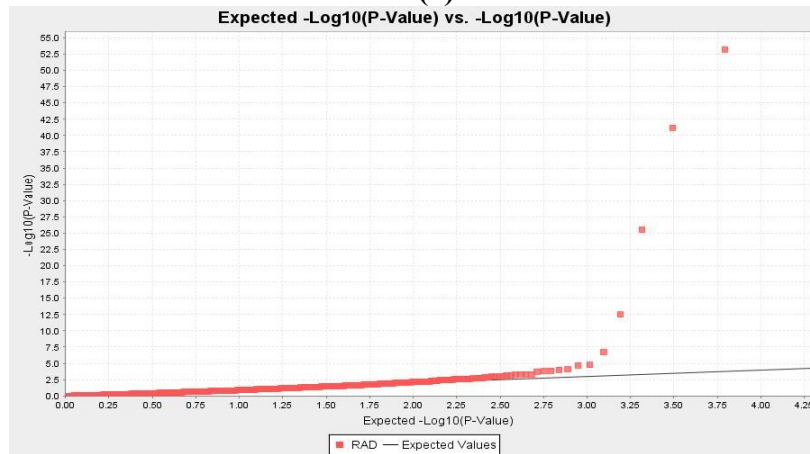
Figure A1a (continued). Quantile-Quantile comparison of GWAS model PCA + K for identifying loci associated with eight root architectural traits in 313 *Brassica* accessions representing five species *B. napus*, *B. oleracea*, *B. rapa*, *B. carinata* and *B. juncea*. Traits include (a) total root length (TRL/cm), (b) total surface area of roots (TRSA/cm²), (c) average root diameter (RAD/cm), (d) number of tips (NTP), (e) total primary root length (TPRL/cm), (f) total lateral root length (TLRL/cm), (g) total tertiary root length (TTRL/cm) and (h) basal link length (BLL/cm). The black line is the expected $-\log_{10}P$ distribution while colored lines are the observed $-\log_{10}P$ distribution for each of the eight root architectural traits.



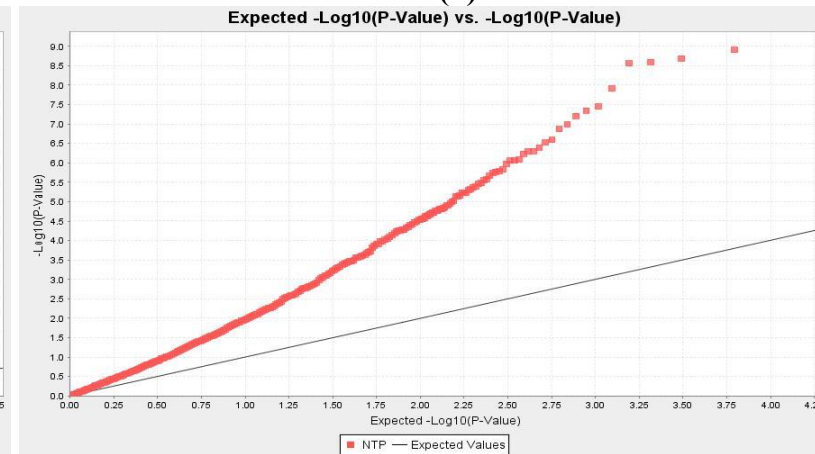
(a)



(b)

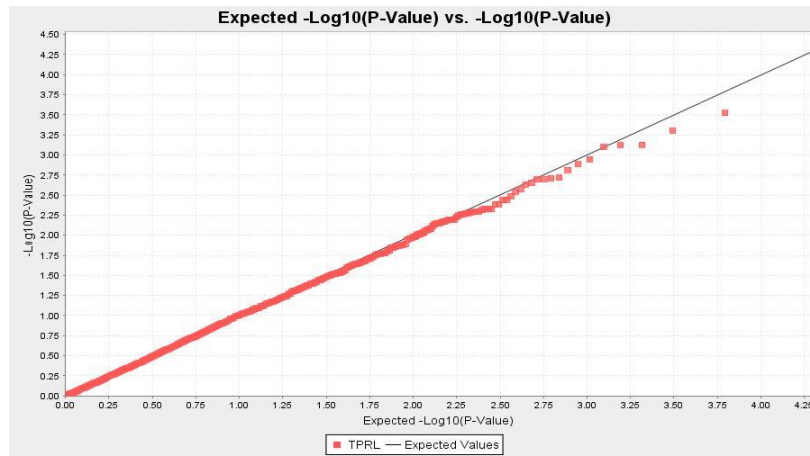


(c)

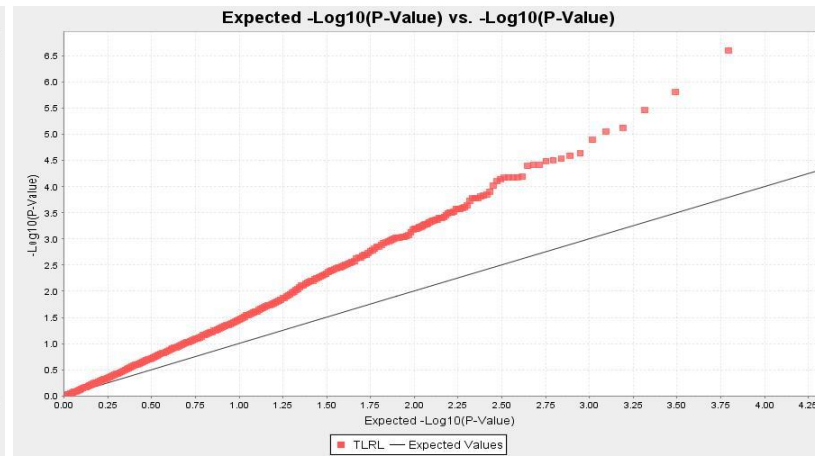


(d)

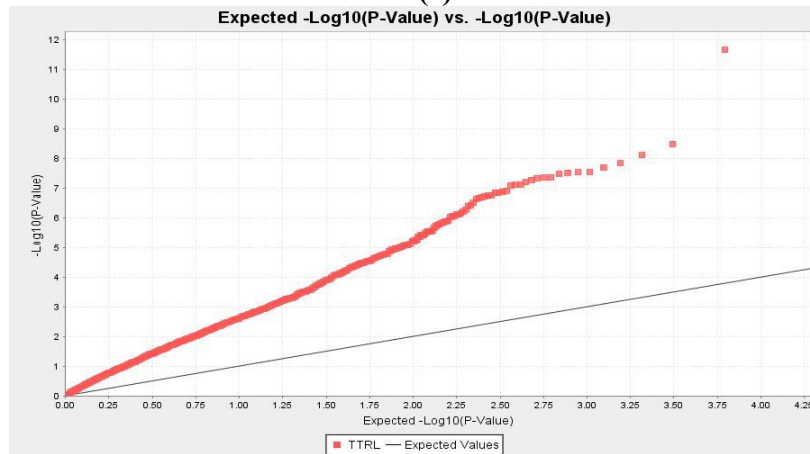
Figure A1b. Quantile-Quantile comparison of GWAS model PCA + D for identifying loci associated with eight root architectural traits in 313 *Brassica* accessions representing five species *B. napus*, *B. oleracea*, *B. rapa*, *B. carinata* and *B. juncea*. Traits include (a) total root length (TRL/cm), (b) total surface area of roots (TRSA/cm²), (c) average root diameter (RAD/cm), (d) number of tips (NTP), (e) total primary root length (TPRL/cm), (f) total lateral root length (TLRL/cm), (g) total tertiary root length (TTRL/cm) and (h) basal link length (BLL/cm). The black line is the expected $-\log_{10} P$ distribution while colored lines are the observed $-\log_{10} P$ distribution for each of the eight root architectural traits.



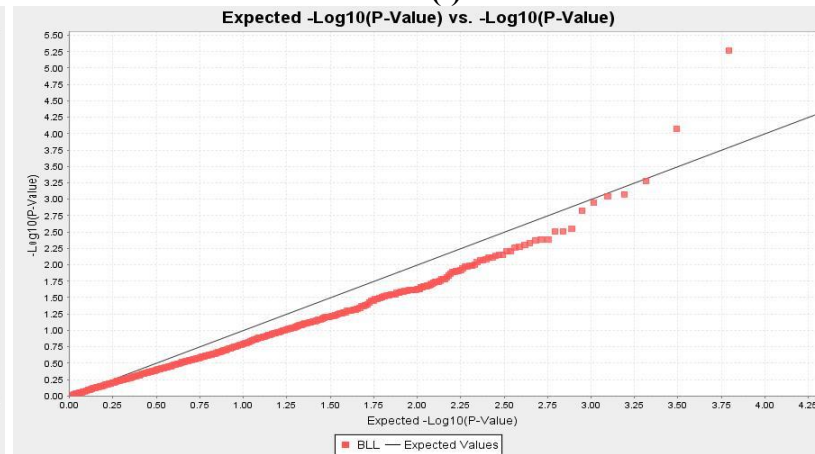
(e)



(f)



(g)



(h)

Figure A1b (continued). Quantile-Quantile comparison of GWAS model PCA + D for identifying loci associated with eight root architectural traits in 313 *Brassica* accessions representing five species *B. napus*, *B. oleracea*, *B. rapa*, *B. carinata* and *B. juncea*. Traits include (a) total root length (TRL/cm), (b) total surface area of roots (TRSA/cm²), (c) average root diameter (RAD/cm), (d) number of tips (NTP), (e) total primary root length (TPRL/cm), (f) total lateral root length (TLRL/cm), (g) total tertiary root length (TTRL/cm) and (h) basal link length (BLL/cm). The black line is the expected $-\log_{10}P$ distribution while colored lines are the observed $-\log_{10}P$ distribution for each of the eight root architectural traits.

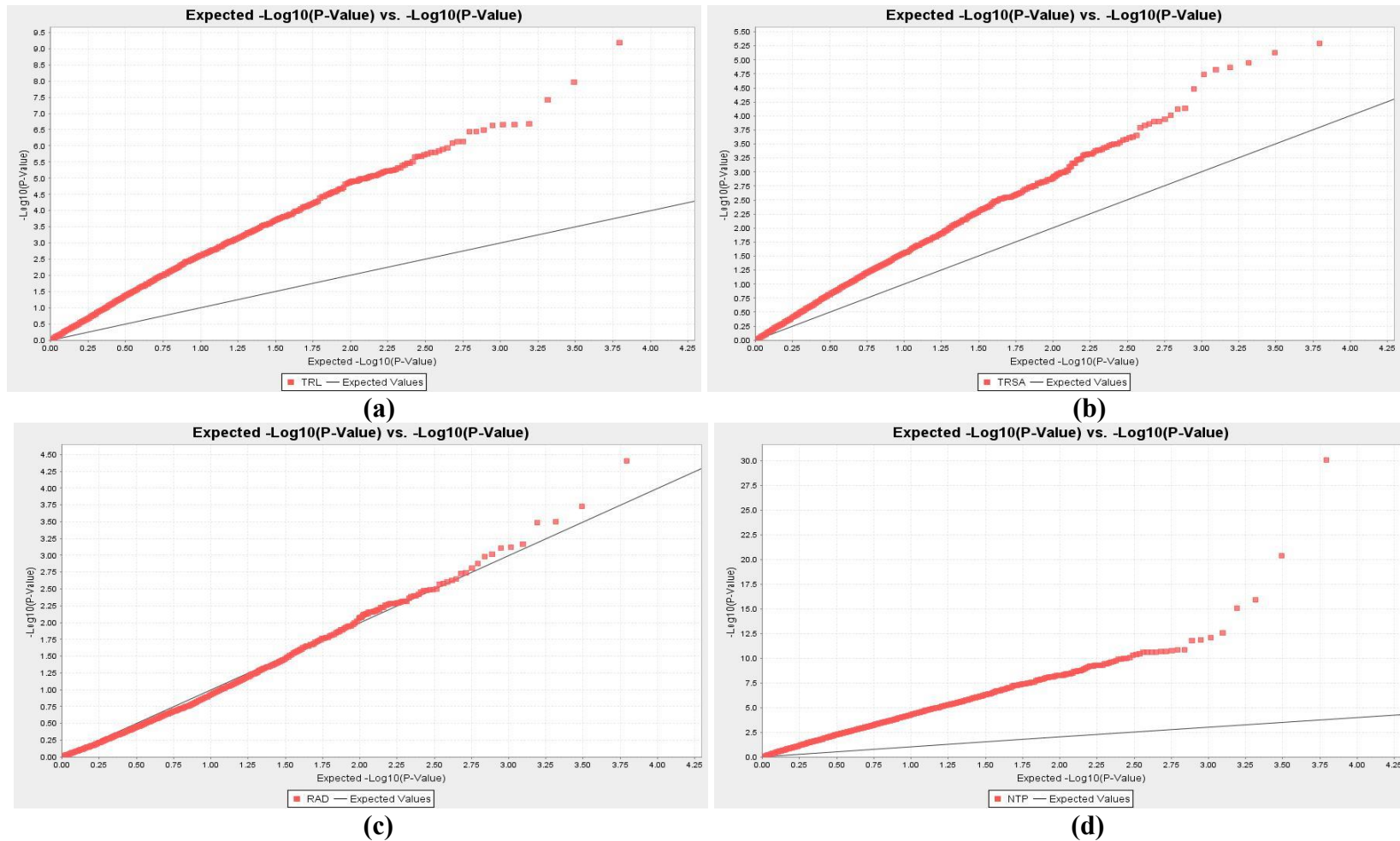
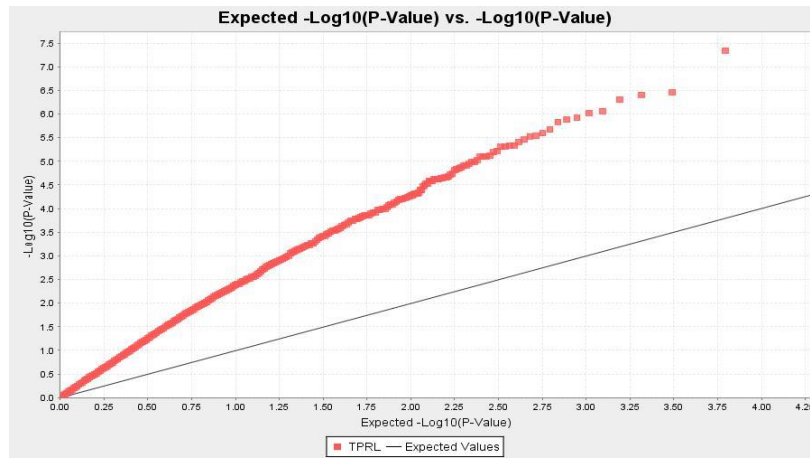
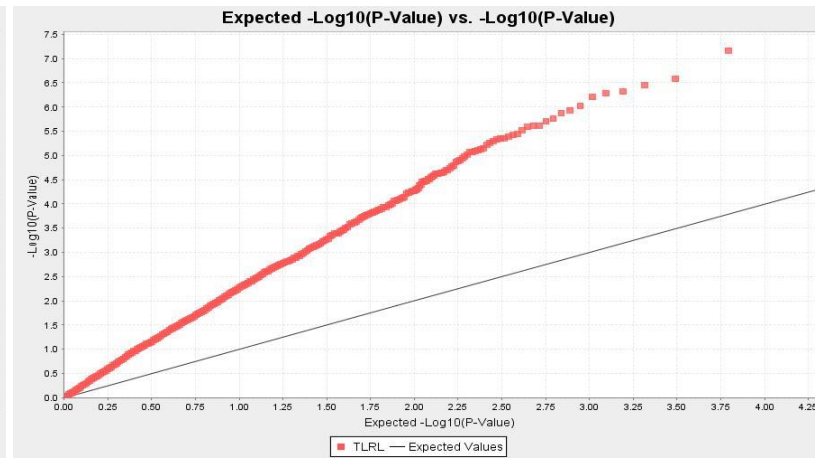


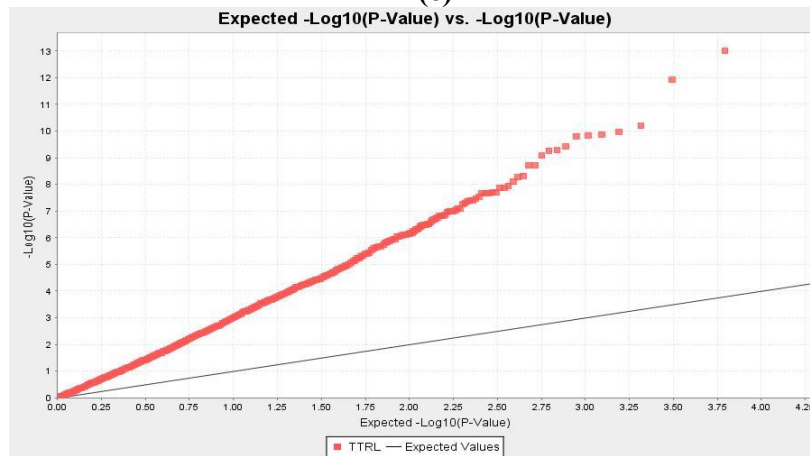
Figure A1c. Quantile-Quantile comparison of GWAS model Q + D for identifying loci associated with eight root architectural traits in 313 *Brassica* accessions representing five species *B. napus*, *B. oleracea*, *B. rapa*, *B. carinata* and *B. juncea*. Traits include (a) total root length (TRL/cm), (b) total surface area of roots (TRSA/cm²), (c) average root diameter (RAD/cm), (d) number of tips (NTP), (e) total primary root length (TPRL/cm), (f) total lateral root length (TLRL/cm), (g) total tertiary root length (TTRL/cm) and (h) basal link length (BLL/cm). The black line is the expected $-\log_{10}P$ distribution while colored lines are the observed $-\log_{10}P$ distribution for each of the eight root architectural traits.



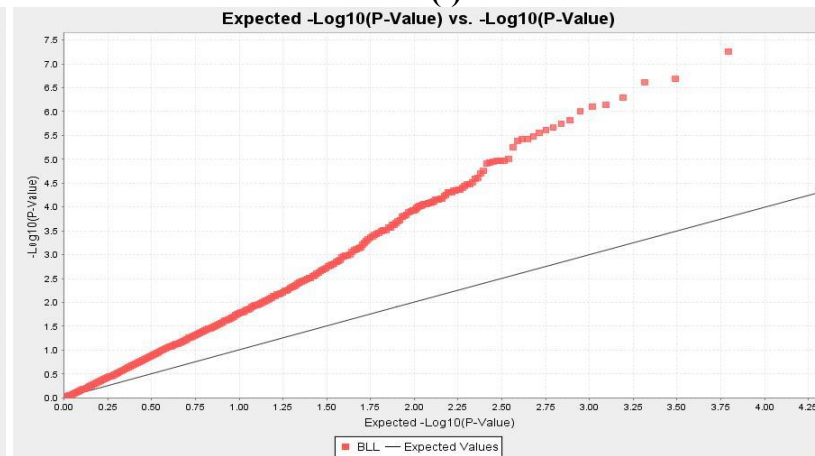
(e)



(f)



(g)



(h)

Figure A1c (continued). Quantile-Quantile comparison of GWAS model Q + D for identifying loci associated with eight root architectural traits in 313 *Brassica* accessions representing five species *B. napus*, *B. oleracea*, *B. rapa*, *B. carinata* and *B. juncea*. Traits include (a) total root length (TRL/cm), (b) total surface area of roots (TRSA/cm²), (c) average root diameter (RAD/cm), (d) number of tips (NTP), (e) total primary root length (TPRL/cm), (f) total lateral root length (TLRL/cm), (g) total tertiary root length (TTRL/cm) and (h) basal link length (BLL/cm). The black line is the expected $-\log_{10}P$ distribution while colored lines are the observed $-\log_{10}P$ distribution for each of the eight root architectural traits.

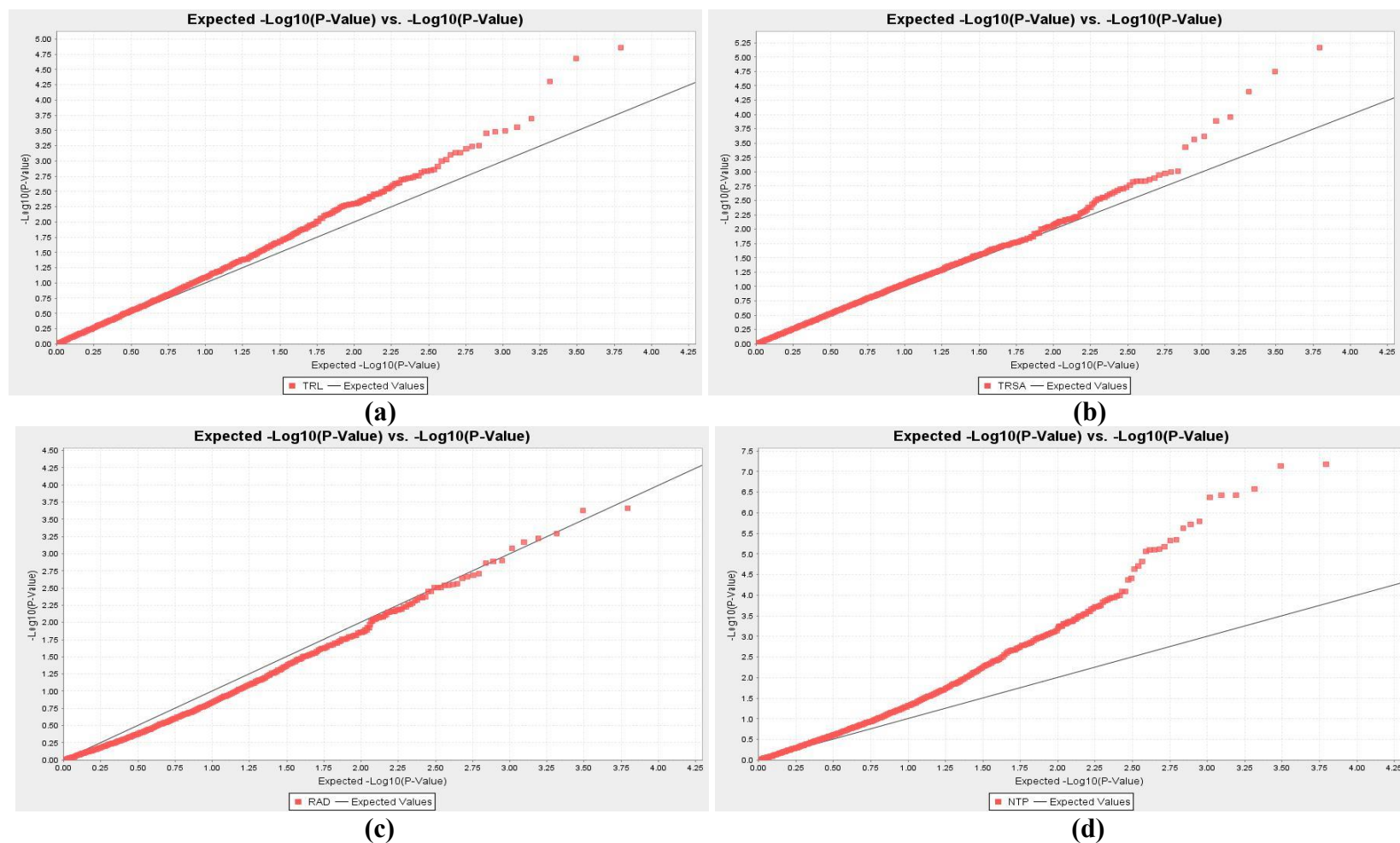


Figure A1d. Quantile-Quantile comparison of GWAS model Q + K for identifying loci associated with eight root architectural traits in 313 *Brassica* accessions representing five species *B. napus*, *B. oleracea*, *B. rapa*, *B. carinata* and *B. juncea*. Traits include (a) total root length (TRL/cm), (b) total surface area of roots (TRSA/cm²), (c) average root diameter (RAD/cm), (d) number of tips (NTP), (e) total primary root length (TPRL/cm), (f) total lateral root length (TLRL/cm), (g) total tertiary root length (TTRL/cm) and (h) basal link length (BLL/cm). The black line is the expected $-\log_{10} P$ distribution while colored lines are the observed $-\log_{10} P$ distribution for each of the eight root architectural traits.

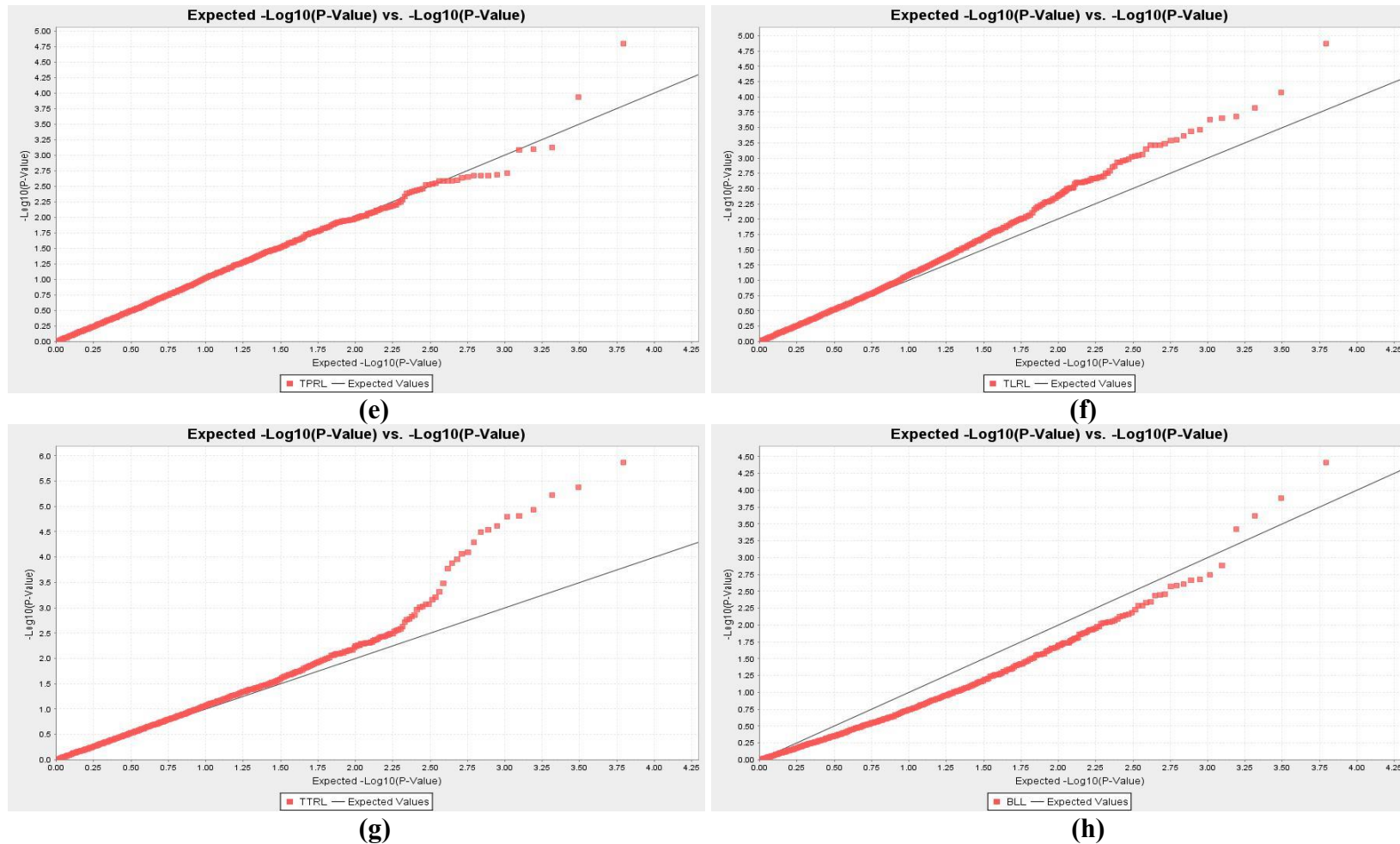


Figure A1d (continued). Quantile-Quantile comparison of GWAS model Q + K for identifying loci associated with eight root architectural traits in 313 *Brassica* accessions representing five species *B. napus*, *B. oleracea*, *B. rapa*, *B. carinata* and *B. juncea*. Traits include (a) total root length (TRL/cm), (b) total surface area of roots (TRSA/cm²), (c) average root diameter (RAD/cm), (d) number of tips (NTP), (e) total primary root length (TPRL/cm), (f) total lateral root length (TLRL/cm), (g) total tertiary root length (TTRL/cm) and (h) basal link length (BLL/cm). The black line is the expected $-\log_{10}P$ distribution while colored lines are the observed $-\log_{10}P$ distribution for each of the eight root architectural traits.

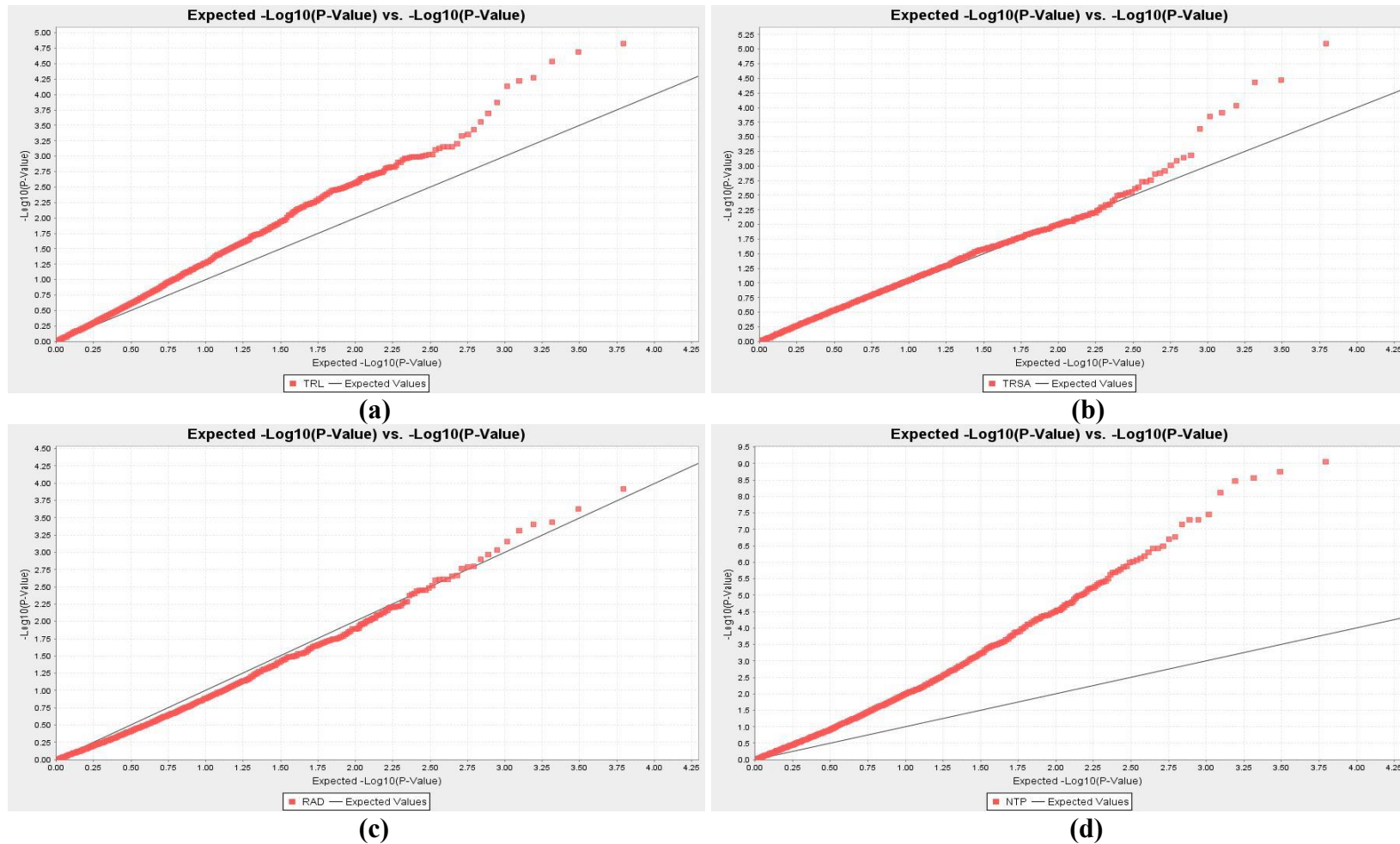


Figure A1e. Quantile-Quantile comparison of GWAS model PCA-only for identifying loci associated with eight root architectural traits in 313 *Brassica* accessions representing five species *B. napus*, *B. oleracea*, *B. rapa*, *B. carinata* and *B. juncea*. Traits include (a) total root length (TRL/cm), (b) total surface area of roots (TRSA/cm²), (c) average root diameter (RAD/cm), (d) number of tips (NTP), (e) total primary root length (TPRL/cm), (f) total lateral root length (TLRL/cm), (g) total tertiary root length (TTRL/cm) and (h) basal link length (BLL/cm). The black line is the expected $-\log_{10} P$ distribution while colored lines are the observed $-\log_{10} P$ distribution for each of the eight root architectural traits.

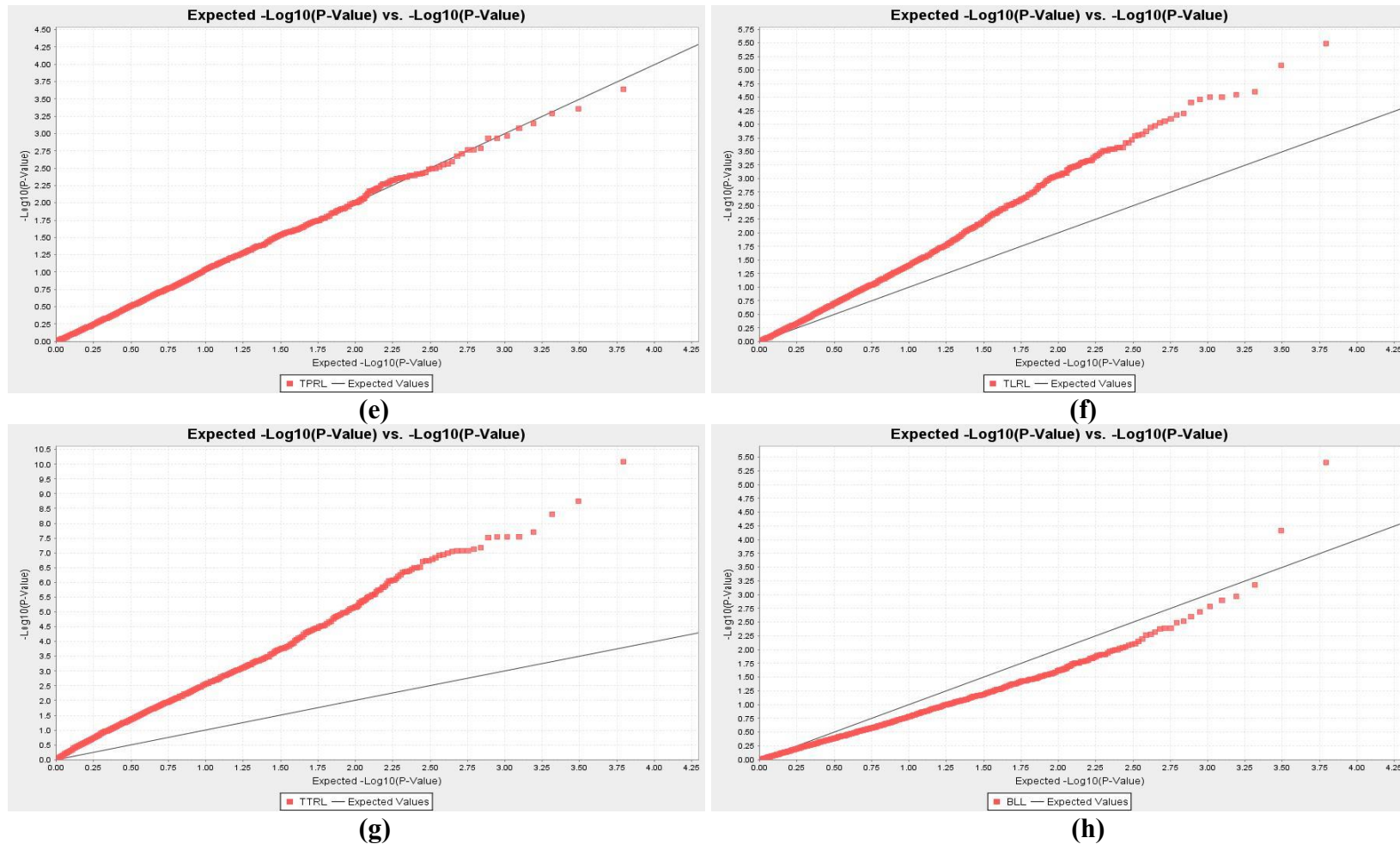


Figure A1e (continued). Quantile-Quantile comparison of GWAS model PCA-only for identifying loci associated with eight root architectural traits in 313 *Brassica* accessions representing five species *B. napus*, *B. oleracea*, *B. rapa*, *B. carinata* and *B. juncea*. Traits include (a) total root length (TRL/cm), (b) total surface area of roots (TRSA/cm²), (c) average root diameter (RAD/cm), (d) number of tips (NTP), (e) total primary root length (TPRL/cm), (f) total lateral root length (TLRL/cm), (g) total tertiary root length (TTRL/cm) and (h) basal link length (BLL/cm). The black line is the expected $-\log_{10}P$ distribution while colored lines are the observed $-\log_{10}P$ distribution for each of the eight root architectural traits.

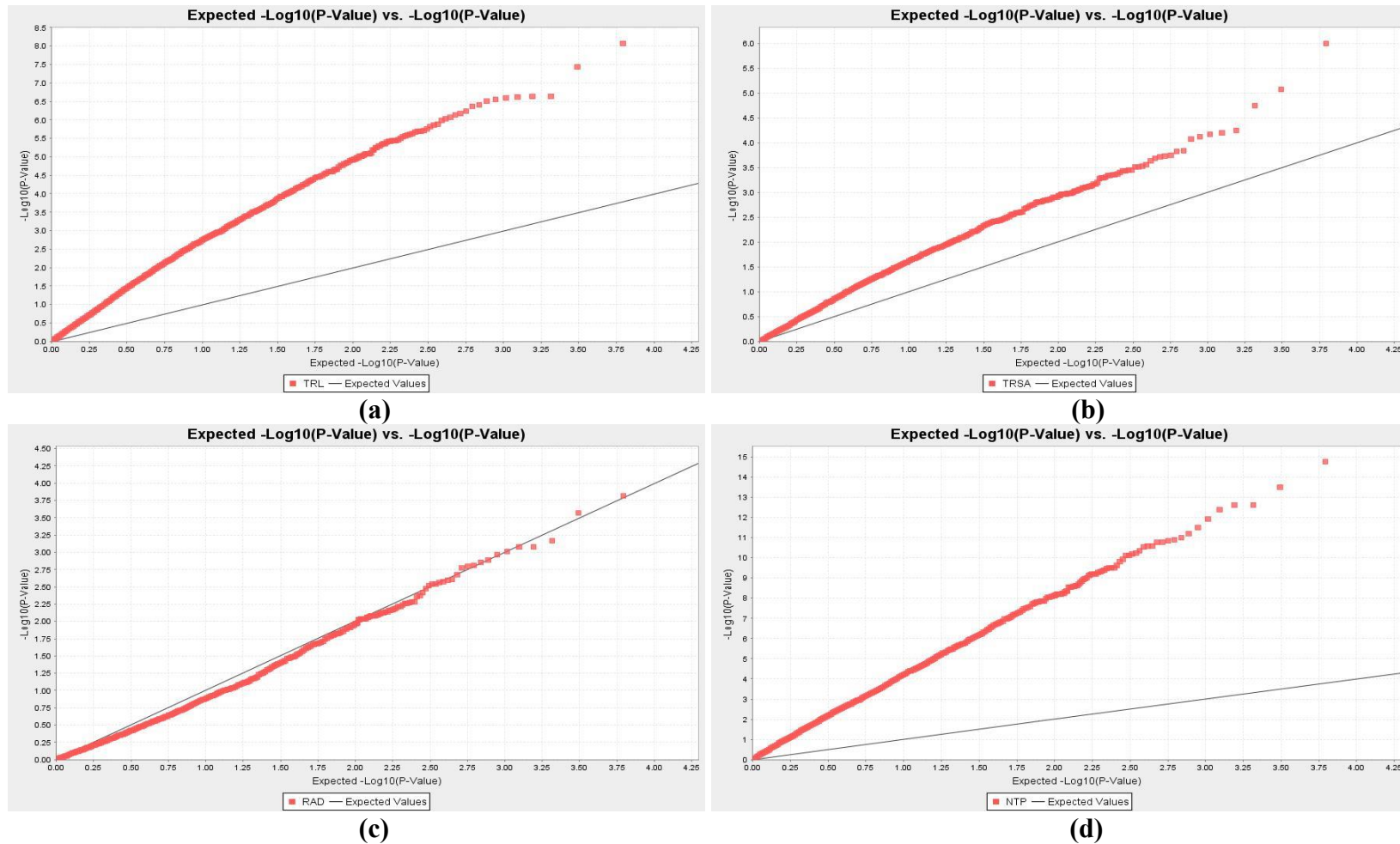
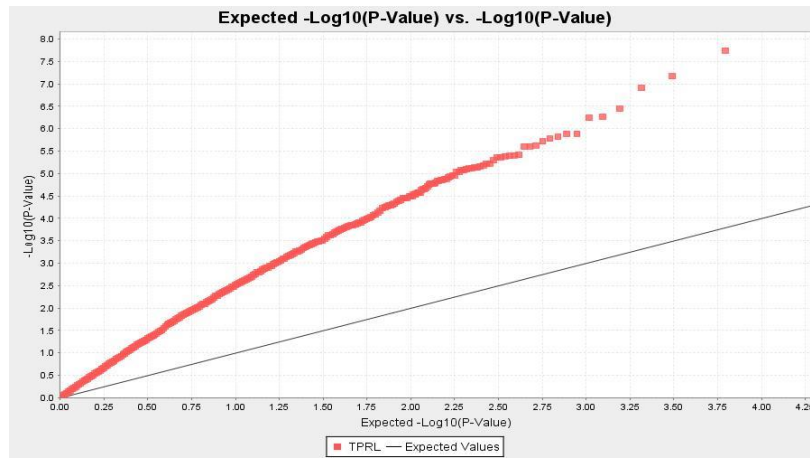
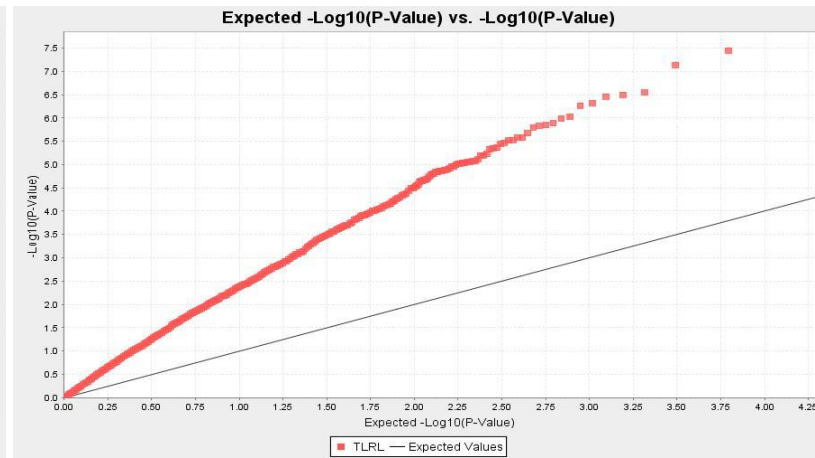


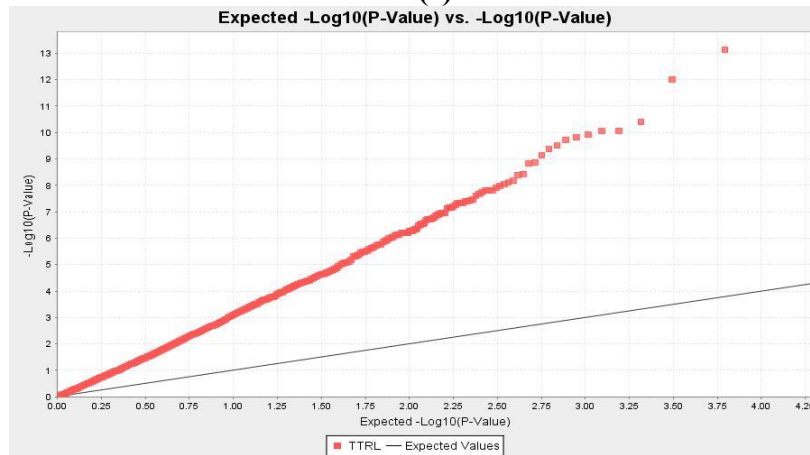
Figure A1f. Quantile-Quantile comparison of GWAS model Q-only for identifying loci associated with eight root architectural traits in 313 *Brassica* accessions representing five species *B. napus*, *B. oleracea*, *B. rapa*, *B. carinata* and *B. juncea*. Traits include (a) total root length (TRL/cm), (b) total surface area of roots (TRSA/cm²), (c) average root diameter (RAD/cm), (d) number of tips (NTP), (e) total primary root length (TPRL/cm), (f) total lateral root length (TLRL/cm), (g) total tertiary root length (TTRL/cm) and (h) basal link length (BLL/cm). The black line is the expected $-\log_{10} P$ distribution while colored lines are the observed $-\log_{10} P$ distribution for each of the eight root architectural traits.



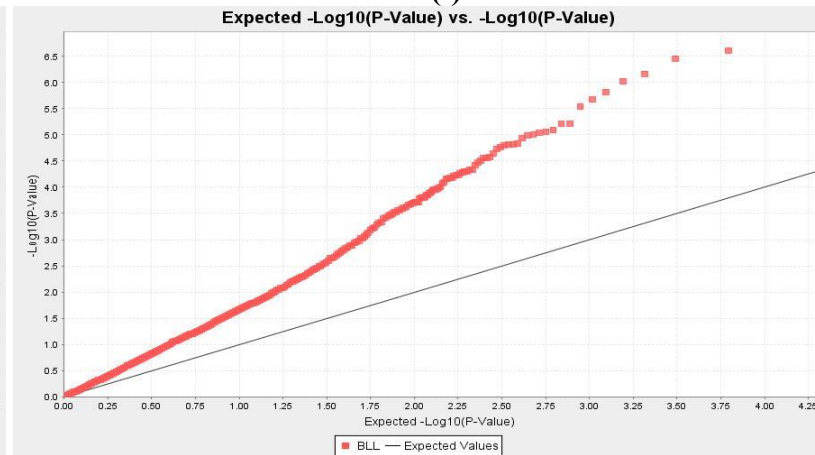
(e)



(f)

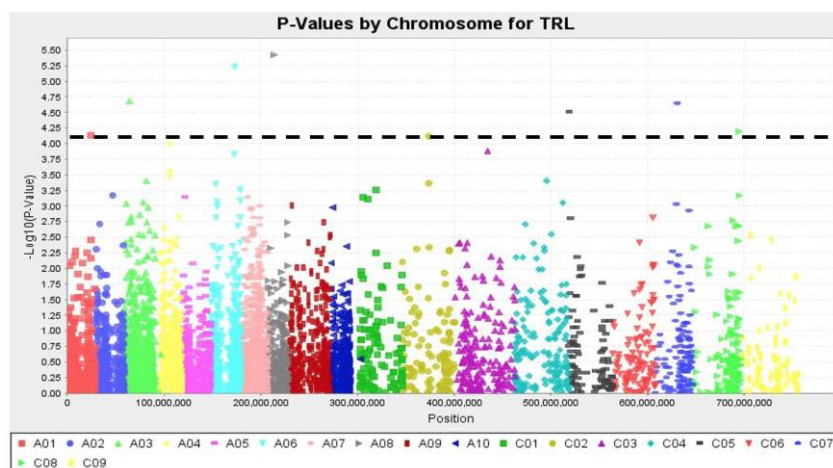


(g)

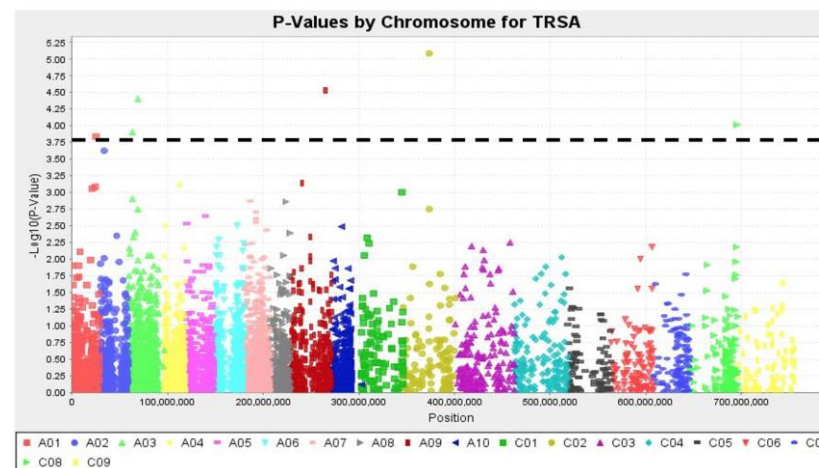


(h)

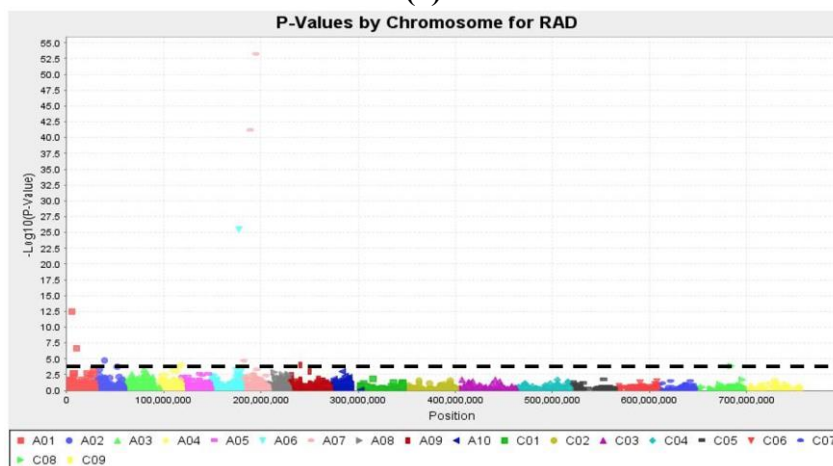
Figure A1f (continued) Quantile-Quantile comparison of GWAS model Q-only for identifying loci associated with eight root architectural traits in 313 *Brassica* accessions representing five species *B. napus*, *B. oleracea*, *B. rapa*, *B. carinata* and *B. juncea*. Traits include (a) total root length (TRL/cm), (b) total surface area of roots (TRSA/cm²), (c) average root diameter (RAD/cm), (d) number of tips (NTP), (e) total primary root length (TPRL/cm), (f) total lateral root length (TLRL/cm), (g) total tertiary root length (TTRL/cm) and (h) basal link length (BLL/cm). The black line is the expected $-\log_{10}P$ distribution while colored lines are the observed $-\log_{10}P$ distribution for each of the eight root architectural traits.



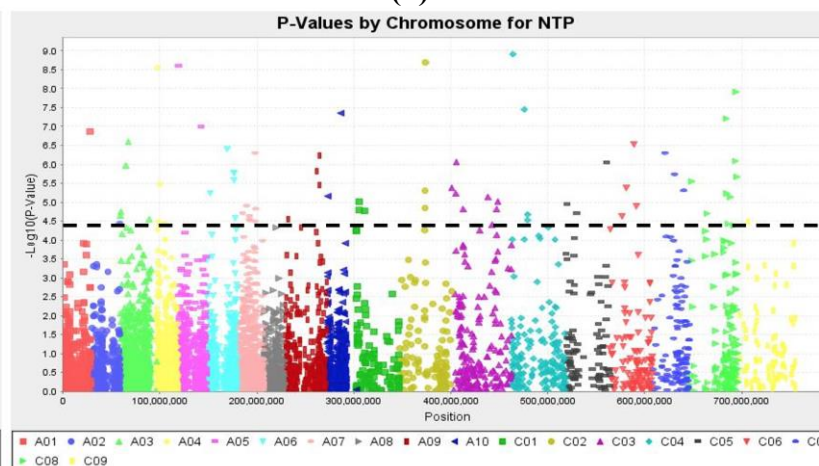
(a)



(b)

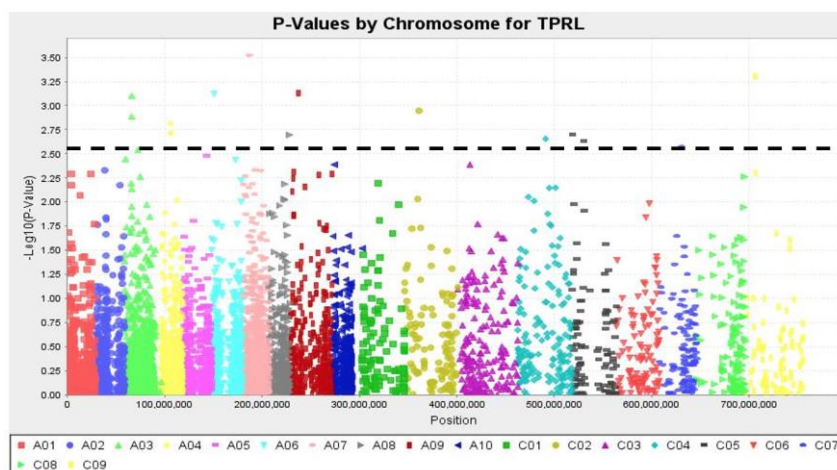


(c)

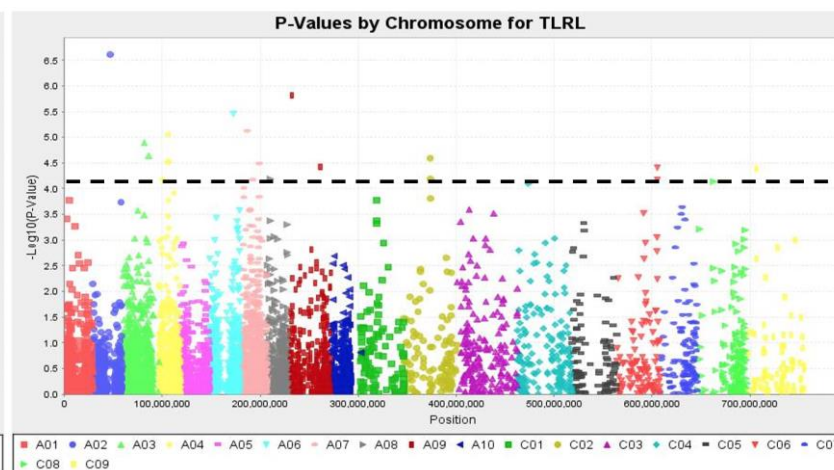


(d)

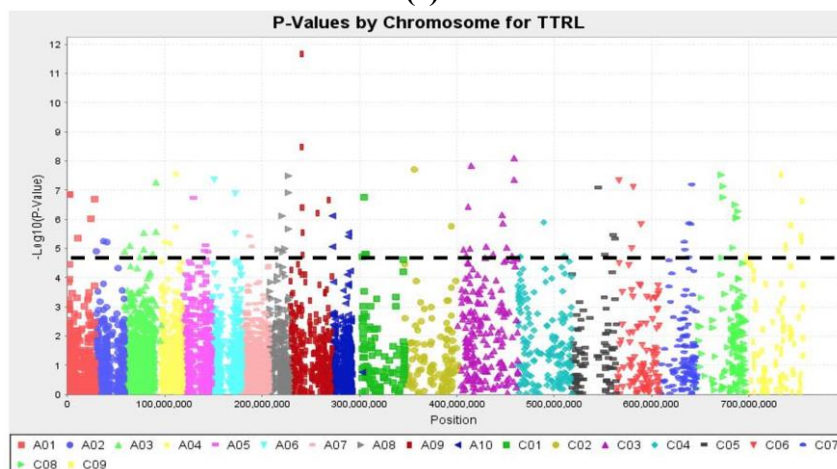
Figure A2a. Manhattan plots of the PCA + D MLM models for identifying root architecture traits loci in 313 *Brassica* accessions representing five species *B. napus*, *B. oleracea*, *B. rapa*, *B. carinata* and *B. juncea*. The dashed horizontal lines indicate the Bonferroni-adjusted significance threshold known as “logarithm-of-odds” (LOD score). The dots above the significance threshold indicate SNPs associated with resistance to each trait.



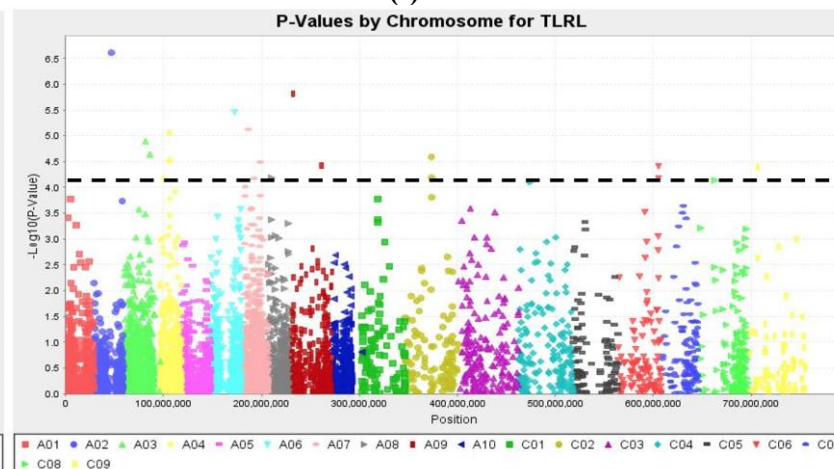
(e)



(f)



(g)



(h)

Figure A2a (continued). Manhattan plots of the PCA + D MLM models for identifying root architecture traits loci in 313 *Brassica* accessions representing five species *B. napus*, *B. oleracea*, *B. rapa*, *B. carinata* and *B. juncea*. The dashed horizontal lines indicate the Bonferroni-adjusted significance threshold known as “logarithm-of-odds” (LOD score). The dots above the significance threshold indicate SNPs associated with resistance to each trait.

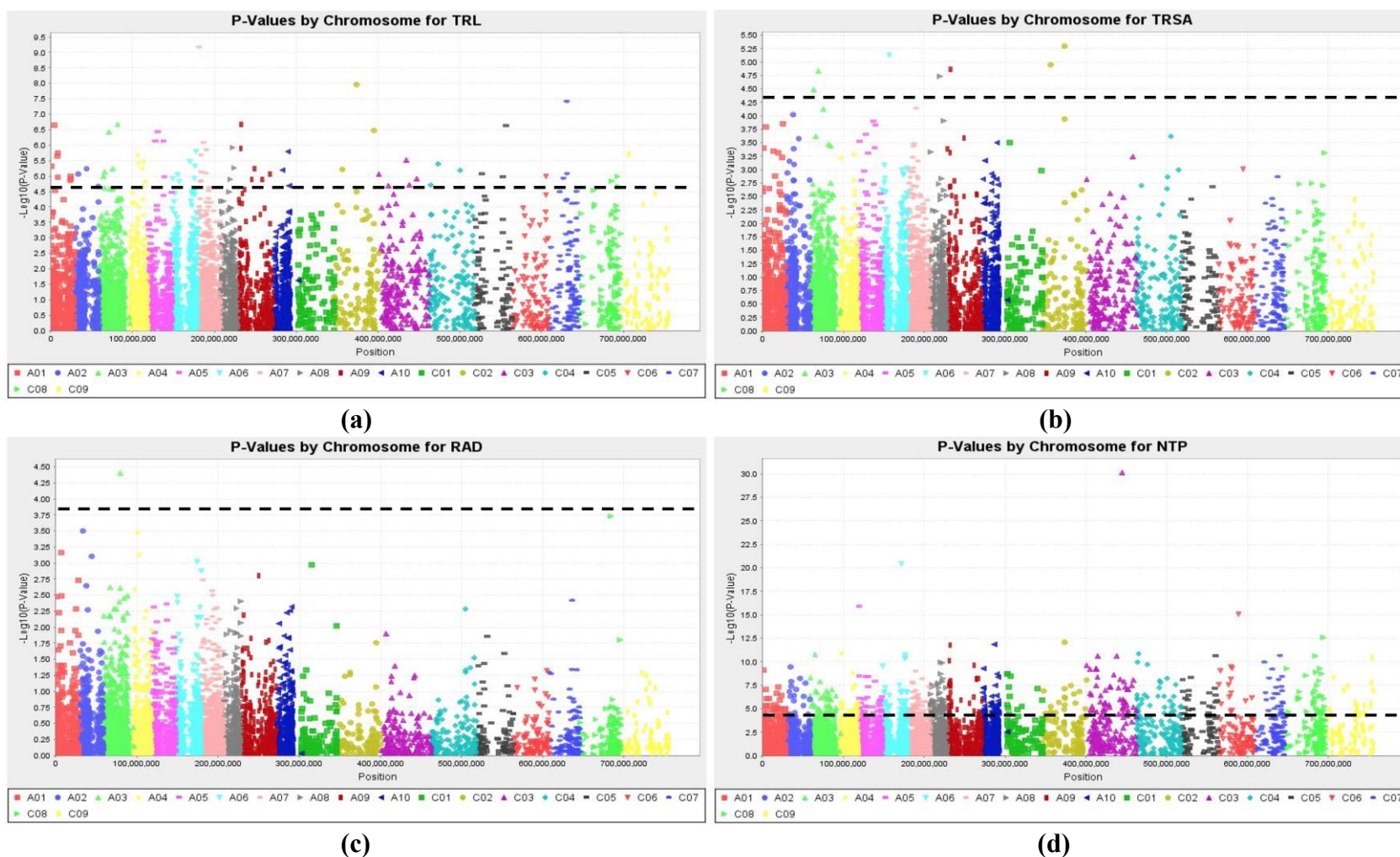
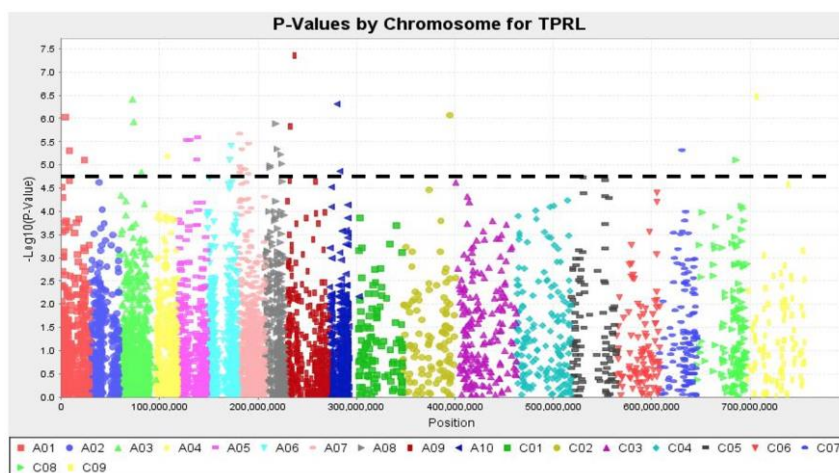
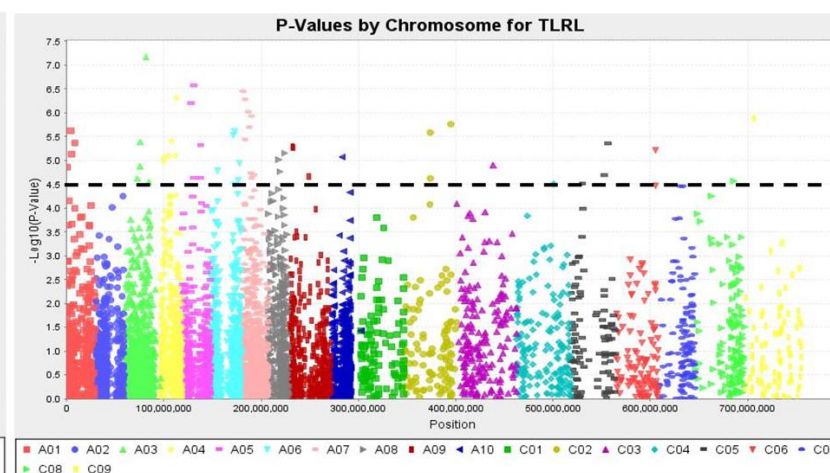


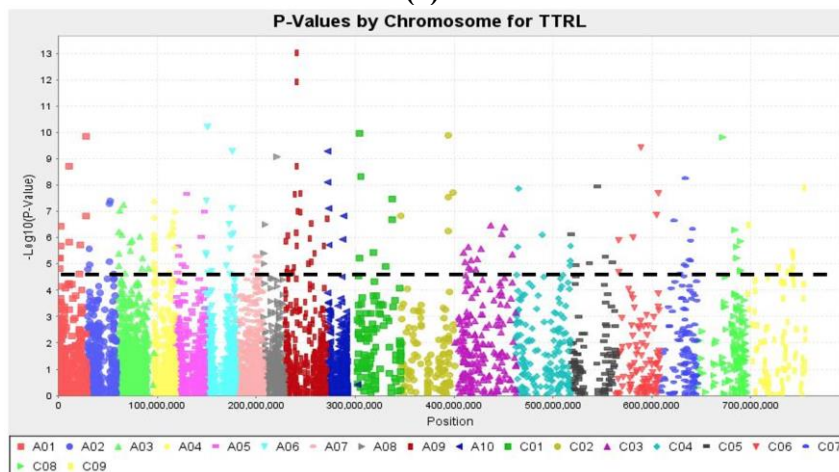
Figure A2b. Manhattan plots of the Q + D MLM models for identifying root architecture traits loci in 313 *Brassica* accessions representing five species *B. napus*, *B. oleracea*, *B. rapa*, *B. carinata* and *B. juncea*. The dashed horizontal lines indicate the Bonferroni-adjusted significance threshold known as “logarithm-of-odds” (LOD score). The dots above the significance threshold indicate SNPs associated with resistance to each trait.



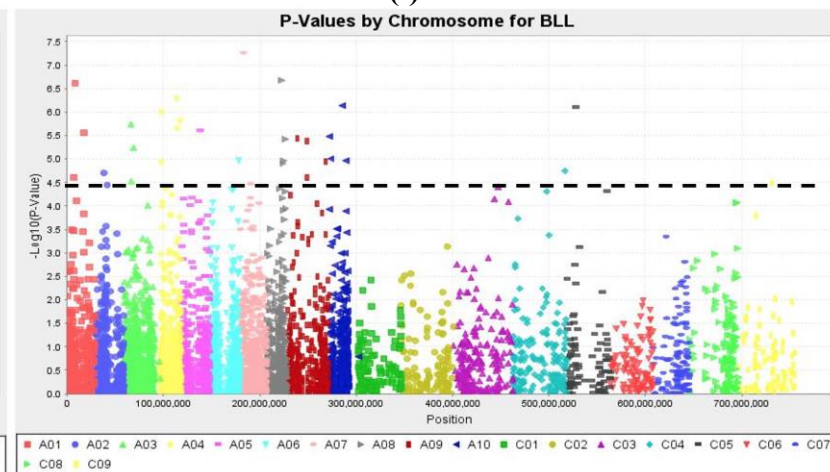
(e)



(f)

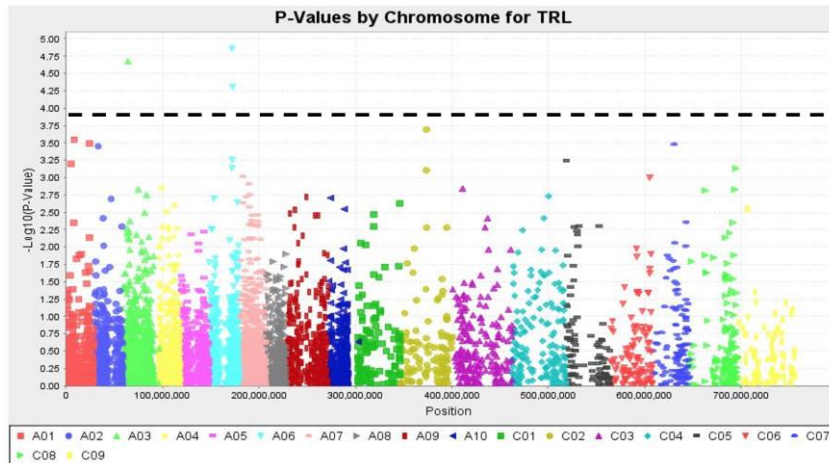


(g)

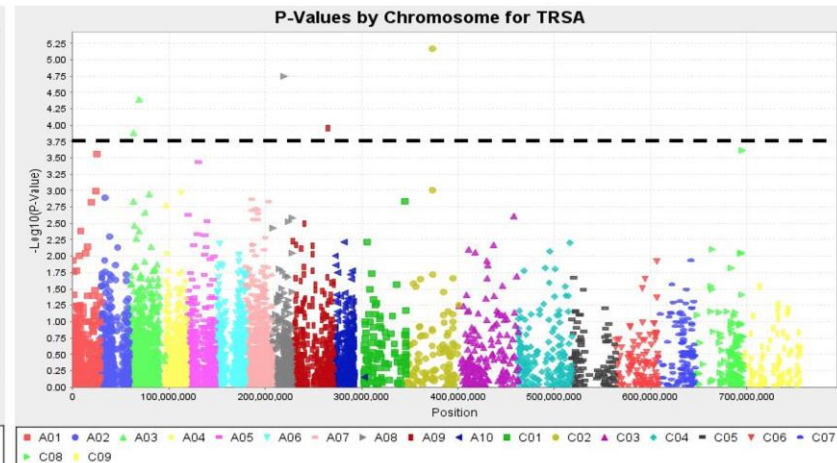


(h)

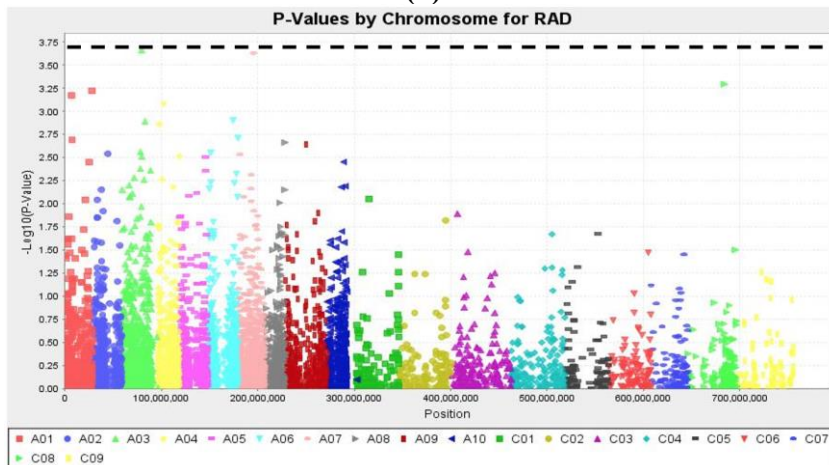
Figure A2b (continued). Manhattan plots of the Q + D MLM models for identifying root architecture traits loci in 313 *Brassica* accessions representing five species *B. napus*, *B. oleracea*, *B. rapa*, *B. carinata* and *B. juncea*. The dashed horizontal lines indicate the Bonferroni-adjusted significance threshold known as “logarithm-of-odds” (LOD score). The dots above the significance threshold indicate SNPs associated with resistance to each trait.



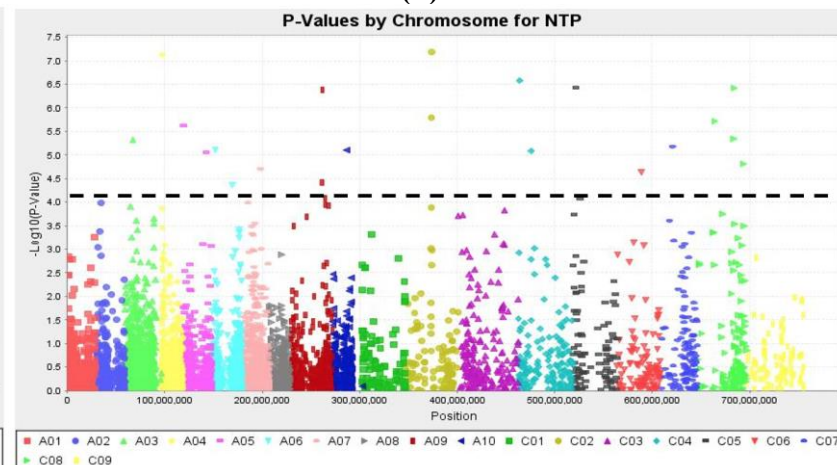
(a)



(b)

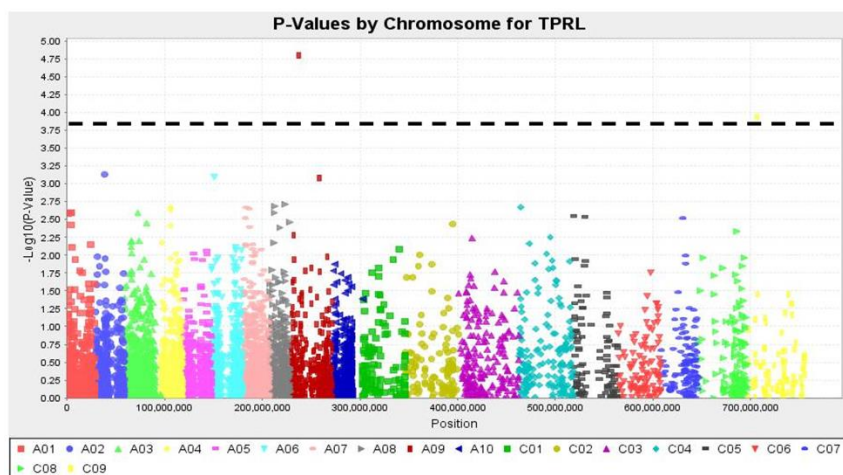


(c)

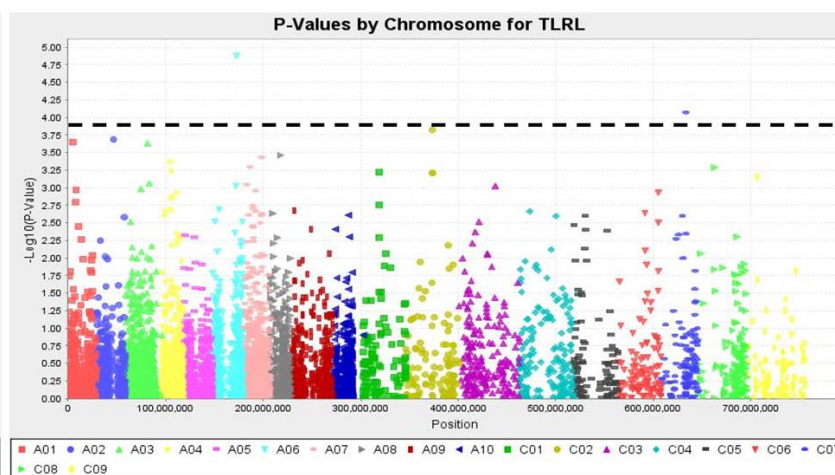


(d)

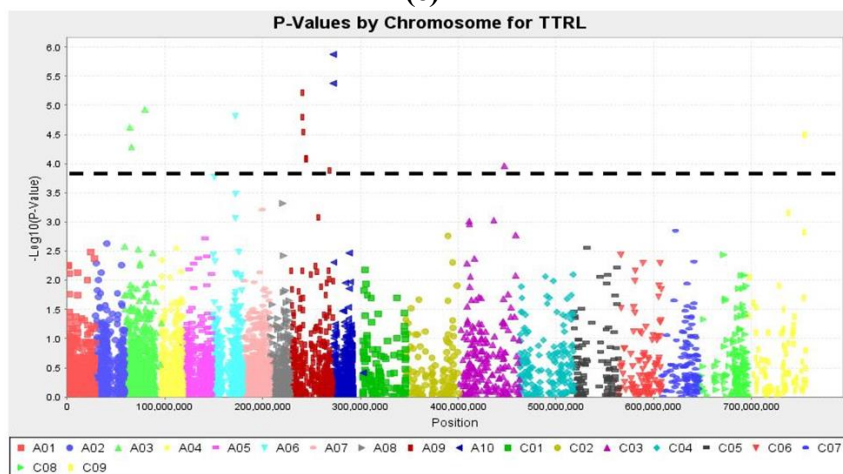
Figure A2c. Manhattan plots of the Q + K MLM models for identifying root architecture traits loci in 313 *Brassica* accessions representing five species *B. napus*, *B. oleracea*, *B. rapa*, *B. carinata* and *B. juncea*. The dashed horizontal lines indicate the Bonferroni-adjusted significance threshold known as “logarithm-of-odds” (LOD score). The dots above the significance threshold indicate SNPs associated with resistance to each trait.



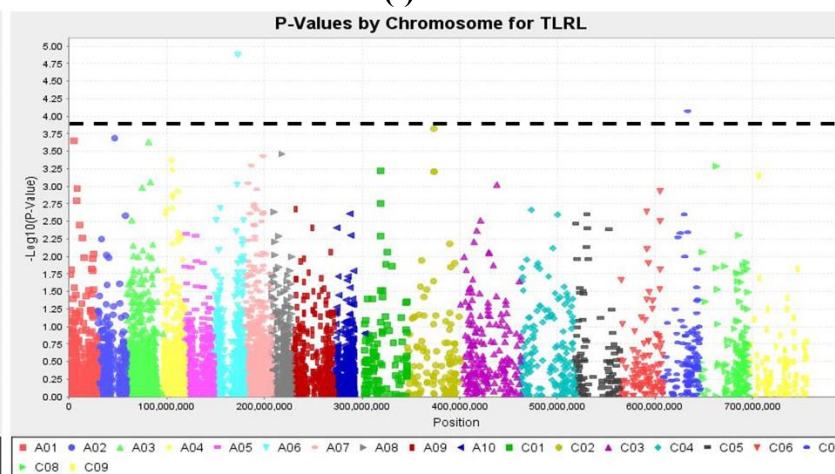
(e)



(f)

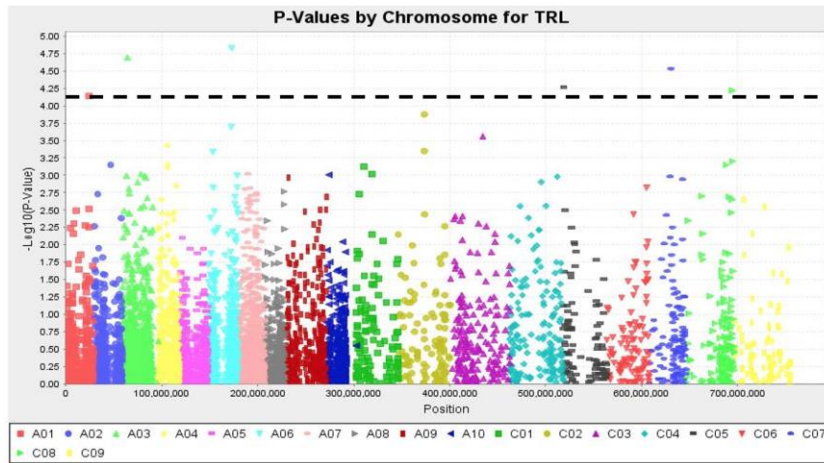


(g)

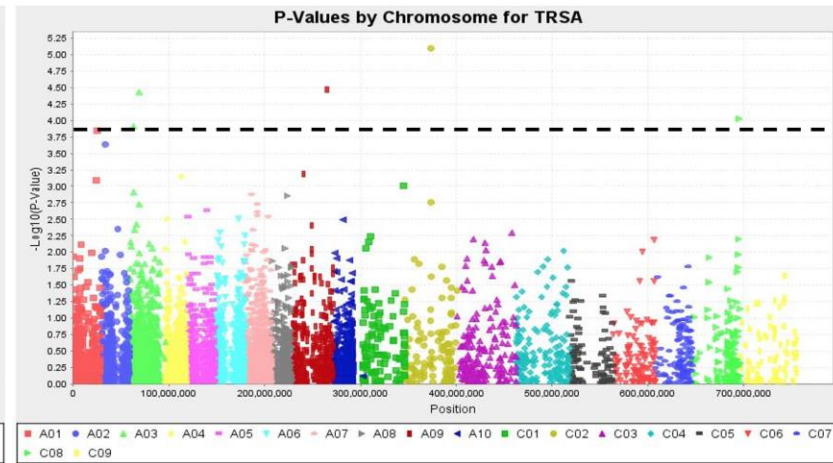


(h)

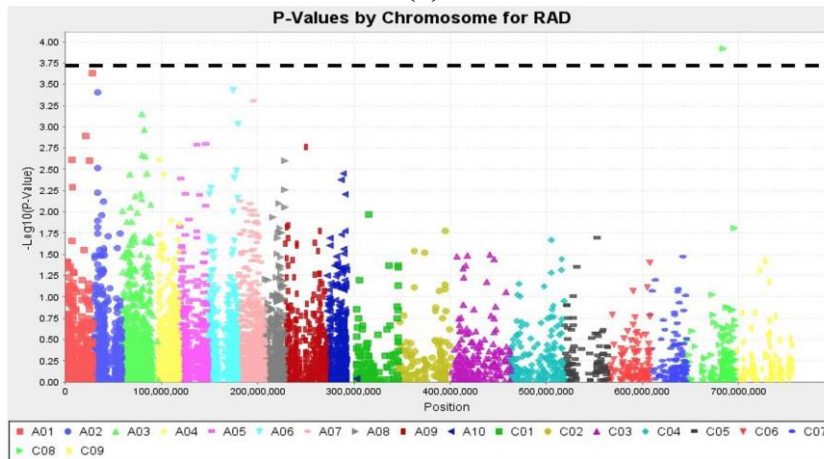
Figure A2c (continued). Manhattan plots of the Q + K MLM models for identifying root architecture traits loci in 313 *Brassica* accessions representing five species *B. napus*, *B. oleracea*, *B. rapa*, *B. carinata* and *B. juncea*. The dashed horizontal lines indicate the Bonferroni-adjusted significance threshold known as “logarithm-of-odds” (LOD score). The dots above the significance threshold indicate SNPs associated with resistance to each trait.



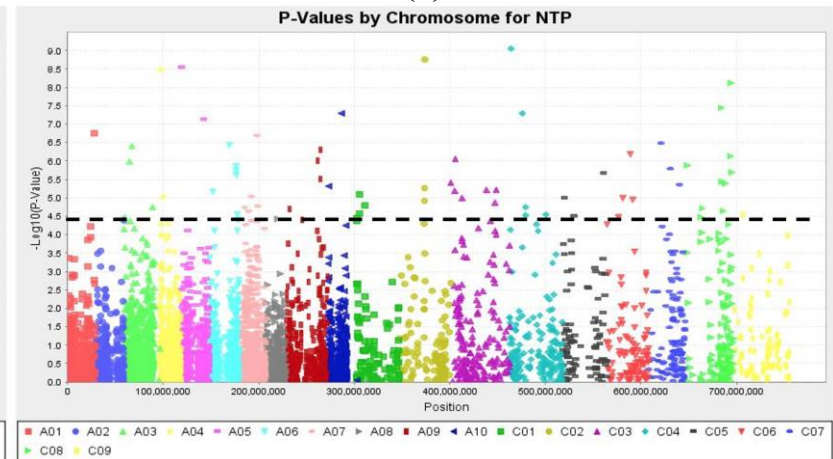
(a)



(b)

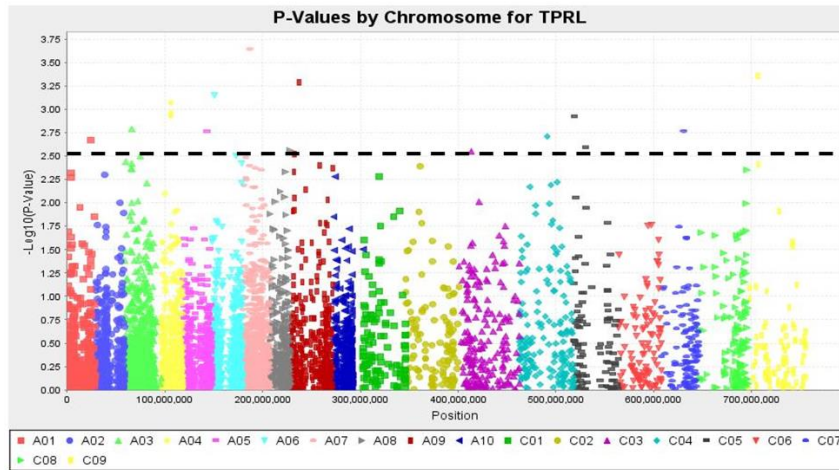


(c)

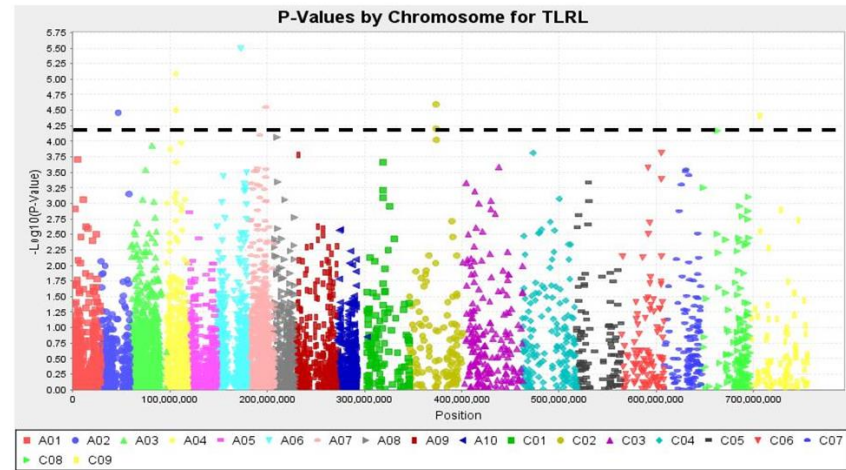


(d)

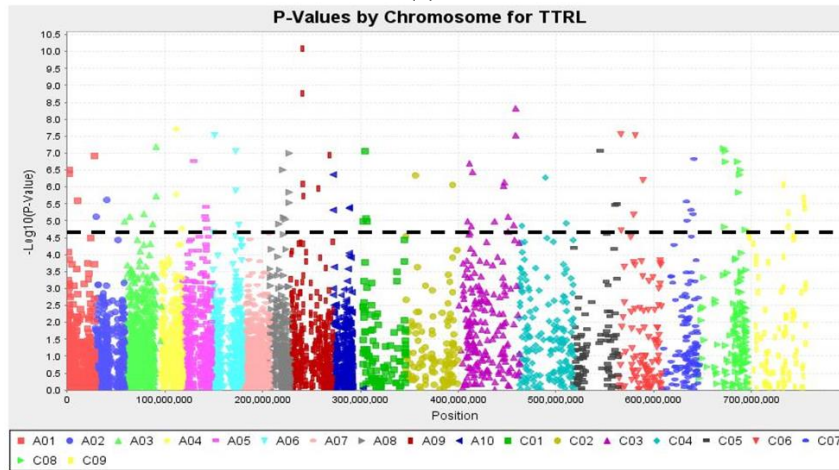
Figure A2d. Manhattan plots of the PCA-only GLM models for identifying root architecture traits loci in 313 *Brassica* accessions representing five species *B. napus*, *B. oleracea*, *B. rapa*, *B. carinata* and *B. juncea*. The dashed horizontal lines indicate the Bonferroni-adjusted significance threshold known as “logarithm-of-odds” (LOD score). The dots above the significance threshold indicate SNPs associated with resistance to each trait.



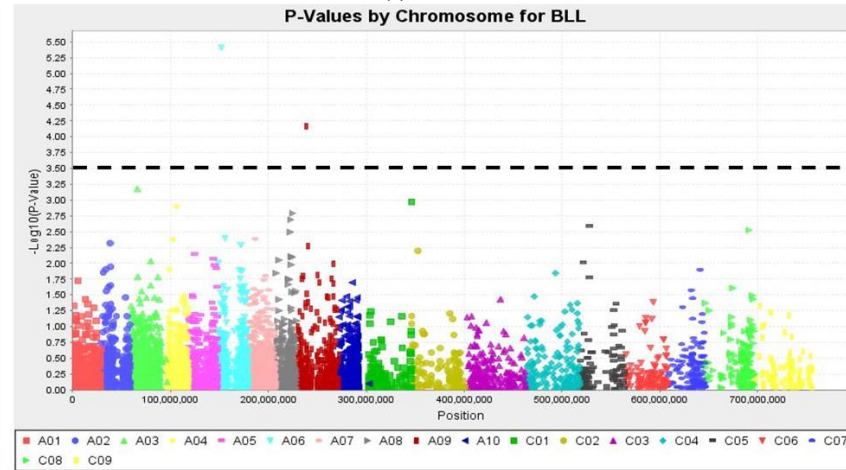
(e)



(f)

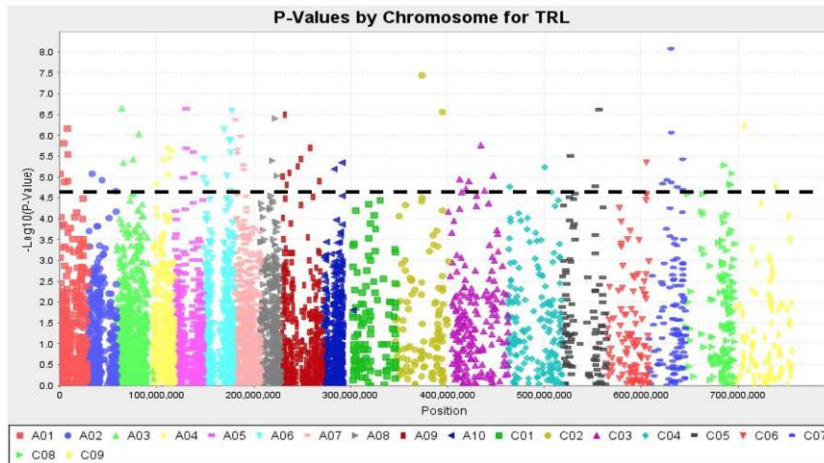


(g)

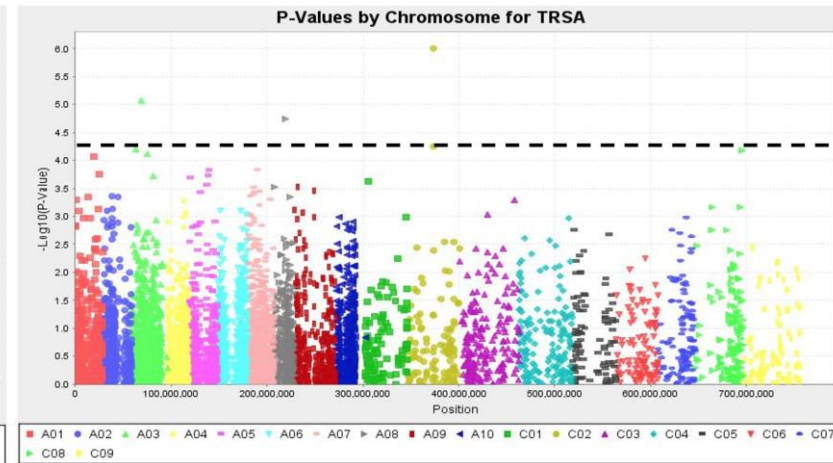


(h)

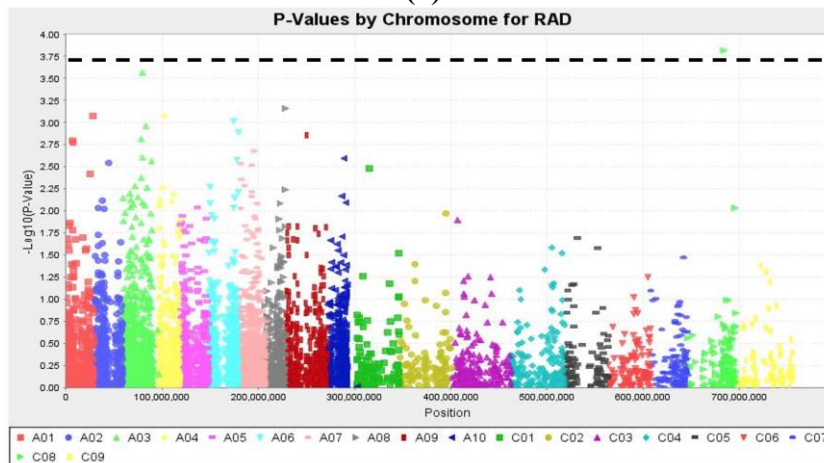
Figure A2d (continued). Manhattan plots of the PCA-only GLM models for identifying root architecture traits loci in 313 *Brassica* accessions representing five species *B. napus*, *B. oleracea*, *B. rapa*, *B. carinata* and *B. juncea*. The dashed horizontal lines indicate the Bonferroni-adjusted significance threshold known as “logarithm-of-odds” (LOD score). The dots above the significance threshold indicate SNPs associated with resistance to each trait.



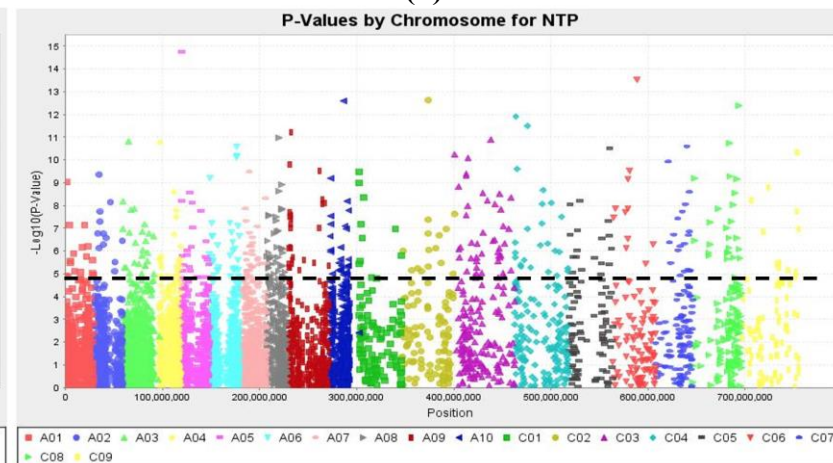
(a)



(b)

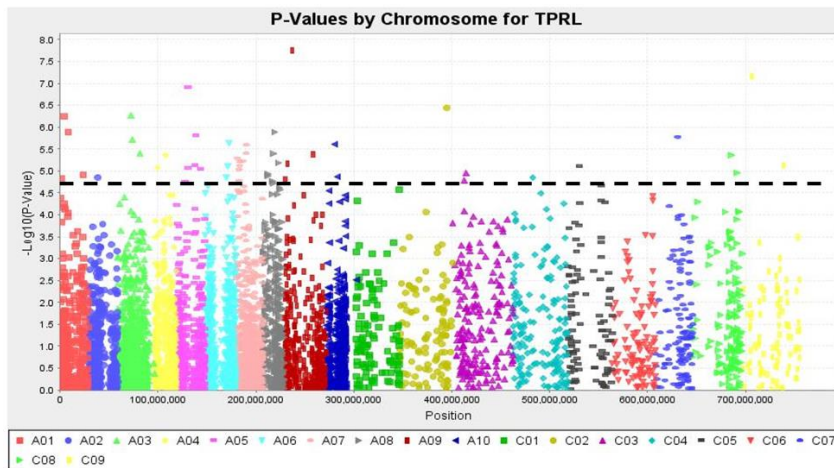


(c)

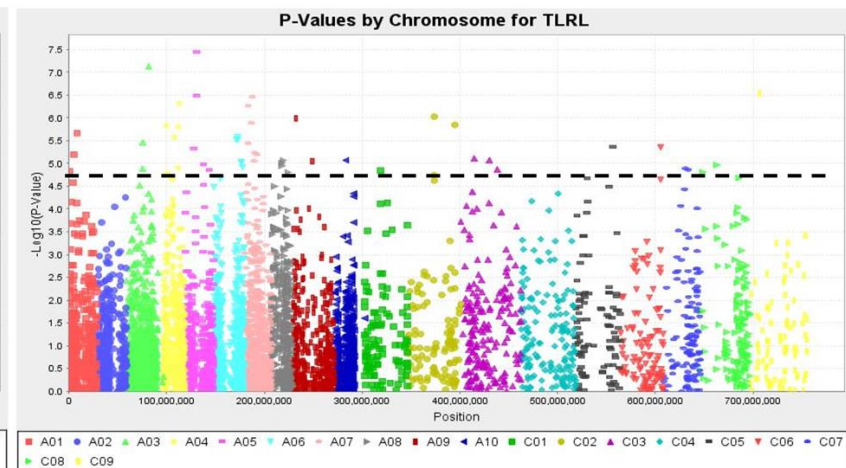


(d)

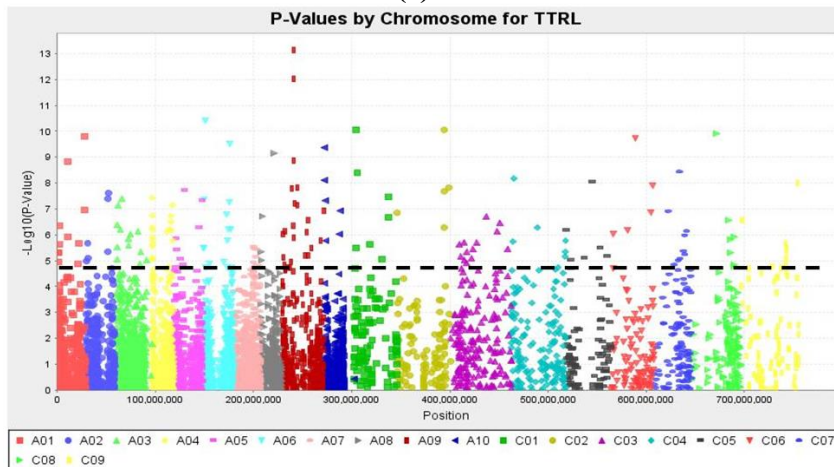
Figure A2e. Manhattan plots of the Q-only GLM models for identifying root architecture traits loci in 313 *Brassica* accessions representing five species *B. napus*, *B. oleracea*, *B. rapa*, *B. carinata* and *B. juncea*. The dashed horizontal lines indicate the Bonferroni-adjusted significance threshold known as “logarithm-of-odds” (LOD score). The dots above the significance threshold indicate SNPs associated with resistance to each trait.



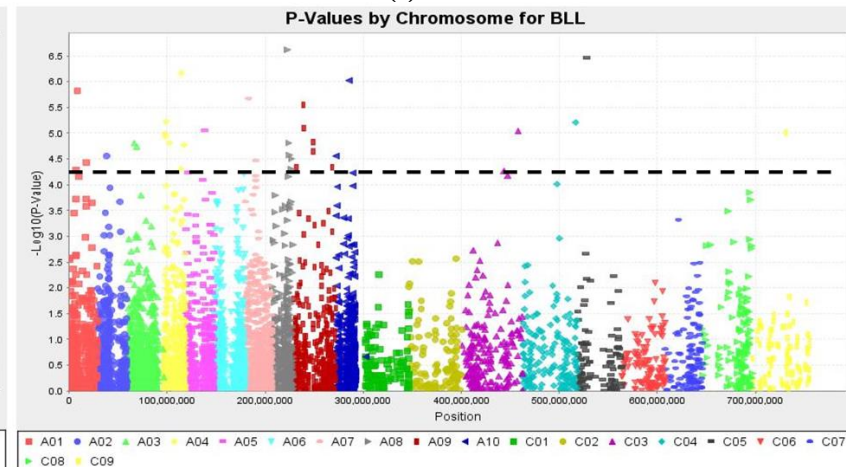
(e)



(f)



(g)



(h)

Figure A2e (continued). Manhattan plots of the Q-only GLM models for identifying root architecture traits loci in 313 *Brassica* accessions representing five species *B. napus*, *B. oleracea*, *B. rapa*, *B. carinata* and *B. juncea*. The dashed horizontal lines indicate the Bonferroni-adjusted significance threshold known as “logarithm-of-odds” (LOD score). The dots above the significance threshold indicate SNPs associated with resistance to each trait.

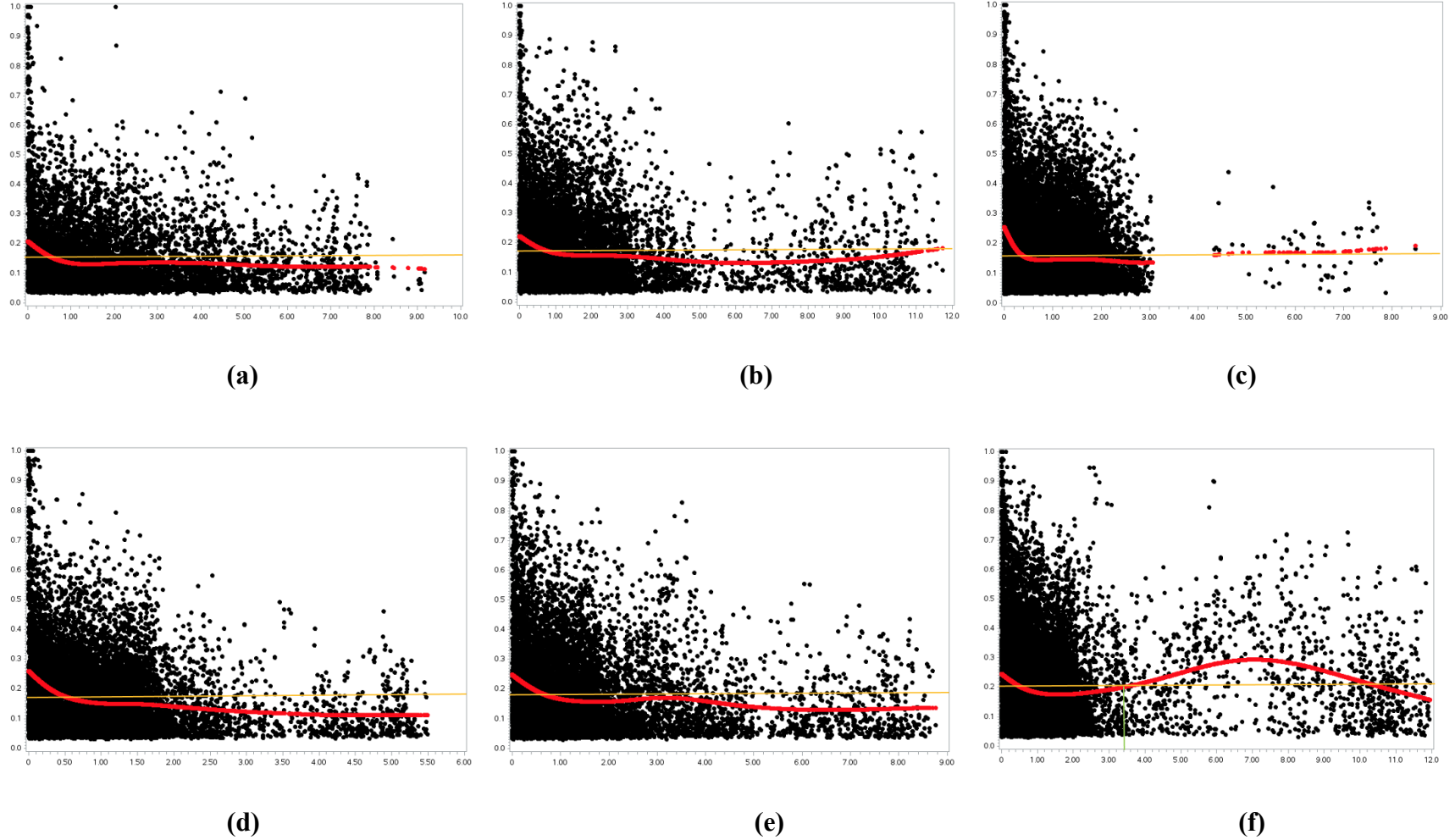


Figure A3. Plots of correlation coefficient (r^2) and physical distance (in Mb) for SNP markers on chromosomes A01 – A10 (a-j) and chromosomes C01 – C09 (k-s). The red curves represent the fitted plots of the data points, while the yellow line represents the background linkage disequilibrium (BLD) or threshold line. The decay of linkage disequilibrium was determined by projecting the intersection of the curves and the BLD line onto the physical distance axis.

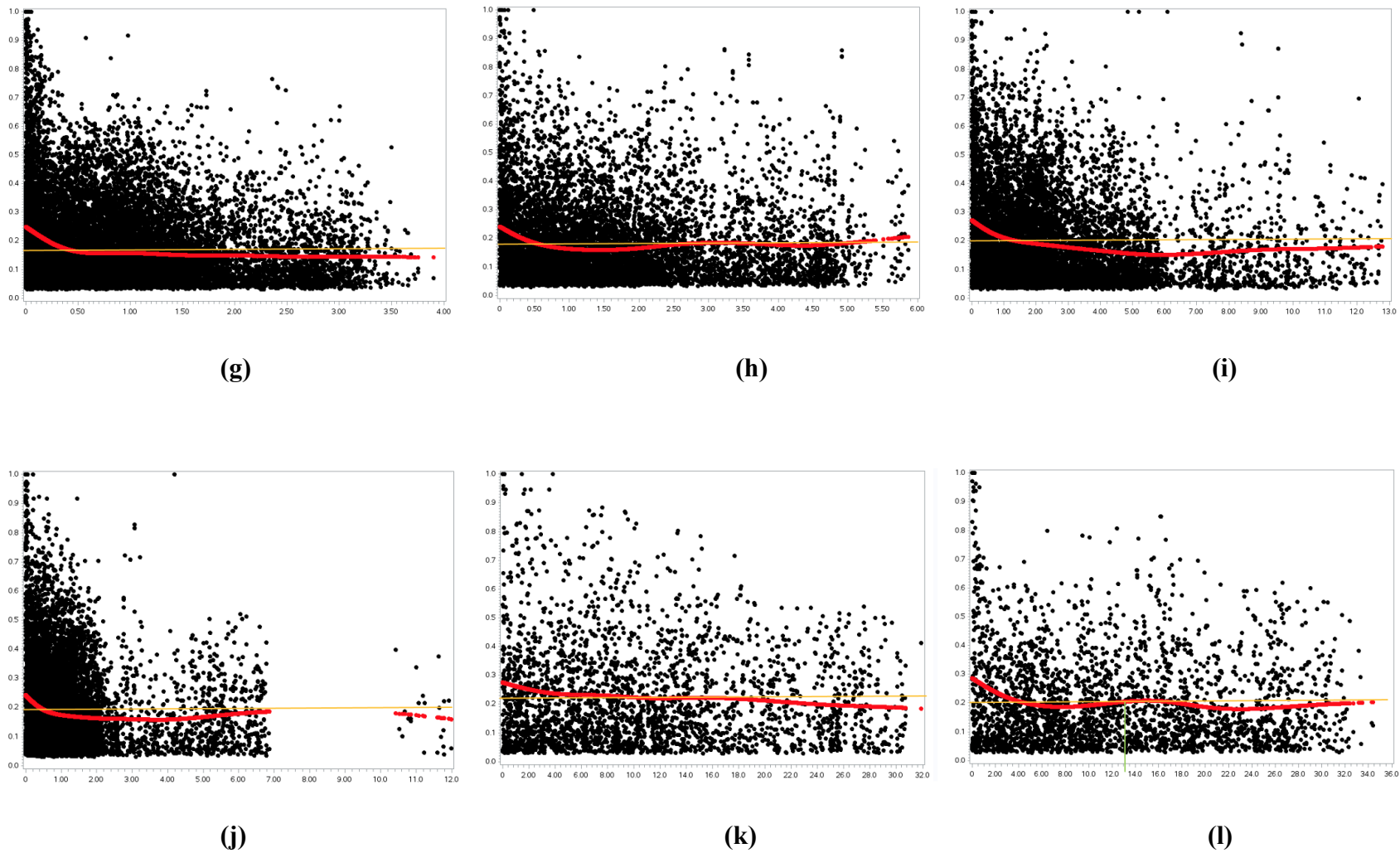


Figure A3 (continued). Plots of correlation coefficient (r^2) and physical distance (in Mb) for SNP markers on chromosomes A01 – A10 (a-j) and chromosomes C01 – C09 (k-s). The red curves represent the fitted plots of the data points, while the yellow line represents the background linkage disequilibrium (BLD) or threshold line. The decay of linkage disequilibrium was determined by projecting the intersection of the curves and the BLD line onto the physical distance axis.

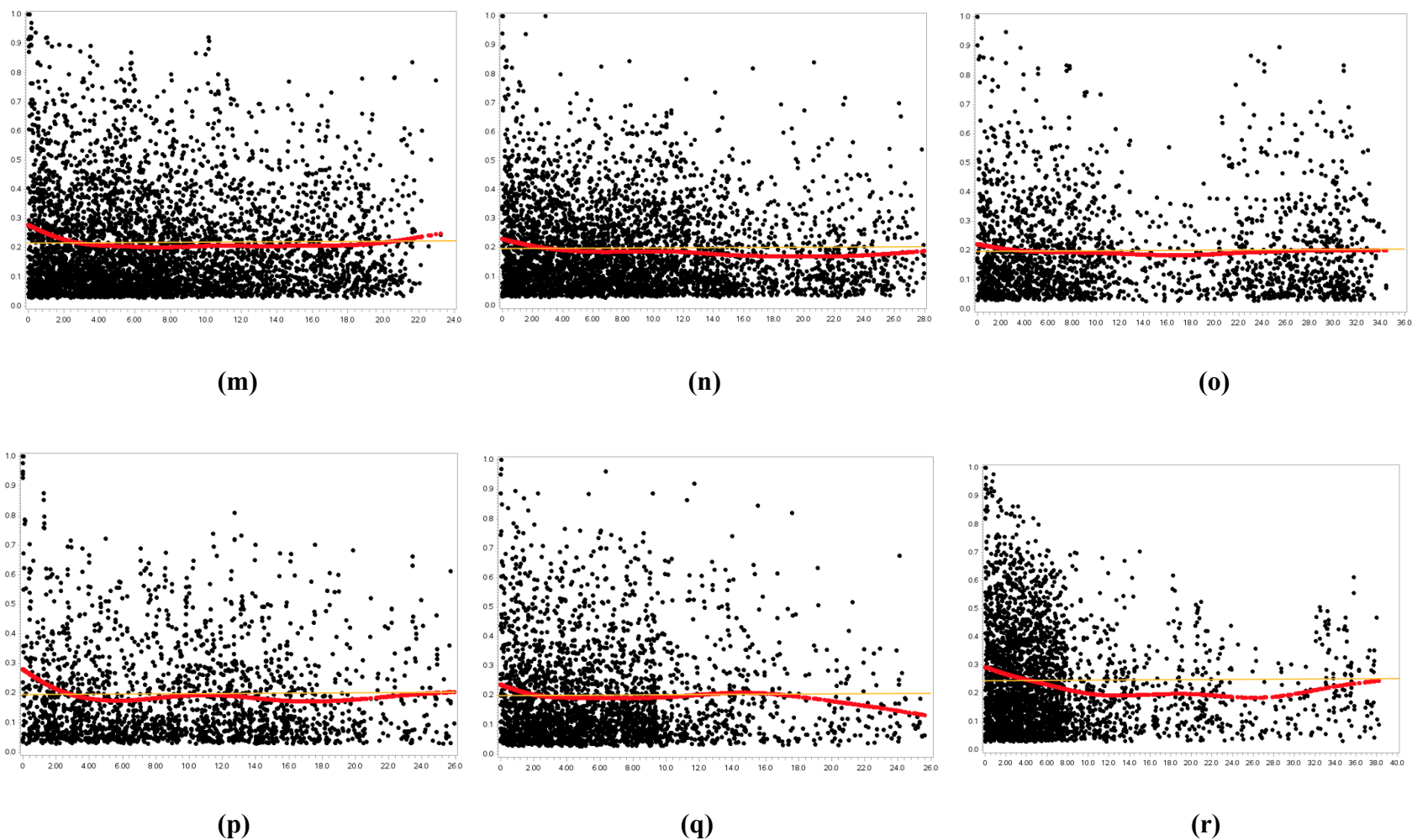
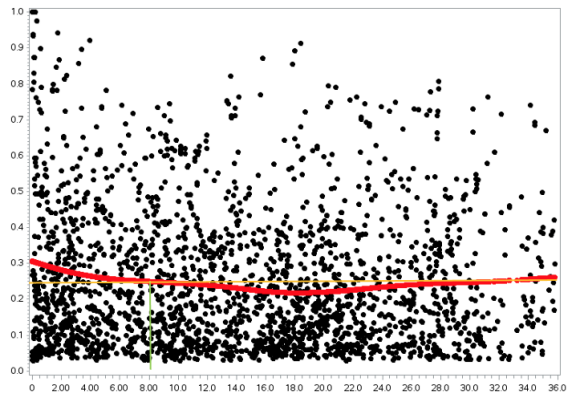


Figure A3 (continued). Plots of correlation coefficient (r^2) and physical distance (in Mb) for SNP markers on chromosomes A01 – A10 (a-j) and chromosomes C01 – C09 (k-s). The red curves represent the fitted plots of the data points, while the yellow line represents the background linkage disequilibrium (BLD) or threshold line. The decay of linkage disequilibrium was determined by projecting the intersection of the curves and the BLD line onto the physical distance axis.



(s)

Figure A3 (continued). Plots of correlation coefficient (r^2) and physical distance (in Mb) for SNP markers on chromosomes A01 – A10 (a-j) and chromosomes C01 – C09 (k-s). The red curves represent the fitted plots of the data points, while the yellow line represents the background linkage disequilibrium (BLD) or threshold line. The decay of linkage disequilibrium was determined by projecting the intersection of the curves and the BLD line onto the physical distance axis.